

A moonlighting enzyme imposes second messenger bistability of drive lifestyle decisions in *E. coli*

Inauguraldissertation

zur
Erlangung der Würde eines Doktors der Philosophie
vorgelegt der
Philosophisch-Naturwissenschaftlichen Fakultät
der Universität Basel

von

Alberto Reinders
aus Weil am Rhein, Deutschland

Basel, 2018

Genehmigt von der Philosophisch-Naturwissenschaftlichen Fakultät auf Antrag von:

Prof. Dr. Urs Jenal

Prof. Dr. Dirk Bumann

Basel, den 10. November 2015

Prof. Dr. Jörg Schibler
Dekan

Table of content

Chapter 1 OUTLINE	11
Cyclic di-GMP: second messenger extraordinaire	11
Introduction	12
Makers and breakers	13
C-di-GMP effectors	17
Physiological roles of c-di-GMP	19
Development and morphogenesis	19
Motile-sessile transition and biofilm formation	23
Role of c-di-GMP in bacterial virulence	27
Conclusion and outlook	29
Author contribution	32
Author information	32
Acknowledgements	32
Chapter 2 PROJECT 1	33
A novel capture compound for the identification and analysis of c-di-GMP binding proteins	33
Abstract	34
Technical note	35
Author contribution	40
Author information	40
Supplemental material	40
Acknowledgements	40
Materials & Methods	41
Bacterial strains and growth conditions	41
Protein expression and purification	41
Protein analysis and c-di-GMP production	41
Extract preparation for CCMS experiments	41
Capturing of c-di-GMP binding proteins	42
Tryptic digest of proteins for MS analysis	42
LC-MS/MS analysis	43
Database search and label-free quantification	43
Chapter 3 PROJECT 2	45
Expression and genetic activation of c-di-GMP-specific phosphodiesterases in <i>Escherichia coli</i>	45
Abstract	46
Importance	47
Introduction	48

Results	50
Expression of PDEs in growing <i>E. coli</i> cells	50
Motile suppressor mutants of a <i>pdeH</i> mutant identify activating mutations in alternative PDEs	50
Pde suppressor alleles restore motility by reducing intracellular c-di-GMP levels	53
Pde suppressor alleles reduce poly-GlcNAc levels and cellulose-dependent attachment	54
PdeL suppressors show increased enzymatic activity	56
PdeL suppressors enhance <i>pdeL</i> transcription	58
PdeL directly regulates its own expression in a c-di-GMP-dependent manner	58
Discussion	61
Author contribution	66
Author information	66
Supplemental material	66
Acknowledgements	66
Materials & Methods	67
Bacterial strains, plasmids, and growth conditions	67
DNA work	67
P1 phage lysate preparation and transduction	67
λ -RED recombineering	67
Suppressor screen	68
Video tracking	69
C-di-GMP measurements	69
Attachment assay	69
Protein purification	69
C-di-GMP hydrolysis assay and data fitting (phosphate sensor assay)	70
Electrophoretic mobility shift assay (EMSA)	71
β -galactosidase reporter assay	71
Strains, plasmids and oligonucleotides	73
Chapter 4 PROJECT 3	81
Stay or go? A bistable molecular switch facilitating	81
bacterial lifestyle transitions	81
Abstract	82
Introduction	83
Results	85
Cra and PdeL are activators of <i>pdeL</i> transcription	85
Cra and PdeL mediate c-di-GMP-dependent transcription of <i>pdeL</i>	86
PdeL is a c-di-GMP sensor	87

Two dimer configurations of PdeL drive c-di-GMP-dependent <i>pdeL</i> transcription	89
C-di-GMP determines PdeL dimer-species configuration	90
PdeL enzyme activity scales with c-di-GMP concentrations	90
PdeL enzyme activity scales with PdeL concentrations	90
PdeL controls the global c-di-GMP pool	91
<i>PdeL</i> expression is highly cooperative and requires the Cra-independent PdeL-box	93
<i>PdeL</i> transcription is bistable	93
Enzymatic feedback loop is not required for <i>pdeL</i> bistability	94
CIB is required for <i>pdeL</i> bistability	95
Bistable expression of <i>pdeL</i> generates bimodal populations	96
The enzymatic feedback loop is required for <i>pdeL</i> bimodality	96
PdeL is a gatekeeper for motile-sessile lifestyle transcription	97
Discussion	99
Author contribution	101
Author information	101
Supplemental material	101
Acknowledgements	101
Materials & Methods	102
Bacterial strains and growth conditions	102
P1 phage lysate preparation and transduction	102
Gene deletions and λ -RED-mediated recombineering	102
Electrophoretic mobility shift assay (EMSA)	102
Protein purification	103
Immunoblotting	103
C-di-GMP hydrolysis assay	104
Cysteine crosslink assay	104
Microscopy	105
Analysis of microscopy images	105
C-di-GMP measurements	105
Absolute protein concentration determination via selected reaction-monitoring (SRM) LC-MS analysis	105
Attachment assay	107
Biofilm escape assay	107
Motility assay	107
Strains, plasmids and oligonucleotides	108
Chapter 5 SUPPLEMENTALS	113
Figure S1 Specificity and DNA-binding affinities of Cra and Pde to <i>pdeL</i> intergenic region	114

Figure S2 Location and properties of PdeL motile suppressor alleles	115
Figure S3 R-state-specific cysteine-crosslink of PdeL (Y268C)	116
Figure S4 Characterization of enzymatic feedback loop-deficient PdeL _{EL} - variant	116
Figure S5 Putative H-NS binding boxes within pdeL intergenic region	117
Chapter 6 OUTLOOK	119
Chapter 7 APPENDICES	121
References	122
Acknowledgements	143
Publication record	145
Co-author affiliations	146
Curriculum vitae	147

Chapter 1 | OUTLINE

Cyclic di-GMP: second messenger extraordinaire

Urs Jenal, Alberto Reinders*, Christian Lori*

*equal contribution

Adapted from:

'Cyclic di-GMP: second messenger extraordinaire'

Nature Reviews Microbiology | February 2017 | vol. 15, issue 5: 271-284

Introduction

Cyclic dinucleotides (CDNs) are highly versatile signaling molecules that control various important biological processes in bacteria. The best-studied example is cyclic di-GMP (c-di-GMP). Known since the late 1980s, it is now recognized as a near-ubiquitous second messenger that coordinates diverse aspects of bacterial growth and behavior, including motility, virulence, biofilm formation and cell cycle progression. The roles of the prototypical second messengers cyclic AMP (cAMP) and cyclic GMP (cGMP) have been studied for more than 50 years, whereas recognition of the cyclic dinucleotides (CDNs), which are larger signaling molecules, has lagged behind. The first CDN was discovered in 1987, when Moshe Benziman reported “an unusual cyclic nucleotide activator” that was able to stimulate cellulose synthase from *Komagataeibacter xylinus* (formerly known as *Gluconacetobacter xylinus*), and identified this compound as bis-(3'-5')-cyclic diguanylic acid (c-di-GMP) [1]. More than 20 years later, c-di-AMP was discovered as a factor that is involved in DNA repair in *Bacillus subtilis* [2] (**Box 1**). Moreover, versions of c-GMP-AMP (cGAMP) that have different chemical linkages were first discovered in bacteria [3] and later in mammalian cells [4], and they were shown to have prominent roles in virulence and the innate immune response, respectively. Despite their chemical similarities, different CDNs seem to have distinct evolutionary origins, and the enzymes that are involved in their synthesis and breakdown are structurally unrelated [2,5,6]. The idea that different CDNs evolved in parallel emphasizes the potency and versatility of this macrocyclic ring with two purine moieties, which is the structural component of these biomolecules, as a key carrier of cellular information.

The discovery of CDNs has provided novel entry points for the study of important biological processes and cell behavior, including how bacteria coordinate their own growth and replication cycle, how they adapt to surfaces by forming multicellular consortia known as biofilms, or how pathogenic bacteria control their virulence and persistence. This was possible by first identifying the enzymes that are involved in the synthesis and degradation of CDNs [7,8], followed by the characterization of specific effectors and target molecules (see below). The field of CDN research is now rapidly expanding, and aspects of the signaling pathways that are involved are being explored at the atomic, molecular and cellular levels. In the past years, we have learned that CDNs are wide- spread and immensely versatile signaling molecules that control bacterial cellular processes at several levels, are well integrated with other global regulatory pathways, such as phosphorylation networks [9] and quorum sensing pathways [10], and crosstalk with other small signaling molecules, including cGMP, cAMP and guanosine tetraphosphate (ppGpp) [11-13]. So far, in bacteria, c-di-GMP is not only the most widespread CDN but also the most intensely studied and best-understood member of this family of second messengers.

Box 1 | CDNs beyond c-di-GMP

The cyclic dinucleotide (CDN) cyclic di-AMP (c-di-AMP) was discovered as a ligand that was bound to the amino-terminal domain of the DNA damage-sensing protein DisA of *Bacillus subtilis* [2]. Biochemical studies identified this domain as diadenylyl cyclase (DAC), which is the founding member of a family of enzymes that converts ATP

into c-di-AMP. Specific phosphodiesterases (PDEs) that contain DHH-DHHA1 or HD domains hydrolyze c-di-AMP into 5'-phosphoadenylyl-(3'-5')-adenosine (pApA) or AMP [14-16]. C-di-AMP is essential in various different bacteria, and dysregulation of c-di-AMP signaling causes abnormal phenotypes [17,18]. A recent report related the essential nature of c-di-AMP in *Listeria monocytogenes* to increased level of guanosine tetraphosphate (ppGpp), which is a global second messenger that has been linked to carbon metabolism and nutrient starvation. Depletion of c-di-AMP in rich media led to an accumulation of ppGpp and altered GTP concentrations, thereby inactivating the pleiotropic transcriptional regulator CodY [19]. In Gram-positive bacteria, c-di-AMP is associated with an increased list of cellular functions. These functions include cell wall homeostasis [18,20-23], DNA integrity [18,24-26], potassium homeostasis [27-30] and osmoprotection [31,32], gene expression [33,34], biofilm formation [35,36], sporulation [37], metabolism [38], antibiotic resistance [39], and, similar to c-di-GMP, cell-mediated adaptive immune response (see below).

cGMP-AMP (cGAMP) is of special interest because it is produced by bacteria and metazoans [3,40]. Bacterial cGAMP exhibits 3'-3' linkage and is synthesized by the dinucleotide synthase DncV, which was originally identified in *Vibrio cholerae* [3]. Structural studies have revealed that, in the first nucleotidyl transfer reaction, DncV preferably recognizes ATP and GTP as acceptor and donor nucleotides, respectively [41]. cGAMP is required for host colonization by *V. cholerae* and for exoelectrogenesis in different members of the Deltaproteobacteria [42,43]. Mammalian cGAMP (2'-3' linkage) has a prominent role in vertebrate innate immunity pathway that is responsible for the surveillance of cytoplasmic DNA [44]. cGAMP is synthesized by cGAMP synthase (cGAS), which is activated by binding to cytoplasmic DNA [45,46]. In turn, cGAMP binds to and activates the host receptor stimulator of interferon genes (STING), which then recruits TANK-binding kinase 1 (TBK1) to phosphorylate interferon regulatory factor 3 (IRF3), ultimately leading to the production of type I interferon (IFN). Evolutionary studies have recently revealed that the function of the cGAS-STING axis is conserved in sea anemones, which diverged from the human lineage more than 500 million years ago. As cGAS in sea anemones produces a bacteria-like 3'-3'-linked CDN that is recognized by its own STING protein, it was proposed that 2'-3'linked cGAMP recently evolved in vertebrates and that during evolution the protein components of this innate immunity pathway remained structurally conserved, whereas chemical changes in the second messenger were driving functional innovation [47].

Recent evidence suggests that c-di-GMP and c-di-AMP, which are secreted by bacteria or released through cell lysis, are also sensed by STING, thereby converging with the cGAS-cGAMP cytosolic DNA-surveillance pathway [48-50]. Interestingly, bacteria seem to have evolved strategies to decrease the production of IFN by avoiding the activation of STING. Group B *Streptococcus* was recently shown to express an ectonucleotidase, CdnP, which hydrolyses extracellular bacterial c-di-AMP to attenuate the cGAS-STING axis [51].

Makers and breakers

The c-di-GMP monomer exhibits two-fold symmetry, with two GMP moieties that are fused by a 5'-3' macrocyclic ring (**Figure 1A**). High-resolution structures of c-di-GMP, in solution or bound to protein, indicate that the ligand exists either as an elongated monomer or as a condensed intercalated dimer [3,52]. At physiological concentrations, c-di-GMP is a monomer in solution [4,53], which suggests that intercalated dimers form through the successive binding of two monomers to specific effector proteins. Cellular levels of c-di-GMP are regulated in response to internal and environmental cues. This is achieved through the activity of two antagonistic enzyme families: diguanylate cyclases (DGCs) and c-di-GMP-specific phosphodiesterases (PDEs) (**Figure 1A**), with equivalent enzymes being responsible for the metabolism of c-di-AMP (**Box 1**). DGCs and PDEs are found in members of all major bacterial phyla, thus representing two of the largest known families of signaling proteins in the bacterial kingdom [2,5,6,54]. The synthesis of c-di-GMP is catalyzed by DGCs through the cooperative action of their two catalytic GGDEF domains, which arrange in an antiparallel manner with one GTP molecule bound to

each protomer. Pioneering structural and mechanistic studies on PleD, which is a DGC from *Caulobacter crescentus*, proposed modes of substrate binding, catalytic mechanism, enzyme activation and product inhibition for this class of enzymes [5,9,55-57]. A mechanism was proposed whereby two GTP molecules are positioned in an antiparallel manner to enable their condensation into c-di-GMP [3,52] (**Figure 1B**). The requirement for dimerization conveys a simple mechanism to control the activity of DGCs by using an accessory domain that forms homodimers in a signal-dependent manner. In the case of PleD or the DGC WspR in *Pseudomonas aeruginosa*, this is facilitated by an amino-terminal receiver domain that dimerizes following phosphorylation [5,11-13,55,58] (**Figure 1B**). Recently, an alternative mechanism for the activation of DGCs was proposed for DgcZ from *Escherichia coli*, which contains a catalytic GGDEF domain that is fused to an N-terminal zinc-binding (CZB) domain. DgcZ is a constitutive dimer and its activity is allosterically regulated by the CZB domain [59] (**Figure 1C**). When zinc is present, the GGDEF domains of DgcZ, although facing each other, are not positioned in a catalytically competent conformation. In the absence of zinc, DgcZ may be activated through the repositioning of the GGDEF domains to enable the formation of phosphodiester bonds between substrate molecules (**Figure 1B**).

The arrangement of the catalytic GGDEF domains was also implicated in the feedback inhibition of c-di-GMP synthesis. Many of these enzymes are subject to non-competitive product inhibition through the binding of c-di-GMP to the allosteric I-site on the surface of the GGDEF domain [5,57]. In PleD and WspR, an intercalated c-di-GMP dimer binds to the I-site and a secondary binding site, thereby immobilizing the GGDEF domains in a non-catalytic state [55,58] (**Figure 1B**). Product inhibition of DGCs may establish precise cellular threshold concentrations of c-di-GMP or contribute to the reduction of stochastic perturbations and increased stability of c-di-GMP signaling networks by maintaining c-di-GMP levels in defined concentration windows [57]. Although a functional connection between the I-site and product inhibition has been clearly established, the binding of c-di-GMP to some GGDEF domains may also have other roles, such as in protein-protein interactions [60] (see below).

Structurally and mechanistically distinct c-di-GMP-specific PDEs that contain an EAL domain or an HD-GYP domain have been described. EAL-type PDEs hydrolyze c-di-GMP in the presence of Mg^{2+} or Mn^{2+} to yield the linear 5'-phosphoguananylyl-(3'-5')-guanosine (pGpG) dinucleotide [8]. EAL domain-containing proteins are active as dimers [61,62] but, in contrast to DGCs, for which the fusion of two GTP molecules requires a dimeric arrangement of the enzyme, this quaternary arrangement does not seem to be required for PDE catalysis. Instead, recent structural studies have implied a regulatory role for EAL domain dimerization. Based on crystal structures, a clam-shell-like opening and closing mechanism of the EAL dimer was proposed to regulate the activity of PDEs [62,63]. The evolutionarily conserved dimerization interface is formed by two helices, with one of them, $\alpha 5$, directly connecting through the $\beta 5$ - $\alpha 5$ loop (loop 6) to two central Asp residues that coordinate the metal ions in the active site [61,62,64] (**Figure 1D**). Structural and biophysical studies revealed that the $\alpha 5$ -loop 6 region undergoes substantial rearrangements during the clam-like opening and closing movements of the EAL dimer. These findings indicate that this part of the protein may function as a 'hinge joint' to couple EAL conformation to catalytic activity through the positioning of metal ions in the active site [62,63].

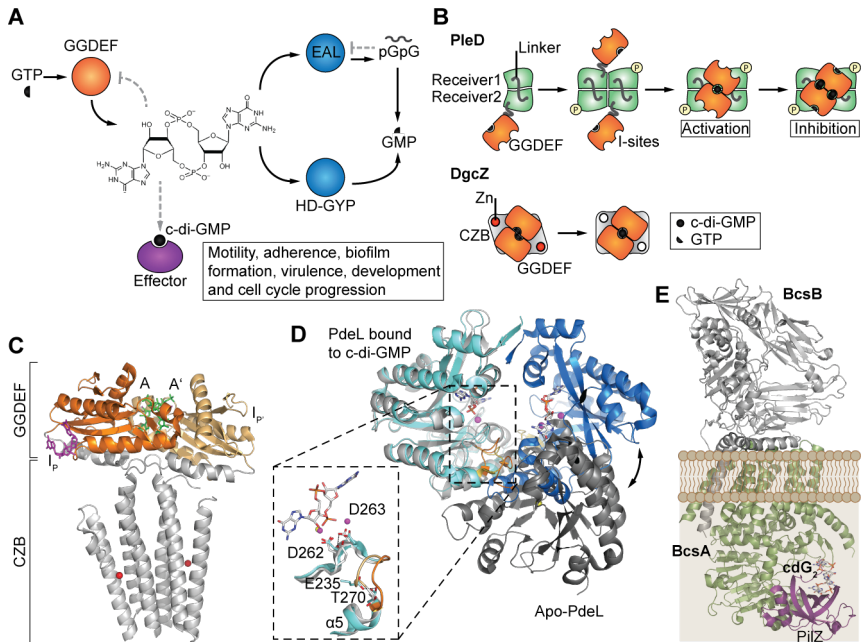


Figure 1 | Components of the c-di-GMP signaling network. (A) Principles of cyclic di-GMP (c-di-GMP) signaling. The c-di-GMP monomer exhibits two-fold symmetry, with two GMP moieties that are fused by a 5'-3' macrocyclic ring. The synthesis of c-di-GMP is catalyzed by diguanylate cyclases (DGCs) through the cooperative action of their two catalytic GGDEF domains (orange). Specific phosphodiesterases (PDEs) that contain EAL or HD-GYP domains (blue) hydrolyze c-di-GMP into 5'-phosphoguanylyl-(3'-5')-guanosine (pGpG) or GMP, respectively. DGCs are subject to product inhibition through the binding of c-di-GMP to an allosteric I-site. Product inhibition of PDEs is accomplished through the competitive binding of pGpG to the active site of the enzyme. Through binding to effector molecules, c-di-GMP regulates diverse cellular processes, including motility, adherence, biofilm formation, virulence, development and cell cycle progression. (B) Schematic of DGC activation. The upper panel shows the phosphorylation-dependent activation of PleD from *Caulobacter crescentus*. The amino-terminal receiver domains and GGDEF domains that are bound to GTP are shown. The phosphorylation-induced dimerization of receiver domains leads to the activation of GGDEF domains. The GTP molecules that are bound by each protomer are positioned in an antiparallel manner to enable the formation of two intermolecular phosphodiester bonds. Binding of c-di-GMP to the I-site and to a secondary binding site on the surface of the GGDEF domain immobilizes the enzyme in a catalytically inactive state. The lower panel shows the metal-dependent activation mechanism of DgcZ from *Escherichia coli*, which contains a catalytic GGDEF domain that is fused to an N-terminal zinc-binding (CZB) domain. DgcZ is a constitutive dimer. In the presence of zinc, the GGDEF domains of DgcZ are not positioned in a catalytically competent conformation. In the absence of zinc, DgcZ may be activated through the repositioning of the GGDEF domains to enable the formation of phosphodiester bonds between the GTP molecules that are bound to each DgcZ protomer. (C) Structure of the DgcZ dimer from *E. coli* (RCSB Protein Data Bank (PDB) entry 4H54) [59]. GGDEF-domains (orange) and zinc-binding CZB domains (grey) are highlighted. Zinc metal ions are depicted as red spheres. The binding of c-di-GMP (magenta) to antipodal inhibitory I-sites (I_p and I_p' from each protomer, respectively) and the binding of the GTP analogue GTPαS (green) to active sites (A and A' from each protomer, respectively) are shown. (D) Overlay of the EAL domains of the phosphodiesterase PdeL in the tight, substrate-bound conformation (blue; PDB entry 4LJ3) and the relaxed, substrate-free (apo) conformation (grey; PDB entry 4LYK) [62]. The

inset shows a zoomed-in view of the active site of PdeL and the conserved loop 6 region. The loop 6 conformations in the relaxed, apo (yellow) and tight c-di-GMP-bound (orange) dimer are indicated. Yellow spheres (Mg^{2+}) and magenta spheres (Ca^{2+}) indicate the positions of catalytic ions in the relaxed and tight protein conformations, respectively. The conserved double-aspartic acid motif (D262, D263) is highlighted. The figure also shows the anchoring glutamate (E235), which determines the structural arrangement of loop 6 through interaction with D263 or the conserved T270, respectively. (E) Activation of the membrane-bound BcsA–BcsB cellulose synthase complex by c-di-GMP. The structure of the *Rhodobacter sphaeroides* BcsA subunit (green), its carboxy-terminal PilZ-domain (magenta) and the BcsB subunit (grey; PDB entry 4P02) are shown [65]. The binding of c-di-GMP to the C-terminal PilZ domain of BcsA releases autoinhibition of its glycosyltransferase activity to activate the complex. A dimer of c-di-GMP bound to the PilZ domain is indicated.

Consistent with this, accessory domains that are known to control PDE activity communicate with the catalytic core by modulating the conformation of the EAL dimerization interface [63]. The observation that substrate binding induces EAL dimerization and also determines the conformation of the $\alpha 5$ -loop 6 region suggested allosteric coupling between EAL domains and the associated regulatory domains, with the $\alpha 5$ -loop 6 region acting as a central communication platform [62-64]. Interestingly, EAL domain-containing proteins that have adopted roles as c-di-GMP effectors seem to use similar c-di-GMP-mediated dimerization and $\alpha 5$ -loop 6 remodeling to regulate cellular processes [66] (see below). A second, unrelated family of c-di-GMP-specific phosphodiesterases contains conserved HD-GYP domains [67]. Recently, the first crystal structure of an active HD-GYP-containing PDE was solved and indicated that a novel trinuclear iron-binding site is involved in catalysis [68]. Whereas EAL-based enzymes generally convert c-di-GMP into the linear product pGpG, HD-GYP hydrolyses c-di-GMP in a one-step reaction to yield two molecules of GMP [68]. Thus, for bacteria that lack HD-GYP domain-containing proteins it remained unclear how pGpG is further catabolized into GMP. This puzzle was solved recently by studies that showed that the oligoribonuclease Orn, which is a ribonuclease that hydrolyses RNAs that are 2–5 nucleotides in length, is the primary enzyme that is capable of degrading pGpG [69,70].

Despite detailed knowledge on the structure and function of DGCs and PDEs, it has remained challenging to assign physiological roles to individual enzymes under laboratory conditions [71]. Genetic studies often fail to reveal clear phenotypes. Thus far, only a few specific input signals have been identified for these enzymes, including oxygen [72], light [61], nitric oxide [73], metals [59], nutrients [74,75] or surface contact [76], which may be owing to the limited physiological conditions that are assayed in the laboratory. Evidence for this was provided by a recent study of PDEs in *E. coli*. Despite a total of 13 PDEs being encoded in the genome of this organism, only PdeH is able to decrease c-di-GMP levels and license motility in growing *E. coli* cells [77,78] (see below). The observations that most PDEs are readily expressed and that a large proportion of these enzymes can be genetically activated to substitute for PdeH in motility control implied that most of these enzymes simply lack the appropriate stimuli under laboratory conditions [79].

DGCs and PDEs also engage in downstream signaling cascades through direct interactions with their effector molecules, thereby spatially controlling cellular processes [60,72,80]. In such supramolecular complexes, these proteins not only regulate the synthesis and degradation of c-di-GMP but can also act as ‘c-di-GMP sensors’ to control the activity of interacting proteins [80].

Box 2 | 1st aim of this thesis

Out of the 13 putatively active PDEs in *E. coli* K-12 we still lack knowledge of the exact physiological functions of most of these PDEs. In fact – under laboratory conditions – only the PDE PdeH seems to license motility in *E. coli* by reducing c-di-GMP levels below the threshold required to activate the flagellar brake protein YcgR. This raised questions regarding expression and activity of the other PDEs. Several possibilities could account for the observation that none of the other proteins are involved in motility control: (i) The remaining PDEs are not expressed. (ii) The input signals activating their enzyme activity are absent under the conditions tested. (iii) Some PDEs might be spatially confined to signal within microdomains without affecting the global c-di-GMP pool. Genetically studying the contribution of DGCs and PDEs to c-di-GMP-responsive output systems is a challenging endeavor, since under laboratory conditions most DGCs and PDEs are present in their inactive state, due to missing input signals. In this work we aim to answer, whether *E. coli* PDEs are restricted to a confined output target or – whether activated – could in principle contribute to a number of c-di-GMP-responsive output system.

C-di-GMP effectors

Although the coordinated control of makers and breakers explains how c-di-GMP levels are controlled in time and space, c-di-GMP pathways ultimately rely on the respective effectors that bind to c-di-GMP and on their downstream targets, which are the cellular components that are regulated by specific c-di-GMP effectors. Given the global influence of c-di-GMP on bacterial cell physiology and the sheer abundance of DGCs and PDEs in some bacteria, it can be assumed that numerous such effectors and cellular targets exist. Several families of effector proteins and RNAs have been identified and are structurally and functionally well characterized [81]. These include mRNA riboswitches [82], transcriptional regulators [83-85], proteins that contain PilZ domains [78,86,87], and proteins that contain degenerate GGDEF and EAL domains [88]. The field has recently come full circle; the discovery of c-di-GMP goes back to the observation that c-di-GMP activates the membrane-bound BcsA–BcsB cellulose synthase complex in *K. xylinus*, thereby increasing the production of this exopolysaccharide matrix component [1]. The availability of the structure of the BcsA–BcsB complex revealed an elegant mechanism, whereby the binding of c-di-GMP to the carboxy-terminal PilZ domain of BcsA releases autoinhibition of its glycosyltransferase activity to activate the complex [65] (**Figure 1E**). This example illustrates how c-di-GMP effectors, such as proteins that contain PilZ domains or the newly discovered YajQ protein family [89], can act as versatile adaptors that link c-di-GMP signal input to the activity of enzymes complexes or transcription factors.

The discovery that c-di-GMP binds to a range of transcription factors, including members of the response regulator or cAMP-responsive protein (Crp) families, in a way that was not predictable from their protein sequence, argued for a more versatile nature of ligand–effector interactions [83,90,91]. This is supported by the identification and characterization of a range of novel c-di-GMP effectors, an endeavor that was greatly aided by the introduction of innovative high-throughput methods and biochemical techniques (**Box 3**). One of the most exciting recent discoveries was the finding that ATPases bind to c-di-GMP. The first example is FleQ, which is a bacterial enhancer-binding protein (bEBP) from *P. aeruginosa*. Whereas

other members of this family of transcription factors are normally activated by phosphorylation, the activity of FleQ is controlled by c-di-GMP [84]. Structural studies have revealed that c-di-GMP interacts with the AAA+ ATPase domain of FleQ at a site that is distinct from the ATP-binding pocket. The binding of c-di-GMP obstructs the ATPase activity of FleQ, thereby altering its quaternary structure and its transcriptional activity [91]. In other bacteria, specific homologues of FleQ have also been identified as c-di-GMP effectors [92,93]. Similarly, c-di-GMP specifically binds to MshE, which is an AAA+ ATPase that is involved in the assembly of mannose-sensitive haemagglutinin pili (MSHA pili) in *Vibrio cholerae* [94-96]. The observation that HxrA, which is an MshE homologue and type 2 secretion (T2S) ATPase from *P. aeruginosa*, also specifically binds to c-di-GMP opened up the exciting possibility that this protein secretion pathway, which uses a pilus-like extrusion mechanism, might also be controlled directly by c-di-GMP [94]. The idea that c-di-GMP globally controls bacterial protein secretion is reinforced by some recent observations that indicate that this second messenger also controls type VI secretion systems (T6SSs) [97], as well as T3SSs [98]. Although the exact role of c-di-GMP in T6SSs remains unclear, its effect on T3SSs seems to be direct and again mediated through a central ATPase, as it was shown that the flagellar export ATPase FliH from a range of distantly related bacteria specifically binds to c-di-GMP [98]. The binding of c-di-GMP to FliH, and to its homologues HrcN and ClpB2 from the T3SS and T6SS, respectively, inhibits ATPase activity, which suggests that it directly interferes with flagellar export and T3S-mediated protein secretion. The authors of this study proposed that the mechanism of c-di-GMP binding might be widely conserved among the rotary export ATPases, which makes c-di-GMP central to the function of many of these secretion proteins [98]. It will be interesting to compare the c-di-GMP binding mode of the individual members of this family once structural information is available. Finally, sensor histidine kinases, which are the central components of phosphorylation pathways in bacteria, have also been identified as targets of c-di-GMP. The histidine kinase cell cycle kinase A (CckA) from *C. crescentus* was shown to bind to c-di-GMP through its catalytic and ATPase domains, which leads to a shift in the kinase-phosphatase activity of this bifunctional enzyme [9] (see below). The discovery that several ATPases act as regulatory hubs for c-di-GMP may reflect the global role of c-di-GMP in monitoring bacterial cell physiology. ATPases often function as central regulatory switches that govern key cellular processes and c-di-GMP seems to control the activity of some of these essential enzymes.

Box 3 | Toolkit for the analysis of CDN and CDN-binding proteins

Several tools and biomarkers were established for the *in vitro* and *in vivo* analysis of cyclic di-GMP (c-di-GMP). This includes sensitive high-performance liquid chromatography-coupled tandem mass spectrometry (HPLC-MS/MS) to accurately determine the concentration of second messengers in cell extracts [99,100], fluorescence-based reporters that are fused to c-di-GMP-dependent promoters or riboswitches [101-104], and a c-di-GMP concentration in individual live cells [105,106]. In the past five years, novel approaches were developed to identify and characterize cyclic dinucleotide (CDN) effector proteins on a global scale. This included affinity pull-down assays followed by mass spectrometry analysis. Trivalent chemical scaffolds with a CDN-binding, a biotin-sorting and a crosslinking moiety were used as capture compounds in combination with streptavidin-coated beads [107,108]. A similar approach used c-di-GMP-coated sepharose beads for affinity pull-down assays [109]. The advantage of these methods is that potential binding proteins can directly be isolated from cell extracts without the need for time-

consuming fractionation or biochemical purification. Moreover, once specific binding proteins have been identified, such pull-down methods can also be used for diagnostic purposes in combination with specific antibodies [110]. Both methods were successfully applied for different bacteria, including *Pseudomonas aeruginosa*, *Salmonella enterica* subsp. *enterica* serovar Typhimurium, *Caulobacter crescentus*, *Listeria monocytogenes*, *Streptomyces venezuelae* or *Bdellovibrio bacteriovorus* [38,85,107,111]. A more indirect approach involves the screening of the complete genome-scale ORF library (ORFeome) and the subsequent testing of cell lysates with a high-throughput binding assay [94,112]. Differential radial capillary action of ligand assay (DRaCALA) was developed to directly mix proteins with labelled nucleotides (such as radiolabeled nucleotides) on a nitrocellulose membrane. After washing the membrane, free ligands will diffuse away, whereas ligands that are specifically bound to proteins will be immobilized at the contact site [112]. The application of these techniques, as well as more conventional approaches, such as isothermal titration calorimetry (ITC) or microscale thermophoresis (MST), has led to the identification of numerous novel effector proteins [27,94,98,111].

Box 4 | 2nd aim of this thesis

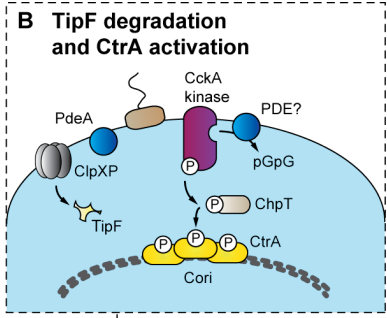
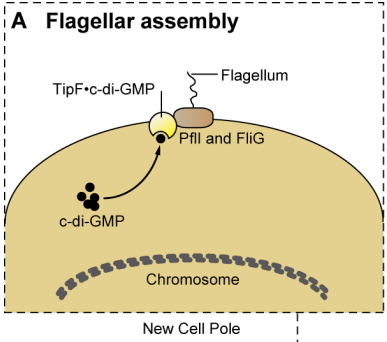
In silico analyses have identified several conserved families of c-di-GMP-binding proteins based on consensus motifs. Apart from the known c-di-GMP-binding proteins such as PilZ, degenerate GGDEF and EAL-domain proteins, a substantial number of non-canonical c-di-GMP-binding proteins have been experimentally identified and characterized so far. The structures of some of these proteins show a high degree of variability regarding the binding of c-di-GMP to them. This makes it challenging – if not impossible – to apply *in silico* approaches to predict and identify novel non-canonical c-di-GMP-binding proteins. The first aim of this work was to develop a novel approach to experimentally identify novel c-di-GMP binding proteins. The method was based on a biochemical approach, which applies a molecule comprised of a covalent link between c-di-GMP, a cross-linking and a sorting moiety. This allowed to capture c-di-GMP-binding proteins out of cell extracts, covalently cross-link the captured proteins, sort them by affinity pull-down and identify them via state-of-the-art mass-spectrometry.

Physiological roles of c-di-GMP

Development and morphogenesis

Several bacteria use c-di-GMP to control morphogenesis and developmental transitions. This includes *C. crescentus*, which is an aquatic organism that has an inherently asymmetric life cycle [113] (**Figure 2**). *C. crescentus* produces two specialized progeny cells during each division cycle – a motile swarmer cell and a sessile stalked cell. Dividing *C. crescentus* cells are highly polarized, with a stalk and adhesive holdfast exposed at one cell pole and a flagellum, pili and chemotaxis apparatus assembled at the opposite pole. The surface-attached stalked cell progeny reinitiates chromosome replication (S phase) and cell division (G2 phase) immediately, whereas the new swarmer cell is motile but blocks replication for an extended period called G1 phase. Replication and division resume when the swarmer cell differentiates into a stalked cell, a process during which it ejects its flagellum, retracts its pili and replaces them with a holdfast and a stalk [113] (**Figure 2**).

Recent studies identified c-di-GMP as a major driver of pole morphogenesis and cell cycle control in *C. crescentus* [9,114,115]. Mutants that were unable to synthesize c-di-GMP lost all polar appendages and showed marked cell morphology aberrations [115].



 [c-di-GMP] <50 nM
 [c-di-GMP] 300-500 nM

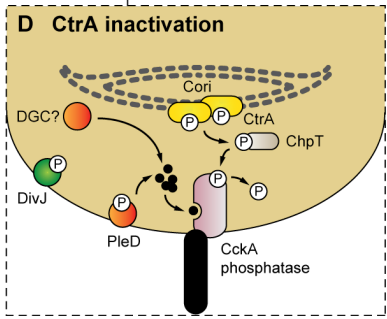
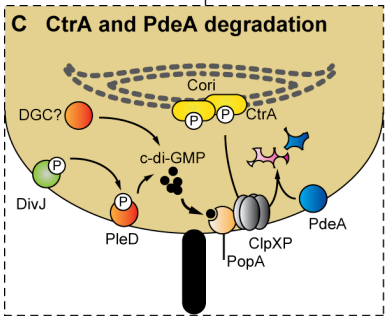
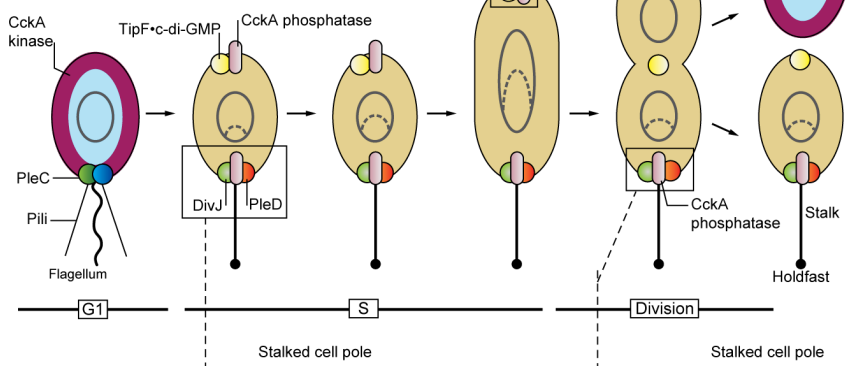


Figure 2 | Role of c-di-GMP in *C. crescentus* pole morphogenesis and cell cycle progression. A schematic of the cell cycle of *Caulobacter crescentus* is shown in the middle of the figure and individual panels highlight stage-specific processes at the stalked and flagellated poles. Motile, flagellated swarmer cells have a replication arrest (G1 phase) before differentiating into a sessile stalked cell and entering S phase and subsequently dividing. Dividing *C. crescentus* cells are highly polarized, with a stalk and adhesive holdfast exposed at one cell pole and a flagellum, pili and chemotaxis apparatus assembled at the opposite pole. The replication status of the circular chromosome is indicated schematically, with swarmer cells being replication silent, whereas chromosome replication initiates in stalked cells. Bacteria use cyclic di-GMP (c-di-GMP) to control pole morphogenesis and developmental transitions. This is achieved through the asymmetric, cell type-specific distribution of c-di-GMP. Levels of c-di-GMP oscillate during the cell cycle of *C. crescentus*, with trough values in the motile swarmer cell, a peak during the swarmer-to-stalked cell transition and intermediate concentrations during cell division. Changes in c-di-GMP concentration are controlled by the opposing action of the diguanylate cyclase (DGC) PleD and the phosphodiesterase (PDE) PdeA. The subcellular localization of PleD, PdeA, the flagellar placement protein TipF, and the sensor histidine kinases PleC, DivJ and CckA are marked at individual stages of the cell cycle. **(A)** Flagellar assembly. Following binding to c-di-GMP, TipF binds to its polar receptor TipN (not shown) to localize to the cell pole, where it recruits the flagellar components PflI and FlhG to initiate flagellar assembly. **(B)** Low levels of c-di-GMP at the flagellated pole of dividing cells and in swarmer cells promote the degradation of TipF by the ClpXP protease and promote the kinase activity of cell cycle kinase A (CckA). CckA activates CtrA through the phosphotransferase ChpT. Phosphorylated CtrA inhibits replication initiation by binding to the *C. crescentus* origin of replication (*Cori*). PdeA and as-yet-unidentified PDEs contribute to the decrease in the concentration of c-di-GMP at this stage of the cell cycle. PleC histidine kinase inhibits the phosphorylation of PleD in swarmer cells, and thus contributes to the decrease in the levels of c-di-GMP (see the central panel). **(C)** During differentiation into stalked cells, CtrA is inactivated and chromosome replication is initiated. PdeA and CtrA are degraded by the ClpXP protease. The ClpXP protease adaptor PopA binds to c-di-GMP and delivers CtrA to the protease. PleD and as-yet-unidentified DGCs contribute to the increase in c-di-GMP levels following entry into S phase and in the predivisional cell. The histidine kinase DivJ promotes the phosphorylation of PleD in stalked cells and thus contributes to the increase in c-di-GMP levels. **(D)** The inactivation of CtrA by the CckA phosphatase during the swarmer-to-stalked cell transition and at the stalked pole of the dividing cell. The binding of c-di-GMP to the catalytic domain of the histidine kinase CckA causes a switch from its default kinase activity to its S phase-specific phosphatase activity. This reverses the phosphate flux through the CckA–ChpT–CtrA cascade and leads to the inactivation of CtrA.

Levels of c-di-GMP oscillate during the cell cycle of *C. crescentus*, with trough values in the motile swarmer cell, a peak during the swarmer-to-stalked cell transition and intermediate concentrations during division [105,115] (**Figure 2**). The increase in the concentration of c-di-GMP during the swarmer-to-stalked cell transition is mainly promoted by PleD, which is a DGC that is activated by phosphorylation when cells enter S phase [115,116]. The activity of PleD is confined to the stalked cell by two antagonistic histidine kinases, PleC and DivJ, which are positioned at opposite poles of dividing cells and differentially segregate into swarmer cell and stalked cell progenies (**Figure 2**). Whereas PleC functions as a phosphatase that keeps the levels of phosphorylated PleD low in swarmer cells, DivJ functions as a kinase to drive the phosphorylation of PleD in stalked cells [116]. In addition, counteracting PDEs are thought to keep c-di-GMP levels low in the motile swarmer cell. One of these PDEs, PdeA, localizes to the flagellated pole before division and later partitions into the new swarmer cell, in which it promotes motility by keeping c-di-GMP levels low. PdeA is removed by specific proteolysis during the swarmer-to-stalked cell transition, which coincides with the activation of PleD, thereby contributing to the sharp increase in c-di-GMP at this stage of the cell cycle [114].

But how does the oscillation of c-di-GMP instigate the exact timing of cell cycle events in *C. crescentus*? One example is illustrated by the TipF–TipN pathway, which regulates flagellar polarity. Following the

binding of c-di-GMP, TipF localizes to the pole opposite to the stalk, where it binds to its polar receptor, the birth scar protein TipN [117] (**Figure 2A**). TipF then recruits flagellar proteins to this subcellular site to initiate flagellar assembly in the pre-divisional cell. TipF is stable when bound to c-di-GMP but is rapidly degraded when c-di-GMP levels decrease in the swarmer cell (**Figure 2B**). The removal of TipF was proposed to reset the flagellar polarization state and avoid incorrect positioning of the flagellar motor at the incipient stalked cell pole [117]. Recent studies also linked oscillations of c-di-GMP to the G1-S phase transition and control of chromosome replication [9]. The transcription factor cell cycle transcriptional regulator A (CtrA) is phosphorylated and active in swarmer cells (G1 phase) in which it binds to the *C. crescentus* origin of replication (Cori) to block replication initiation [113] (**Figure 2B**). During differentiation into stalked cells, CtrA is inactivated and replication is initiated. The activity of CtrA is controlled by the bifunctional cell cycle histidine kinase CckA, which phosphorylates and thus activates CtrA through the phosphotransferase protein ChpT. CckA exhibits kinase activity in the swarmer cell but adopts marked phosphatase activity during the G1-S transition, thereby reversing the phosphate flux through the CckA-ChpT-CtrA cascade and inactivating CtrA. Concurrent with its dephosphorylation, CtrA is degraded by the ClpXP protease [113] (**Figure 2C**). Both the dephosphorylation and degradation of CtrA are controlled by the increase in c-di-GMP during the G1-S phase transition. The degradation of CtrA is mediated by the ClpXP protease adaptor PopA, which binds to c-di-GMP and delivers CtrA to the protease [88,118,119], whereas the dephosphorylation of CtrA results from c-di-GMP directly interfering with the CckA kinase-phosphatase switch (**Figure 2D**). Biochemical and structural studies have shown that c-di-GMP binds to the catalytic and ATP-binding domain of CckA, thereby inhibiting its default kinase activity and stimulating its phosphatase activity [9,120]. By controlling a key cell cycle kinase to drive the G1-S phase transition in *C. crescentus*, c-di-GMP has adopted a role similar to cyclins in eukaryotes, which drive the cell cycle by regulating the activity of cyclin-dependent kinases [121]. Moreover, c-di-GMP spatially controls the activity of CckA during division to promote the asymmetric replication of future daughter cells. In predivisional cells, CckA localizes to opposite cell poles, adopting kinase and phosphatase activity at the flagellated and stalked pole, respectively (**Figure 2**). This leads to a gradient of phosphorylated CtrA in the cell and to the asymmetric initiation of replication, with Cori at the stalked cell pole being activated before cell division is completed, whereas the Cori at the flagellated pole remains inactive [122,123]. The asymmetric distribution of c-di-GMP was proposed to control the differential activity of CckA at opposite poles. Although the bulk of dividing cells experience high levels of c-di-GMP, a microenvironment that has low levels of c-di-GMP was proposed to promote the kinase activity of CckA at the flagellated pole [9] (**Figure 2**). The authors of this study proposed that this mechanism could shield CckA molecules that are sequestered to the flagellated pole from the cellular pool of c-di-GMP. How such a microenvironment with low c-di-GMP levels is organized and which PDEs are involved in this spatial control remain to be shown.

The asymmetric distribution of c-di-GMP during cell division was also observed in other bacteria, which argues that this might represent a general principle to control cell behavior and/or reproduction [105].

For example, during the cell cycle of *P. aeruginosa*, c-di-GMP levels decrease a short period after cell division in the daughter cell that inherits the polar flagellum. This pattern is caused by the asymmetric distribution of Pch, which is a PDE that localizes to the chemotaxis machinery at the flagellated cell pole during division [106]. Similar to the G1 phase of the cell cycle of *C. crescentus*, a decrease in c-di-GMP at this stage of the cell cycle of *P. aeruginosa* may promote diversity in the swimming behavior, which, in turn, could help *P. aeruginosa* to adapt to new environments. In addition to contributing to cell polarity and the determination of cell fate in unicellular bacteria, c-di-GMP also controls complex multicellular behavior in bacteria. For example, *streptomyces* undergo an elaborate life cycle with two distinct filamentous cell forms. Germinating spores develop into vegetative hyphae, which grow into a substrate to scavenge nutrients. Following nutrient depletion, aerial hyphae are formed, which eventually differentiate into long chains of spores [124]. Recently, c-di-GMP was found to have a key role in the transition from vegetative mycelial growth to the formation of a reproductive aerial mycelium [85]. The deletion of genes that encode proteins that are involved in the metabolism of c-di-GMP had a notable effect on colony morphology and development [124]. Moreover, increasing internal levels of c-di-GMP blocked development, whereas decreasing levels of c-di-GMP caused premature spore production by bypassing the formation of aerial hyphae [85]. Premature sporulation is also observed in mutants that lack BldD, the master regulator of *Streptomyces* development that represses a global regulon of approximately 170 sporulation genes [124]. Recently, a direct connection between these two key components of developmental control was identified when BldD was shown to be a c-di-GMP effector protein that represses its target genes in a manner that is dependent on c-di-GMP binding [85]. Thus, a decrease in cytoplasmic levels of c-di-GMP may cause the disassembly of the BldD dimer and its inactivation, and thus the induction of sporulation genes. Other studies in *Myxococcus xanthus* [92,125], *Bdellovibrio bacteriovorus* [126] and *cyanobacteria* [127] further highlight the broad effect of c-di-GMP on development and morphogenesis in bacteria.

Motile-sessile transition and biofilm formation

Controlling the motile–sessile transition of bacteria is a universal feature of c-di-GMP. Generally, low levels of c-di-GMP are associated with the motility of individual cells, whereas increased concentrations of c-di-GMP promote surface attachment and the formation of biofilms. However, rather than being a simple on–off switch, complex regulatory steps seem to be involved in a multistage process that leads to surface colonization [128]. In line with the idea that motility is one of the primary processes that is targeted by c-di-GMP, the assembly and activity of the bacterial flagellar motor is highly regulated by this second messenger. This includes the regulation of flagellar gene expression [83,84], motor assembly [98,117] and motor function [78,129]. Although controlling flagellar gene expression is likely to be part of a long-term adaptation strategy, tuning motor activity might be important for bacteria to rapidly change their behavior during the colonization of a surface.

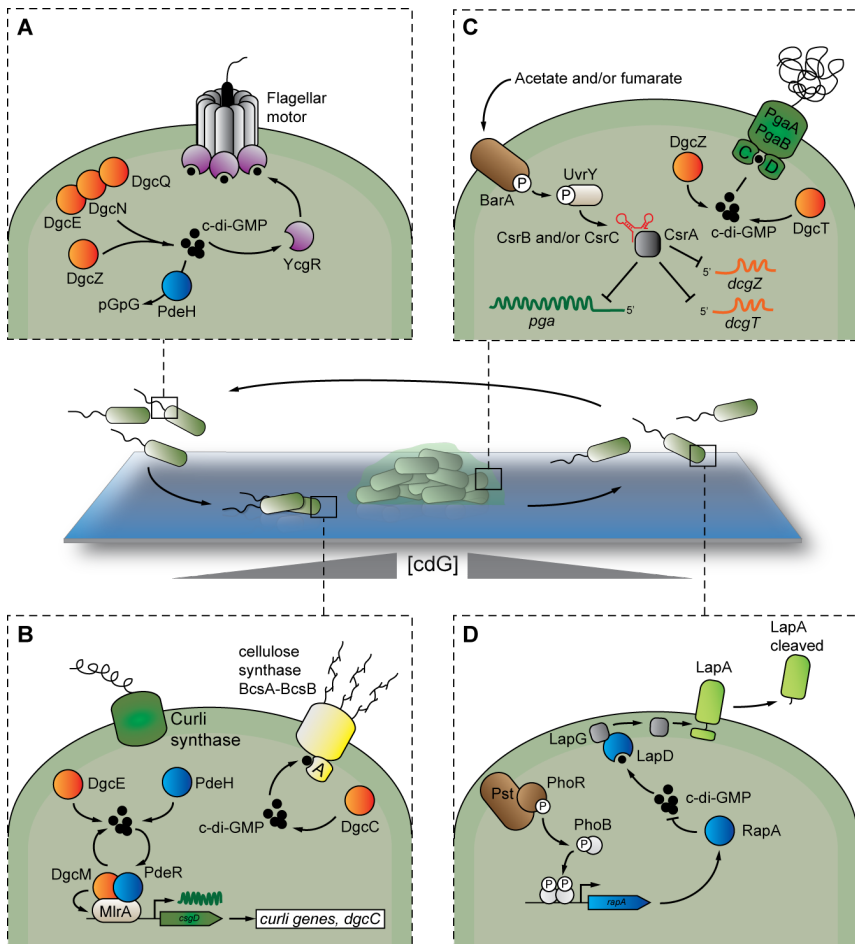


Figure 3 | Role of c-di-GMP in biofilm formation and dispersal. Bacterial surface attachment, biofilm formation and dispersal are indicated schematically in the central panel. **(A)** Cyclic di-GMP (c-di-GMP)-mediated control of flagellar motility in *Escherichia coli*. In its c-di-GMP-bound form, the c-di-GMP effector YcgR interacts with and curbs the flagellar motor, which leads to the obstruction of motor function. PdeH inactivates YcgR by keeping c-di-GMP levels low and thereby enabling motor function. **(B)** c-di-GMP-dependent production of the biofilm matrix components amyloid curli fibers and cellulose in *E. coli*. The global DgcE and PdeH module controls the overall levels of c-di-GMP, and increased levels of the second messenger are sensed by the local DgcM and PdeR module to activate the transcription factor MirA. This transcription factor induces the expression of the global transcription factor CsgD, which then activates the expression of curli components and DgcC. In turn, DgcC stimulates the synthesis of c-di-GMP, which allosterically activates the production of cellulose by binding to the BcsA–BcsB complex. **(C)** c-di-GMP-mediated synthesis of the alternative exopolysaccharide poly-β-1,6-N-acetylglucosamine (PGA) in *E. coli*. The biogenesis and secretion of PGA require the Pga

complex, which comprises the two transmembrane proteins PgaA and PgaB, and the two inner membrane components PgaC and PgaD. The carbon storage regulator (Csr) global regulatory system represses the *pga* genes, which encode components of the PGA synthesis machinery (PgaA, PgaB, PgaC (represented by single letter 'C' in this panel) and PgaD (represented by single letter 'D' in this panel)), and *dgcT* and *dgcZ*, which encode two diguanylate cyclases (DGCs) that are responsible for the allosteric activation of PgaC and PgaD. The histidine kinase BarA is stimulated by short-chain fatty acids and activates the expression of two small RNAs, CsrB and CsrC, through the phosphorylation of the response regulator UvrY. In turn, CsrB and CsrC antagonize the translation inhibitor CsrA and thus enable the expression of *pga*, *dgcT* and *dgcZ*. Intracellular levels of c-di-GMP increase through the action of DgcT and DgcZ. The binding of c-di-GMP to PgaC and PgaD allosterically activates the Pga complex. (D) Biofilm dispersal mechanism in *Pseudomonas fluorescens* Pf01. The LapA surface protein mediates surface adhesion and contributes to the stabilization of biofilms in *P. fluorescens*. Under conditions of phosphate starvation, LapA is degraded by the periplasmic protease LapG, which results in biofilm dispersal. If enough phosphate is available, LapG is sequestered by its partner LapD in its c-di-GMP-bound conformation. When phosphate becomes limited, the phosphodiesterase (PDE) RapA is expressed through the Pst-PhoR-PhoB phosphate control system, which leads to a decrease in the levels of c-di-GMP, a conformational change in apo-LapD and the release of the LapG protease, which cleaves the LapA adhesin. pGpG, 5'-phosphoguananylyl-(3'-5')-guanosine.

For example, in *E. coli* and *Salmonella enterica* subsp. *enterica* serovar Typhimurium, increased levels of c-di-GMP result in the obstruction of motor function by the c-di-GMP effector protein YcgR, which, in its c-di-GMP-bound form, interacts with the flagellar rotor–stator interface [78,130,131] (**Figure 3A**). To block the activity of YcgR and promote swimming, these bacteria co-express the PDE PdeH and flagellar genes. A similar mechanism was proposed to tune motility in *B. subtilis*, in which PdeH controls motility by preventing flagellar obstruction by the YcgR homologue DgrA [132]. YcgR homologues also control flagellar function in *pseudomonads* [133,134]. Intriguingly, in *P. aeruginosa*, the YcgR homologue FlgZ controls swarming motility by specifically interacting with the MotC–MotD flagellar stator, which is required for surface-associated motility [133]. YcgR in *E. coli* exhibits high binding affinity for c-di-GMP, which suggests that small spikes in the level of c-di-GMP are sufficient to adjust the flagellar motor and to initiate surface attachment. Consecutive steps of surface colonization may involve an incremental increase in the level of c-di-GMP and the sequential activation of distinct cellular processes, such as surface motility or the production of adhesins and components of the biofilm matrix. This could be accomplished through the successive involvement of DGCs that have distinct levels of feedback inhibition [57] and through the activation of c-di-GMP receptors that have gradually decreased affinities [135]. For example, in *P. aeruginosa*, different DGCs, PDEs and effector proteins are required at discrete stages of biofilm formation [128].

On contact with a surface, bacteria rapidly change their behavior, expose adhesins, activate surface organelles and produce an extracellular matrix to protect developing microcolonies. This adaptation is coordinated by c-di-GMP at the transcriptional (see, for example, Ref. [136]), translational (see, for example, Ref. [137]) and post-translational levels (see, for example, Ref. [110]). For example, c-di-GMP regulates type IV pili (T4P), which are the prototypical surface adherence and motility organelles, in various bacteria, including *M. xanthus* [138], *V. cholerae* [95], *P. aeruginosa* [139], *C. crescentus* [115] or *Clostridium difficile* [140] (see below). Similarly, in *E. coli*, the production of the two principal biofilm matrix components – curli fibers and cellulose – is regulated by c-di-GMP [141]. During biofilm formation, c-di-GMP levels increase as a result of σ^S (also known as RpoS)-induced expression of DgcE

(formerly known as YegE) [77] and other DGCs, and the consecutive downregulation of the PDE PdeH (formerly known as YhjH) [77], which acts as a gatekeeper for motility and is part of the large flagellar regulon [78,142].

Box 5 | 3rd aim of this thesis

In response to environmental changes, bacteria frequently switch their lifestyle from a motile single-cell to a community-based surface attached lifestyle. This is achieved through downstream effectors, which bind c-di-GMP to elicit the corresponding cellular function. As c-di-GMP acts primarily on the post-translational level and many effector proteins have binding affinities in the low to mid nanomolar range, c-di-GMP is able to stage a rapid and hypersensitive response. Given that many bacterial species harbor a whole array of DGCs and PDEs, this raises the problem of network robustness. How is a deterministic cellular response ensured and buffered against stochastic noise in expression and activity of DGCs and PDEs?

In this work, we studied PdeL from *E. coli*, a protein with dual role as transcription factor and c-di-GMP specific phosphodiesterase. We ask, whether PdeL acts as a buffer for c-di-GMP noise to facilitate rapid and robust lifestyle transitions in *E. coli*.

Increased global levels of c-di-GMP induce a local control module that consists of DgcM and the trigger enzyme PdeR (**Box 6**), which form a DGC–PDE pair that directly interacts with and stimulates the transcription factor MrA (**Figure 3B**); this activates the expression of the central curli regulator CsgD. Interestingly, PdeR and DgcM do not primarily exhibit a catalytic role but rather sense the global increase in c-di-GMP and function as co-activators for MrA [80]. CsgD then induces the transcription of curli genes and *dgcC*, which encodes the primary DGC that stimulates the synthesis of c-di-GMP, which, in turn, allosterically activates the production of cellulose by binding to the BcsA–BcsB complex [65] (**Figure 1E, 3B**). This is a key example of how different levels of the c-di-GMP signaling network are interconnected to gradually activate and coordinate a cellular response, which, in this case, tunes the expression of matrix components. An alternative exopolysaccharide, poly- β -1,6-N-acetylglucosamine (PGA), can promote surface adherence and biofilm formation in *E. coli*. The biogenesis and secretion of PGA require the PGA complex (comprising PgaA, PgaB, PgaC and PgaD) and its allosteric activation by c-di-GMP. Both the *pgaABCD* operon and the genes that encode the two DGCs, DgcT and DgcZ, are controlled by the carbon storage regulator (Csr) system, a global regulatory system that mediates virulence and biofilm formation in *E. coli* [143]. Recent findings indicate that c-di-GMP activates the PGA complex by binding directly to both PgaC and PgaD, which are the two inner membrane components of the PGA complex, to stimulate their glycosyltransferase activity [110] (**Figure 3C**).

Although the processes that drive biofilm formation are relatively well understood, the mechanisms that underlie biofilm dispersal have remained understudied. Given the prominent role of c-di-GMP in biofilm formation, careful control of the levels of this second messenger must also be linked to active biofilm dispersal [144]. A potential escape mechanism was identified in *Pseudomonas fluorescens*, in which the LapA surface protein mediates surface adhesion and the stabilization of biofilms [145]. At high c-di-GMP levels, c-di-GMP binds to LapD to help sequester the LapG protease in the periplasm. When c-di-GMP

levels decrease following the induction of the PDE RapA, LapD is inactivated, thereby releasing the protease to cleave the LapA adhesin and weaken the biofilm (Figure 3D).

As biofilms contribute to acute and chronic infections, it is not surprising that the c-di-GMP network is under selective pressure in human patients. Slow-growing autoaggregative *P. aeruginosa* isolates from the respiratory tracts of patients with cystic fibrosis were shown to have mutations that lead to marked activation of some of the major DGCs [146,147]. The observation that such variants effectively persisted in animal models and in the presence of subinhibitory concentration of antibiotics, despite decreased growth rates in vitro, indicated that they may have an important role in persistence during antimicrobial chemotherapy [146].

Box 6 | Moonlighting enzymes

The term moonlighting originates from proteins, which, apart from their primary, have a secondary (unrelated) function [148,149]. Up to date many moonlighting enzymes have been described such as in *C. crescentus*, where the essential metabolic enzyme CtpS is an integral cytoskeletal component contributing to the crescentoid shape. In this particular case the enzyme activity does not affect cell-shaping, since mutations in the active site residues still retained its ability to form cytoskeletal filaments [150]. Moonlighting enzymes are also represented in transcription factors. A prominent example is the metabolic enzyme and transcription factor PutA, which is present throughout many bacterial species including *E. coli*. PutA catalyzes the first step in the proline degradation pathway, namely the irreversible conversion of L-proline to (S)-1-pyrroline-5-carboxylate. In its reduced and proline-bound state, PutA localizes to the membrane where it functions as an enzyme, whereas oxidation and absence of proline leads to translocation of PutA to the DNA to repress expression of the *put* operon [151,152]. This mechanism allows PutA to entirely shut off its expression once proline is depleted, to which PutA itself contributes.

In both examples the two functions are mutually exclusive and the enzymatic activity is functionally uncoupled from transcription or generation of cytoskeletal elements in the case of CtpS. However, in the previously described example, of c-di-GMP-dependent *csgD* expression this is not the case. The primary role of the PDE PdeR is not to deplete the cellular c-di-GMP pool but rather to translate the c-di-GMP status of the cell into further downstream signaling. Thus both functions of PdeR are functionally coupled, since the authors showed that abolished c-di-GMP binding of PdeR fully abrogated c-di-GMP-dependent *csgD* transcription [80]. This functional coupling defines a special class of moonlighting enzymes, namely 'trigger enzymes'.

Role of c-di-GMP in bacterial virulence

The virulence of animal and plant pathogens has been shown to be modulated by c-di-GMP [54]. Processes that are controlled by c-di-GMP include host cell adherence, the secretion of virulence factors, cytotoxicity, invasion, resistance to oxidative stress and the modulation of the immune response of the host. Importantly, recent findings have linked c-di-GMP to the most prominent secretion systems for virulence factors, including T2SSs, T3SSs and T6SSs [94,97,98]. This opens up the possibility that c-di-GMP interferes with these processes on a more global scale. Studies in *C. difficile* have highlighted the importance of c-di-GMP in virulence. In contrast to most gram-positive bacteria, *C. difficile* encodes numerous enzymes that are involved in the turnover of c-di-GMP [153]. During the course of infection, *C. difficile* undergoes a c-di-GMP-mediated switch from a motile to a surface-adherent state, whereby cells adhere to the intestinal mucosa through T4P and other adhesins [154]. This transition is mediated

by a total of 16 c-di-GMP-responsive riboswitches, 12 of which are off switches (type I) and four are on switches (type II) [155]. Through these regulatory elements, c-di-GMP controls the expression of flagella, pili, adhesion factors and other virulence factors, including the toxins TcdA (also known as ToxA) and TcdB, which are the main virulence factors of *C. difficile* [140,155-158] (Figure 4). For example, a collagen-binding protein (CBP) and its specific protease are inversely controlled by type I and type II riboswitches, respectively [155]. Expression of the protease at low c-di-GMP concentrations effectively prevents host cell adherence, whereas expression of the CBP at high c-di-GMP concentrations promotes attachment to host tissue. Thus, c-di-GMP-mediated riboswitches control *C. difficile* host colonization by coordinating motility, toxin production, surface adhesion and biofilm formation.

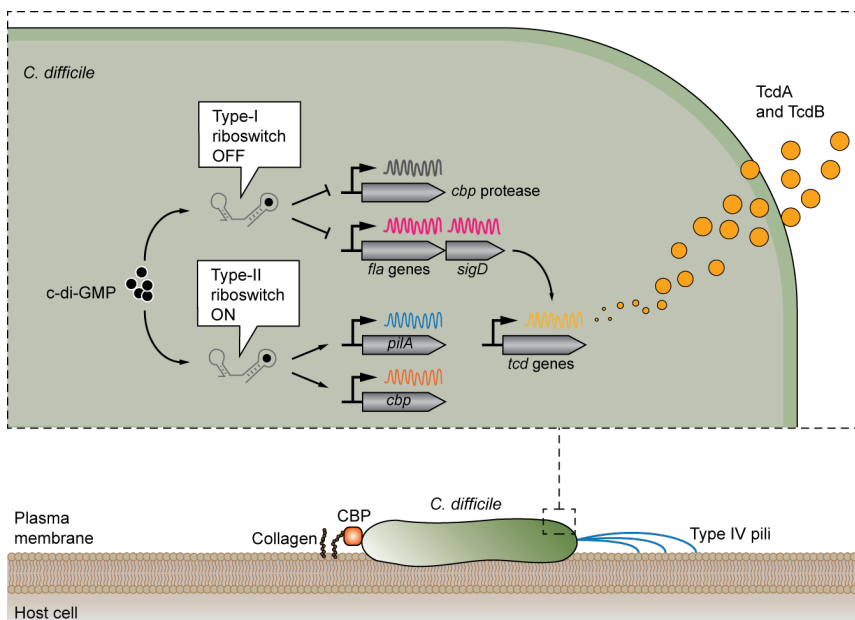


Figure 4 | Role of c-di-GMP in the virulence of *Clostridium difficile*. Cyclic di-GMP (c-di-GMP)-mediated riboswitches control host colonization by *Clostridium difficile*. Type I riboswitches and type II riboswitches control the expression of factors that are involved in motility, surface attachment and virulence, including the toxins TcdA and TcdB. Type I riboswitches (off switches) inhibit translation following the binding of c-di-GMP, whereas type II riboswitches (on switches) promote the translation of target genes when bound to c-di-GMP. Increasing levels of c-di-GMP stimulate the expression of adhesion factors, such as type IV pili and collagen-binding proteins (CBP), and inhibit the expression of flagellar genes and the CBP protease to promote host colonization. When the concentration of c-di-GMP is low, cells express motility and anti-adhesion genes. In addition, the gene that encodes the sigma factor SigD is co-regulated with flagellar genes, leading to the expression of the SigD-dependent toxins TcdA and TcdB, which are the main virulence factors of *C. difficile*.

The prominent role of c-di-GMP in virulence is exemplified by the outbreak of *E. coli* O104:H4 in Germany in 2011, which caused an unusually high incidence of haemolytic uraemic syndrome (HUS) [159]. The genome of the causative strain showed characteristics of both enterohaemorrhagic *E. coli* (EHEC) and enteroaggregative *E. coli* (EAEC), and revealed the presence of a highly-expressed DGC (encoded by *dgcX*), which is prevalent in EAEC O104:H4 strains [160]. This indicated that the outbreak strain and EAEC in general produce high levels of c-di-GMP and are likely to form biofilms in the host. The observation that *dgcX* is inserted at the *attB* locus, the integration site for phage λ , and is flanked by prophage elements, suggested that the gene was acquired by horizontal gene transfer. The analysis of *E. coli* O104:H4 also emphasized the key importance of adaptation and regulatory flexibility of the c-di-GMP network. Although marked adherence, together with the expression of Shiga toxin, is a key virulence factor of *E. coli* O104:H4, this strain produces curli but is cellulose negative. The authors of this study speculated that the marked pro-inflammatory effect of curli, together with the absence of cellulose (which normally counteracts this effect), may facilitate entry into the bloodstream and kidneys, in which this pathogen can cause life-threatening HUS [160].

Given their widespread abundance in bacteria and their importance in bacterial virulence, it is not surprising that bacterial CDNs are sensed by the immune system of the host. Recent evidence suggests a prominent role for c-di-GMP and c-di-AMP as pathogen-associated molecular patterns (PAMPs), which are specifically recognized by the innate immune system of the host (**Box 1**).

Conclusion and outlook

This introduction summarized some of the recent findings that describe the mechanistic and functional aspects of c-di-GMP signaling in bacteria. Although c-di-AMP was discovered more recently, the field is rapidly advancing and exposing a physiological complexity that is comparable to the c-di-GMP network (**Box 1**). It is possible that additional CDNs still await discovery, providing even greater signaling diversity by varying either the nucleotide composition or linkage chemistry. However, why are CDNs so prevalent in the control of important biological processes in bacteria? One major advantage of second messenger-based networks over other information-transfer systems that are based on protein-protein interactions might be the ease with which they are able to evolve. For example, the recruitment of additional cellular processes into an existing c-di-GMP network seems relatively straight-forward, considering that c-di-GMP often binds to the surface of pre-existing protein domains with only a few amino acids that contribute to ligand affinity and specificity (**Figure 5A**). Simple recruitment of additional effectors, together with the rapid expansion of makers and breakers by gene duplication, might thus have predisposed CDN-based regulatory networks for the coordination of global metabolic and behavioral transitions in bacteria.

CDN-based second messengers also provide various advantages in signal transduction. On the one hand, their rapid cellular diffusion stages an instantaneous and global internal response. On the other hand, CDNs may act in a highly specific manner either through temporal or spatial control [161,162]. For example, the combination of DGCs or PDEs that have distinct inhibition constants and substrate affinities, respectively, together with effector proteins or RNAs of matching c-di-GMP affinities would permit cells to regulate different processes in a highly specific manner (**Figure 5B**).

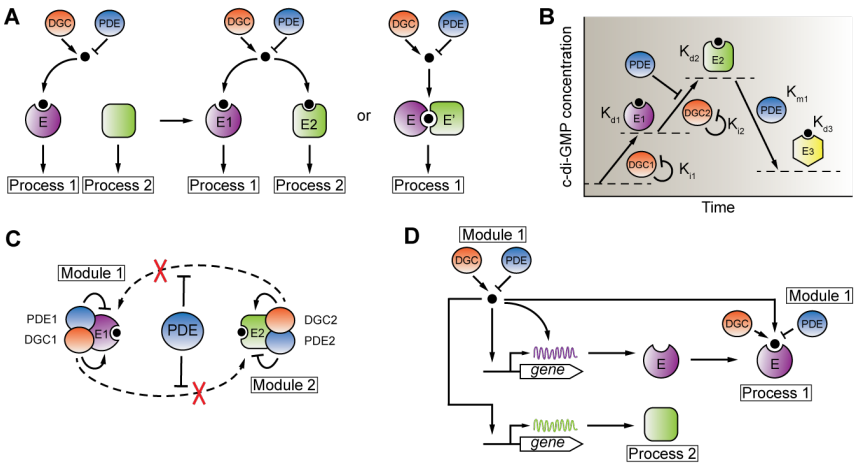


Figure 5 | General concepts of c-di-GMP signaling modules. (A) Evolutionary diagram of the incorporation of a new cellular process into an existing cyclic dinucleotide (CDN) network. Minor modifications to the surface of a specific protein can mediate the specific binding of cyclic di-GMP (c-di-GMP; rendering it an effector protein (E)), which, in turn, can modulate the activity and stability of the protein (E2) or its interaction with a partner (E-E'). **(B), (C)** The network architecture that is involved in pathway-specific signaling. c-di-GMP-dependent processes can be specifically regulated by temporal (part B) or spatial (part C) separation. Temporal regulation can depend on effector proteins with different ligand-binding affinities (K_d) and on diguanylate cyclases (DGCs) and/or phosphodiesterase (PDEs) with specific inhibition (K_i) and activation constants (K_m), respectively. This mode of regulation establishes precise cellular thresholds of c-di-GMP levels, thereby activating specific downstream effectors and pathways. Spatially separated signaling relies on some form of compartmentalization. For example, a specific DGC-PDE module (DGC1-PDE1 or DGC2-PDE2) interacts with its specific effector (E1 or E2, respectively). To avoid unwanted crosstalk between individual DGC-PDE modules and other effectors and cellular pathways, spatially confined modules need to be effectively separated. This can occur through the action of the module-specific PDE (PDE1 or PDE2) or by a general cellular PDE that prevents the leakage of c-di-GMP into other compartments. **(D)** c-di-GMP can control the same biological process at different levels. For example, c-di-GMP can control gene expression (transcription and translation) or the activity of one of the resulting proteins. Expression and allosteric control can be mediated by the same module, comprising a DGC and PDE, or can be modulated independently by different DGC and PDE modules. c-di-GMP molecules are indicated as blue circles or as a spatial gradient in part C.

Alternatively, the spatial organization of DGCs and/or PDEs that interact directly with their respective targets, together with effective mechanisms that isolate individual signaling modules from each other, would permit parallel CDN signaling modules with highly specific readouts (**Figure 5C**). CDNs, such as c-di-GMP, control the expression, activity, stability, localization and interaction of specific proteins (see, for example, Refs. [85,110,117,163]). Moreover, c-di-GMP can control the same biological process at different levels, including transcriptional and translational control or allosteric control (**Figure 5D**; see, for example, Ref. [94]). Such a multilayered signaling architecture can impose tight control over strictly unidirectional cellular processes, such as cell cycle progression, or processes that have considerable metabolic cost, such as the motile–sessile switch. It also enables bacteria to rapidly sample the environment and adjust their behavior without the need for de novo protein synthesis. In addition, the c-di-GMP network could function to integrate two distinct processes but, at the same time, uncouple them if necessary through the use of distinct DGC–PDE modules (**Figure 5D**). An example of such a process is illustrated by the production of curli and cellulose in *E. coli* (see above). Finally, this signaling network could be used to define activity windows for specific cellular processes; for example, by the sequential control of gene expression (module 1) and inactivation of a downstream effector (module 2), which is either turned off by c-di-GMP or subject to c-di-GMP-mediated degradation.

Despite the advances in the field of CDN research, important questions remain to be addressed in the future. For example, are there additional CDNs to be included in this emerging signaling paradigm? Which cellular activities do specific CDN networks control and how extensively do these compounds interfere with basic cellular processes in bacteria? What are the important environmental input signals that control these regulatory systems? What is the exact architecture of CDN networks and how do they contribute to the highly dynamic behavior of bacterial cells? Finally, how are CDN-based networks integrated with other signaling networks, such as quorum sensing pathways, phosphorylation cascades or ppGpp-dependent pathways? It is safe to predict that this field of research will continue to provide exciting novel insights into bacterial signaling, growth and behavior. Future steps should include the development of tools to quantitatively describe CDN network dynamics. This will provide the basis for the mathematical description of these systems and eventually afford the predictive power to experimentally test and refine important network parameters. Moreover, the field has now advanced sufficiently to re-evaluate the therapeutic potential of CDNs. For example, agonists of the host receptor stimulator of interferon genes (STING) are currently being explored as candidate stimulants for anticancer immune activity [164]. Given that STING has been shown to bind to c-di-GMP and c-di-AMP (**Box 1**), similar approaches could be assessed as strategies for the treatment of bacterial infections [165,166].

Author contribution

Abstract, introduction, conclusion and chapter 'Role of c-di-GMP in bacterial virulence' were written by UJ. Chapters 'Makers and breakers', 'Motile-sessile transition and biofilm formation' were written by AR. Chapters 'C-di-GMP effectors', 'Development and morphogenesis' as well as box texts were written by CL. Figures were designed by AR. Figure legends were written by AR. For final submission, all texts were revised and edited by UJ.

Author information

Correspondence should be addressed to urs.jenal@unibas.ch.

Acknowledgements

The authors thank the reviewers for very constructive comments that have helped to improve both the accuracy and quality of the article from which this introduction was adapted. Work in the author's laboratory was supported by the Swiss National Science Foundation (grant 310030B_147090 to UJ) and by a European Research Council (ERC) Advanced Research Grant (322809 to UJ).

Chapter 2 | PROJECT 1

A novel capture compound for the identification and analysis of c-di-GMP binding proteins

Jutta Nesper[†], Alberto Reinders^{*}, Timo Glatter^{*}, Alexander Schmidt, Urs Jenal

^{*}equal contribution

[†]deceased November 15th, 2016

Adapted from:

‘A novel capture compound for the identification and analysis of
c-di-GMP binding proteins’

Journal of Proteomics | May 2012 | vol. 75, issue 15: 4874-4878

Technical note

Abstract

The second messenger cyclic di-GMP is a near-ubiquitous signaling molecule that globally alters bacterial cell physiology to promote biofilm formation and community behavior. Much progress was made in recent years towards the identification and characterization of diguanylate cyclases and phosphodiesterases, enzymes involved in the synthesis and degradation of this signaling compound. In contrast, our knowledge of the nature and mechanistic details of c-di-GMP effector proteins lags behind, primarily because effective tools for their specific enrichment and rapid analysis are missing. In this report, we demonstrate that a novel tri-functional c-di-GMP-specific Capture Compound (cdG-CC) can be effectively used to identify and validate c-di-GMP binding proteins. The cdG-CC was able to specifically and efficiently pull down bona fide c-di-GMP effector proteins. Furthermore, in combination with mass spectrometry (CCMS), this technology robustly identified a substantial fraction of the known c-di-GMP signaling components directly from cell extracts of different model organisms. Finally, we applied the CCMS technique to profile c-di-GMP binding proteins of *Pseudomonas aeruginosa* and *Salmonella enterica* serovar typhimurium. Our studies establish CCMS as a powerful and versatile tool to identify and analyze components of the cellular c-di-GMP pathway in a wide range of different organisms.

Technical note

Cyclic di-GMP is a ubiquitous second messenger regulating growth and behavior of a wide range of gram-positive and gram-negative bacteria. In particular, c-di-GMP mediates the switch between single cell behavior and a community lifestyle called biofilm, which is often associated with chronic infections of bacterial pathogens [167]. Major components of the regulatory network are the GGDEF, EAL, and HD-GYP domains that are widespread in bacteria and catalyze c-di-GMP synthesis and degradation, respectively [168]. The list of cellular processes controlled by c-di-GMP is ever-increasing and includes the biosynthesis and secretion of surface adhesins and exopolysaccharide (EPS) matrix components, different forms of cellular motility, long-term survival and response to environmental stress, synthesis of secondary metabolites, regulated proteolysis and cell cycle progression, delivery of anti-bacterial toxins, intracellular growth and the production of virulence factors in a range of animal and plant pathogens [82,168,169]. Despite of this wide variety of cellular functions that are modulated by c-di-GMP, the list of effector proteins has remained relatively sparse [82,168,169]. These include PilZ, small switch-like domains that undergo conformational change upon binding c-di-GMP. In addition, several members of the CRP/FNR and response regulator superfamilies of transcription regulators were shown to specifically bind c-di-GMP. Finally, a subgroup of GGDEF and EAL domains was recognized as c-di-GMP effector proteins adopting their novel functionality through the combined loss of catalytic activity and exploitation of their allosteric and active site binding pockets, respectively. While most known effector proteins were discovered through an “educated guess” approach that was based on their functional linkage to c-di-GMP mediated cellular processes, unbiased screening for novel effectors was hampered primarily by the lack of reliable and effective biochemical tools for their enrichment and isolation. Only one global recent study used a chemical proteomics approach to identify c-di-GMP binding proteins in *P. aeruginosa* [109]. Here we introduce a novel tri-functional capture molecule (cdGCC) as an effective tool to identify specific c-di-GMP binding proteins directly from a complex mixture of macromolecules. The compound is based on a chemical scaffold harboring specificity, reactivity, and sorting properties (**Figure 1A**) [170,171]. C-di-GMP provides the selectivity for capturing proteins. Upon UV irradiation, the photo-reactivity group forms a highly reactive nitrene [172] that interacts with proteins bound by the selectivity function, thereby forming an irreversible covalent crosslink. Biotin as sorting function then allows for the efficient and facile isolation of the captured proteins by binding of the compound to streptavidin coated magnetic beads.

These results encouraged us to probe if the capture compound can be applied for the selective enrichment of c-di-GMP binding proteins from a more complex mixture of proteins. To test this, we captured soluble c-di-GMP binding proteins from cell extracts and probed immunoblots with PopA specific antibodies. PopA is a GGDEF effector protein that regulates cell cycle progression in *C. crescentus* in response to a cellular upshift of c-di-GMP during the G1-S phase transition [88,114].

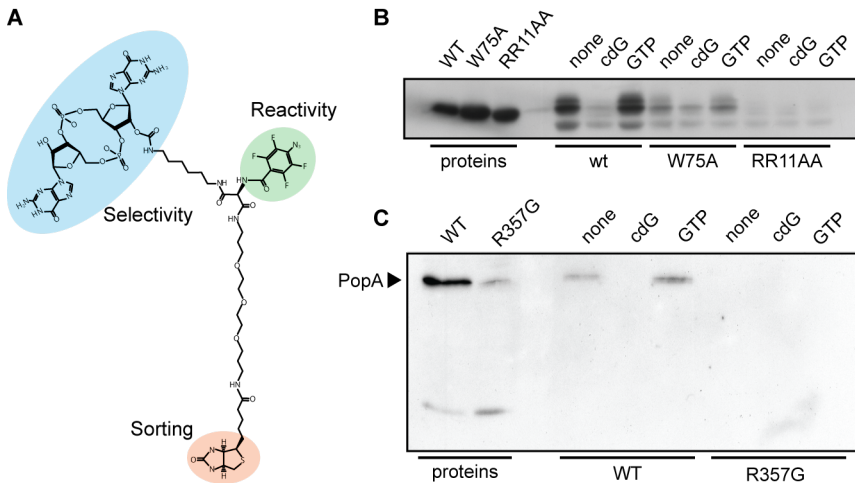


Figure 1 | The cdG-CC can specifically pull down bona fide c-di-GMP binding proteins from purified and from crude cell extracts. (A) Chemical structure of cdG-CC. **(B)** Immunoblot of purified and captured DgrA (wt), DgrA W75A and DgrA RR11AA. In all capture experiments 10 μ M cdG-CC was present, in competition experiments the proteins were preincubated with a 100x excess of c-di-GMP (cdG) or GTP. All proteins were His-tagged and detected using anti-His antibodies. **(C)** Immunoblot of PopA. PopA (wt) or the PopA I-site mutant R357G was expressed in NA1000 Δ popA (lanes marked with 'proteins'; note that this I-site mutant is less abundant in the cell). PopA was captured in the presence of 3 μ M cdG-CC. Addition of 1 mM c-di-GMP but not 1 mM GTP prevented the binding to the cdG-CC. In contrast the PopA I-site mutant could not be captured at all. PopA was detected using anti-PopA antibodies.

To bind c-di-GMP PopA utilizes a conserved and well-defined binding pocket, which, in related catalytic GGDEF domains, is used as an allosteric I-site for product inhibition of the diguanylate cyclase (DGC) activity [55,57]. As shown in **Figure 1C**, PopA with a known K_d for c-di-GMP of 2.5 μ M, was readily captured from *C. crescentus* cell lysates using 3 μ M cdG-CC and a total of 400 μ g soluble protein. Pull down of PopA was inhibited in the presence of a large excess of c-di-GMP (1 mM), while GTP did not interfere with cdG-CC binding (**Figure 1C**), arguing that the cdG-CC interaction with PopA is highly specific. Likewise, no PopA was bound to the cdG-CC when using a strain expressing a PopA mutant that lacks the highly conserved Arg residue of the canonical RxxD I-site binding motif (R357G) [88] (**Figure 1C**). This indicated that the cdG-CC can enrich c-di-GMP binding proteins directly from whole cell extracts in a highly specific manner and that this compound is suited for a global isolation procedure of c-di-GMP binding proteins. Therefore, we combined capture experiments with the analysis of isolated proteins by LC-MS/MS (CCMS, [170,171]). When applying 10, 5 or 2.5 μ M cdG-CC with 400 μ g of soluble *C. crescentus* proteins, nine of eleven proteins predicted to contain either a PilZ, GGDEF or EAL domain (**Table 1A & Table S1A**) were significantly enriched as compared to the competition control based on

the spectral counts of the identified peptides. In addition to the analysis of soluble proteins we also aimed at evaluating the efficiency of CCMS for the enrichment of c-di-GMP binding proteins from membrane fractions. Although the numbers of spectral counts were lower as compared to proteins from the soluble fraction, three of the five integral membrane proteins predicted to bind c-di-GMP were identified when 400 µg DDM solubilized membrane proteins and 10 µM cdG-CC were used for CCMS (Table 1A & Table S1A). Only four of the known components of the *C. crescentus* c-di-GMP network were not identified by CCMS. Two of these are integral membrane proteins with several predicted membrane-spanning domains in their N-terminal regions (CC0740, CC0896). It is possible that they were not solubilized by the detergent used or not detected by LC-MS/MS. Another possibility is that they are not expressed, as it might be the case for the not captured soluble proteins CC3094 and CC3148.

Table 1 – identified known c-di-GMP binding proteins.						
Protein name	ID	Domain architecture	CCMS experiment/CCMS competition ^a			
			No. spectral counts of identified peptides			
A) <i>C. crescentus</i>						
Soluble fraction			1	Experiment No. ^b		
PopA	CCNA_01918	GGDEF	20/1	25/3	3	
PleD	CCNA_02546	Rec-Rec-GGDEF	18/0	21/2	15/5	
DgcA	CCNA_03394	GGDEF	5/0	3/0	1/0	
DgcB	CCNA_01926	GGDEF	12/1	16/3	10/2	
CC0655	CCNA_00692	PAC-GGDEF-EAL	8/0	18/0	19/0	
CC1086	CCNA_01140	PAS-EAL	8/0	5/0	4/0	
PdeA	CCNA_03507	GGDEF-EAL	3/0	5/0	6/0	
DgrA	CCNA_01671	PilZ	5/0	6/3	6/1	
DgrB	CCNA_03268	PilZ		2/0		
Membrane fraction				Experiment No. ^c		
TipF	CCNA_00747	EAL	3/0	23/13		
PdeB	CCNA_00089	3x(MHYT)-PAS-GGDEF-EAL	3/0	6/0		
CC0857	CCNA_00900	CHASE4-GGDEF-EAL		2/0		
B) Soluble proteins of <i>P. aeruginosa</i>						
			1	2	3	Experiment No. ^d
FimX	PA4959	PAS-GDSIF-EVL	9/0	10/0	9/0	8/0
	PA3353	PilZ	5/0	6/0	6/0	10/0
WspR	PA3702	Rec-GGEF	2/0	2/0	2/0	
	PA0012	PilZ			2/0	1/0
	PA0169	GGEEF	2/0	2/0	2/0	
	PA4843	Rec-Rec-GGEF		2/0	2/0	5/0
	PA2989	PilZ	1/0	1/0	1/0	1/0
	PA0290	PAS-Rec-GGEF	1/0	2/0		2/0
	PA2567	GAF-SPTRF-EAL		1/0	1/0	1/0
	PA4608	PilZ	1/0	2/0	2/0	2/0
FleQ	PA1097	Rec-AAA-HTH	11/0	3/0	2/0	4/0

^a All competition experiments were performed in the presence of 1 mM c-di-GMP.
^b 3 independent experiments are indicated using 10, 5 or 2.5 µM cdG-CC respectively.
^c 2 independent experiments are indicated using 10 µM cdG-CC.
^d Experiment 1 was performed with 10 µM cdG-CC, experiment 2 with 7.5 µM cdG-CC, experiment 3 with 2.5 µM cdG-CC, experiment 4 with 2.5 µM cdG-CC and experiment 5 with 1.25 µM cdG-CC.

To expand these studies to a different organism, we attempted to identify known c-di-GMP binding proteins from *P. aeruginosa* PA01. With 42 GGDEF and EAL domain proteins, eight PilZ domain proteins,

two HD-GYP domain proteins, and the transcriptional regulator FleQ that was shown to bind c-di-GMP [173], the complexity of the c-di-GMP signaling network in this organism is much higher than in *C. crescentus*. Using 10 μM , 7.5 μM , 5 μM , 2.5 μM and 1.25 μM cdG-CC and 350 μg of soluble protein extract, 11 of these proteins were unambiguously identified by CCMS (**Table 1B & Table S1B**). This includes four PilZ domain proteins, four GGDEF, two composite GGDEF-EAL domain proteins and FleQ. The fraction of potential c-di-GMP binders from *P. aeruginosa* isolated by CCMS is substantially lower (11 of 33 predicted soluble proteins) as compared to *C. crescentus* but is comparable to a recent study using sepharose-coupled c-di-GMP to pull down c-di-GMP binding proteins [109]. That study identified 14 of the soluble and three of the membrane anchored proteins known or predicted to bind c-di-GMP. Six of these proteins were identified in both studies, including the PilZ domain proteins PA0012, PA2989, PA3353, and PA4908, the GGDEF domain protein PA3702 and FleQ. In addition to known or predicted c-di-GMP binding proteins we identified 54 novel putative c-di-GMP binding proteins in at least two of five independent CCMS experiments performed with 7.5 μM cdG-CC (**Table S3**). The identified proteins were classified according to their annotated function (www.pseudomonas.com) [174] (**Figure S1**). The largest group of identified proteins is of unknown function (30.4%). The others are annotated as being involved in amino acid biosynthesis and metabolism (16.1%), energy metabolism (12.5%), nucleotide biosynthesis and metabolism (8.9%), chemotaxis (7.1%), polysaccharide biosynthesis (3.6%) and some additional pathways. Düvel et al. [109] have reported 140 novel putative c-di-GMP binding proteins. Interestingly, only five proteins (PA1458, PA3348, PA3801, PA4310, and PA4489) were identified in both approaches indicating that the different compounds used for the experiments might be specific for a certain subset of proteins. Alternatively, it is possible that one or both methods generate a set of false positives e.g. by pulling out intact protein complexes containing only one specific effector. Clearly, target validation with alternative techniques is required to confirm bona fide c-di-GMP binding proteins.

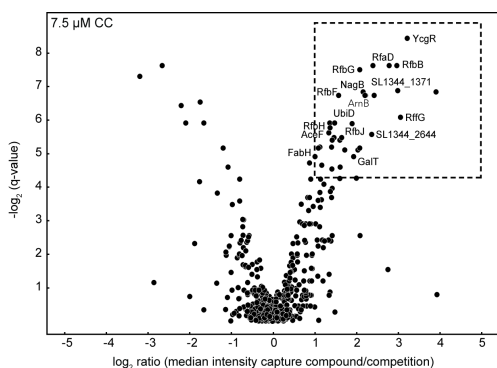


Figure 2 | Volcano plot based visualization of proteins significantly enriched by CCMS of *S. typhimurium*. Following capturing, LC-MS/MS analysis and label-free quantification, log₂-intensity ratio of all detected peptide features between capturing and competition experiment were calculated and plotted versus values derived from significance analysis. Proteins within the significance thresholds for q-values <0.05 and intensity ratios >2-fold are indicated in a box. Experiments in triplicate were performed in the presence of 7.5 μM cdG-CC and with 1 mM c-di-GMP added to the competition reactions.

To expand our analysis, we included *S. typhimurium* in our cdG-CC based CCMS experiments. This organism was chosen to perform an unbiased CCMS experiment because its c-di-GMP network appears to be of lower complexity as compared to other bacterial species [175]. In contrast to the CCMS experiments with *C. crescentus* and *P. aeruginosa*, in which spectral counts were extracted for known c-di-GMP binders, we tested whether CCMS is capable to enrich for c-di-GMP binding proteins upon MS1 label-free quantification. CCMS experiments were performed in triplicates with 350 µg soluble whole cell proteins using 7.5 µM cdG-CC and competition controls with an excess of c-di-GMP (1 mM) (**Table S2A**). Following mass spectrometry analysis and label-free quantification (**Table S2B**) significant differences in protein enrichment between cdG-CC experiments and control samples with competing c-di-GMP were visualized in a volcano plot. The graph shows a significant enrichment (>2 fold) of 36 proteins as compared to the control with a q-value <0.05 (**Table S2C & Figure 2**). Among the enriched proteins is the PilZ domain protein YcgR (**Fig. 2**) [176]. Many of the identified components that were not previously associated with the c-di-GMP network were metabolic proteins and proteins involved in fatty acid and LPS biosynthesis (**Figure 2**). Such proteins might be of interest in the light of switching between a virulent planktonic and a surface attached persistent lifestyle. However, since some of these proteins might be allosterically regulated by other nucleotides, they first need to be validated regarding a specific c-di-GMP binding. Similarly, other potential non-specific binders might be highly abundant proteins, such as five tRNA-related proteins or the chaperone GroEL (**Table S2C**).

In this study, we demonstrate that the novel c-di-GMP specific Capture Compound is a powerful tool to validate known c-di-GMP effectors and to identify novel c-di-GMP binding proteins. Through the use of a photo-reactivity group that forms a covalent bond between the cdG-CC and captured proteins stringent wash conditions can be applied to increase the specificity. Moreover, this feature allows capturing of low affinity binders and low abundant proteins and reduces the probability to pull-out entire protein complexes. Our CCMS experiments with *S. enterica* and *P. aeruginosa* identified a broad range of putative c-di-GMP binding proteins belonging to different classes and biological pathways that will give further insights into the complex c-di-GMP signaling network in these organisms.

Author contribution

JN established CCMS protocol and conduction validation experiments. CCMS experiments with *C. crescentus* were performed by JN. AR performed CCMS experiments with *P. aeruginosa* and *S. typhimurium*. Mass-spectrometry experiments were conducted by TG and AS. JN, AR, TG and UJ analyzed the data. JN, AR, TG and UJ wrote the paper.

Author information

Correspondence should be addressed to urs.jenal@unibas.ch.

Supplemental material

Supplemental materials Figure S1, Table S1, S2 & S3 are available in the online version of the publication.

Acknowledgements

We thank Samuel Steiner for help in optimization of Capture Compound binding assays. We also thank Benoît-Joseph Laventie for the annotation of *P. aeruginosa* proteins. This work was supported by the Swiss National Science Foundation (SNF) Sinergia grant CRSII3_127422.

Materials & Methods

Bacterial strains and growth conditions

C. crescentus NA1000 was grown in peptone yeast extract (PYE). Strain UJ2827 (NA1000 Δ popA) containing either plasmid pAD38 expressing wild-type popA or plasmid pAD39 expressing popA (R357G) [88] was grown in PYE containing 2.5 mg/ml tetracycline. *P. aeruginosa* PA01 and *S. typhimurium* SL1344 were grown in LB.

Protein expression and purification

His-tagged DgrA wild-type and mutants DgrAW75A and DgrARR11AA were expressed in *E. coli* BL21DE3 (Novagen) from plasmids pET42b::dgrA, pET42b::dgrA (W75A) or pET42b::dgrA (RR11AA) and purified as described [177]. The proteins were dialyzed against PBS containing 1 mM DTT.

Protein analysis and c-di-GMP production

Proteins were separated by SDS-PAGE and detected by immunoblot analysis. His-tagged DgrA was visualized using anti-His antibodies (Qiagen) and horseradish conjugated rabbit anti-mouse antibodies (Dako). PopA was visualized using anti-PopA antibodies [88] and horseradish conjugated swine anti rabbit antibodies (Dako). Protein concentrations were determined either with Bradford assays or by measuring absorption at 280 nM with a NanoDrop device (Thermo Scientific). C-di-GMP was synthesized and purified as described in [178].

Extract preparation for CCMS experiments

C. crescentus cells were grown in PYE and *P. aeruginosa* and *S. typhimurium* in LB to mid logarithmic phase and pelleted by centrifugation for 20 min at 5'000 x g. The pellet was resuspended in lysis buffer (6.7 mM MES, 6.7 mM HEPES, 200 mM NaCl, 6.7 mM KAc, pH 7.5 and, for *P. aeruginosa* and *S. typhimurium*, 10 mM β -mercaptoethanol) and protease inhibitor (complete mini, EDTA-free, Roche) as well as DNaseI (Roche) was added. Cells were lysed by passing it 3 x at 20'000 psi through a French pressure cell. After centrifugation at 100'000 x g for 1 h the supernatant was used directly for CCMS experiments of soluble proteins. The lysates of *P. aeruginosa* and *S. typhimurium* were additionally passed through a PD10 (GE healthcare) to remove nucleotides.

After centrifugation at 100'000 g the pellet was washed once in lysis buffer and resuspended in the same buffer before n-dodecyl- β -D-maltopyranoside (DDM, Anatrace) was added to a final concentration of 1 %, and incubated for 1 hour at 4°C with gentle agitation on a rotary wheel. After centrifugation at 100'000x g for 1 hour the supernatant was used directly for CCMS experiments of membrane proteins.

Capturing of c-di-GMP binding proteins

The capture experiments were essentially carried out as described for other Capture Compounds [179,180] but were optimized for the cdG-CC using known c-di-GMP proteins as positive controls. All experiments were performed in 200 μ L 12-tube PCR strips (Thermo Scientific). 400 μ g of the soluble protein fractions (350 μ g for *P. aeruginosa* and *S. typhimurium*) were mixed with the indicated amounts of cdG-CC (Caprotec Bioanalytics GmbH, Berlin) and with 20 μ L 5x capture buffer (100 mM HEPES, 250 mM KAc, 50 mM MgAc, 50 % glycerol, pH 7.5). The volume was adjusted with H₂O to 100 μ L and incubated for 2 h at 4°C in the dark on a rotary wheel. The reaction was then UV irradiated for 4 min using a caproBox (Caprotec Bioanalytics GmbH, Berlin). 50 μ L magnetic streptavidin beads (Dynabeads MyOne Streptavidin C1, Invitrogen) and 25 μ L 5x wash buffer (250 mM Tris pH 7.5, 5 M NaCl, 0.1 % n-octyl- β -glucopyranoside (β -OG)) were added and the mixture was incubated for 45 min at 4°C on a rotary wheel. The beads were then collected with a magnet (caproMag, Caprotec Bioanalytics GmbH, Berlin) and washed 6 times with 200 μ L 1x wash buffer. For immunoblot analysis the beads were resuspended in 25 μ L sample buffer and loaded on a SDS polyacrylamide gel. For LC-MS/MS analyses the beads were prepared directly for digestion (see below). In control experiments run in parallel, c-di-GMP or GTP was added to protein extracts up to a final concentration of 1 mM and incubated for 30 min at 4°C on a rotary wheel before the cdG-CC was added.

Capturing of membrane proteins was performed with the following modifications: The capture mixture was incubated overnight at 4°C instead of 2 h; β -OG was replaced in the wash buffers with 0.1 % DDM for the first six washing steps; the magnetic beads were treated by two additional washing steps with buffer containing 0.05 % DDM and by one additional washing step with buffer containing 0.025 % DDM. Capture experiments with purified proteins were performed in the presence of 0.5 μ M protein and were incubated with the cdG-CC for one hour. Control experiments were carried out in the presence of a 100-fold excess of c-di-GMP or GTP as compared to the cdG-CC concentration.

Tryptic digest of proteins for MS analysis

Magnetic beads with captured soluble proteins were washed 1x with 200 μ L H₂O, 6 times with 80 % acetonitrile and 2 times with H₂O and then resuspended in 20 μ L 100 mM ammonium bicarbonate. 0.5 μ L 200 mM TCEP (sulfhydryl reductant tris[2-carboxyethyl]-phosphine) was added and the beads were incubated for 1 h at 60°C. After addition of 0.5 μ L 400 mM iodoacetamide and incubation for 30 min at 25°C in the dark, 0.5 μ L 500 mM N-acetyl cysteine was added and the beads were further incubated for 10 min at 25°C. Finally, 1 μ g porcine trypsin (Promega) was added and the solution incubated for 16 h at 37°C.

Membrane proteins coupled to streptavidin coated magnetic beads were treated as follows. The beads were washed 3 times with 100 mM ammonium bicarbonate containing 2M urea. The beads were then resuspended in 20 μ L 100 mM ammonium bicarbonate, 8 M urea. TCEP, iodoacetamide and N-acetyl cysteine were added to the same amounts as indicated for the soluble proteins and the beads were incubated as outlined for soluble proteins. 1 μ g of endoproteinase Lys-C (Wako) was added and the

solution was incubated for 16 h at 37°C. Following the addition of 80 µl 100 mM ammonium bicarbonate, 1 µg porcine trypsin was added and incubated for 6 h at 37°C.

For soluble and membrane proteins the beads were removed and the peptides were purified using C18 Microspin columns (Harvard Apparatus) and dried in a speed vac.

LC-MS/MS analysis

LC-MS/MS analyses were performed on a dual pressure LTQ-Orbitrap Velos mass spectrometer, which was connected to an electrospray ion source (both Thermo Scientific). Peptide separation was carried out using an easy nano-LC systems (Thermo Scientific) equipped with a RP-HPLC column (75 µm x 15 cm) packed with C18 resin (Magic C18 AQ 3 µm; Michrom BioResources) using a linear gradient from 96 % solvent A (0.15 % formic acid, 2 % acetonitrile) and 4 % solvent B (98 % acetonitrile, 0.15 % formic acid) to 35 % solvent B over 40 minutes at a flow rate of 0.3 µL/min. The data acquisition mode was set to obtain one high resolution MS scan in the FT part of the mass spectrometer at a resolution of 60,000 FWHM followed by MS/MS scans in the linear ion trap of the 20 most intense ions. To increase the efficiency of MS/MS attempts, the charged state screening modus was enabled to exclude unassigned and singly charges ions.

Collusion induced dissociation was triggered when the precursor exceeded 100 ion counts. The dynamic exclusion duration was set to 15 sec. The ion accumulation time was set to 300 ms (MS) and 50 ms (MS/MS).

Database search and label-free quantification

Mass spectrometry raw spectra were converted into mascot generic files (mgf) and searched with MASCOT version 2.3. *C. crescentus* and *S. typhimurium* uniprot/tremble databases were downloaded via the European Bioinformatics Institute (EBI, <http://www.ebi.ac.uk/>) and *P. aeruginosa* NCBI-database was downloaded via the NCBI homepage (<http://www.ncbi.nlm.nih.gov/>).

In silico trypsin digestion was performed after lysine and arginine (unless followed by proline) tolerating two missed cleavages in fully tryptic peptides. Database search parameters were set to allow oxidized methionines (+15.99491 Da) as variable modifications and carboxyamidomethylation (+57.021464 Da) of cysteine residues as fixed modification. For MASCOT searches using high-resolution scans the precursor mass tolerance was set to 15 ppm. and the fragment mass tolerance was set to 0.6 Da. The protein FDR was set to 1 %.

Mascot searches of *C. crescentus* and *P. aeruginosa* CCMS experiments were imported into Scaffold (Proteomesoftware, Version 3), which was used to extract spectral count.

For label-free quantification the files were imported into Progenesis LC-MS software (Nonlinear Dynamics, Version 4.0). Data in .mgf format were exported directly from Progenesis LC-MS and MS/MS spectra were searched using the MASCOT against a decoy database of the predicted proteome from *S. typhimurium*. Search parameters were the same as described above. Results from the database search were imported into Progenesis LC-MS, mapping peptide identifications to MS1 features. The peak areas

of all MS1 features annotated with the same peptide sequence were summed, per LC-MS run. Next, peptide area ratios between samples with cdG-CC and competing cdG as well as accompanying q-values (i.e. p-values adjusted for multiple testing) were calculated using an in-house developed R script (available upon request) employing the Limma package [181] of BioConductor. As ribosomal proteins are common contaminations using enrichment matrices, those proteins were not considered for quantitative analysis.

Chapter 3 | PROJECT 2

Expression and genetic activation of c-di-GMP-specific phosphodiesterases in *Escherichia coli*

Alberto Reinders, Chee-Seng Hee, Adam Mazur, Shogo Ozaki, Tilman Schirmer and Urs Jenal
*deceased November 27th, 2012

Adapted from:
'Expression and genetic activation of c-di-GMP-specific phosphodiesterases in *Escherichia coli*'
Journal of Bacteriology | November 2015 | vol. 198, issue 3: 448-462

Abstract

Intracellular levels of the bacterial second messenger cyclic di-GMP (c-di-GMP) are controlled by antagonistic activities of diguanylate cyclases and phosphodiesterases. The phosphodiesterase PdeH was identified as a key regulator of motility in *Escherichia coli*, while deletions of any of the other 12 genes encoding potential phosphodiesterases did not interfere with motility. To analyze the roles of *E. coli* phosphodiesterases, we demonstrated that most of these proteins are expressed under laboratory conditions. We next isolated suppressor mutations in six phosphodiesterase genes, which reinstate motility in the absence of PdeH by reducing cellular levels of c-di-GMP. Expression of all mutant alleles also led to a reduction of biofilm formation. Thus, all of these proteins are *bona fide* phosphodiesterases that are capable of interfering with different c-di-GMP-responsive output systems by affecting the global c-di-GMP pool. This argues that *E. coli* possesses several phosphodiesterases that are inactive under laboratory conditions because they lack appropriate input signals. Finally, one of these phosphodiesterases, PdeL, was studied in more detail. We demonstrated that this protein acts as a transcription factor to control its own expression. Motile suppressor alleles led to a strong increase of PdeL activity and elevated *pdeL* transcription, suggesting that enzymatic activity and transcriptional control are coupled. In agreement with this, we showed that overall cellular levels of c-di-GMP control *pdeL* transcription and that this control depends on PdeL itself. We thus propose that PdeL acts both as an enzyme and as a c-di-GMP sensor to couple transcriptional activity to the c-di-GMP status of the cell.

Importance

Most bacteria possess multiple diguanylate cyclases and phosphodiesterases. Genetic studies have proposed that these enzymes show signaling specificity by contributing to distinct cellular processes without much cross talk. Thus, spatial separation of individual c-di-GMP signaling units was postulated. However, since most cyclases and phosphodiesterases harbor N-terminal signal input domains, it is equally possible that most of these enzymes lack their activating signals under laboratory conditions, thereby simulating signaling specificity on a genetic level. We demonstrate that a subset of *E. coli* phosphodiesterases can be activated genetically to affect the global c-di-GMP pool and thus influence different c-di-GMP-dependent processes. Although this does not exclude spatial confinement of individual phosphodiesterases, this study emphasizes the importance of environmental signals for activation of phosphodiesterases.

Introduction

The second messenger cyclic di-GMP (c-di-GMP) is a nearly ubiquitous small signaling molecule which greatly affects bacterial growth and behavior. In particular, c-di-GMP controls important cellular and behavioral processes in a wide range of bacteria, including motility and chemotaxis, surface colonization and the formation of communities, virulence and persistence, and cell cycle progression (for reviews, see references [7,54,161]). The key enzymes involved in c-di-GMP metabolism are diguanylate cyclases (DGCs) [8] and phosphodiesterases (PDEs) [182]. Together, DGCs and PDEs constitute one of the largest families of bacterial signaling proteins, with tens of thousands of members currently deposited in the protein databases. Contributing to an explanation for this enormous multiplicity and diversity is the observation that most bacteria contain multiple representatives, often a few tens, of these proteins [7]. For example, the genomes of *Escherichia coli* K-12 strains contain genes encoding a total of 29 proteins harboring a GGDEF and/or EAL domain, the catalytic units of DGC and PDE enzyme activities, respectively [183]. Moreover, throughout evolution, many of the formerly catalytic members of this family seem to have adopted novel functionalities as c-di-GMP effector proteins [88,117,184-186] or as protein interaction platforms that have lost the connection to their original effector altogether [162].

This caused some confusion in the field in the early years and raised the question of why bacteria evolved multiple DGCs and PDEs to control a small signaling molecule that likely shows rapid diffusion within bacterial cells, thereby providing limited options for signaling specificity. One possible explanation for this phenomenon is that individual representatives are expressed under specific environmental conditions or are specialized for specific cellular tasks which normally are kept separate from each other in either time or space [54]. In the case of temporal sequestration, one would expect that only a subset of these enzymes is expressed at any given time or environmental situation. The other possibility is that cells express and display multiple members of this enzyme family to be able to rapidly respond to a diverse range of signaling inputs. In this case, one would expect that most or possibly all enzymes are expressed at any given time but that the majority of them are not active due to the absence of an input signal. In the past few years, the amount of information about biochemical and structural characteristics of DGCs and PDEs has increased rapidly [5,58,61,187]. Despite such rapid progress, *in vivo* results often remain controversial. Considering that specific components of this signaling network might not be expressed or might not receive the appropriate stimuli to be active, genetic studies relying solely on mutant phenotypes will not give conclusive answers.

Here we address these questions by analyzing the expression and activities of multiple PDEs in *E. coli* K-12. This organism has a total of 16 EAL domain proteins, only 3 of which show obvious degeneration of consensus amino acid motifs required for catalytic activity (**Figure 1A & B**). Among the other 13 proteins, only 7 have been characterized in detail and identified as PDEs [72,80,188-192]. The functions of the other members of this family that potentially are able to catalyze c-di-GMP hydrolysis remain unclear. To identify additional candidate PDEs, we made use of a genetic approach by sequentially isolating activating gain-of-function mutations in specific members of the EAL domain proteins. Our analysis is

based on some recent reports demonstrating that PdeH (YhjH), a highly active PDE that globally controls c-di-GMP levels in *E. coli*, is primarily responsible for motility control in this organism [78,188,193]. The *pdeH* gene is coregulated with flagellar genes, and mutants lacking PdeH show increased c-di-GMP levels and poor motility. PdeH licenses flagellar motility in the exponential and early postexponential phases by keeping c-di-GMP levels low. Upon entry into stationary phase, c-di-GMP levels increase partially due to FlhDC-dependent downregulation of *pdeH* [142], leading to activation of the c-di-GMP effector protein YcgR, which interacts with the flagellar motor to curb its activity [78,130]. Thus, in growing *E. coli* cells, PdeH has a central role in maintaining cell motility by keeping the cellular concentration of c-di-GMP below a threshold level that is able to activate YcgR. The observation that *pdeH* mutants showed poor motility also suggested that under these conditions, no other PDE was expressed or active (enough) to functionally substitute for this PDE. We thus hypothesized that mutations activating any of the other PDEs would be able to restore the motility of the *pdeH* mutant. If so, this would then allow us to identify silent PDEs by genetically uncoupling their activities from the unknown signals that are normally required for their activation. We present genetic and biochemical evidence that a large fraction of the remaining potential PDEs can indeed be activated genetically to substitute for the function of PdeH. This argues in favor of the idea that these proteins are *bona fide* PDEs that are able to interfere with the general cellular pool of c-di-GMP and that, under laboratory conditions, these proteins lack the appropriate signal(s) to become active.

Please note that throughout this report we use the systematic nomenclature for *E. coli* DGCs and PDEs that was recently proposed by Hengge et al. [77]. To make it easier for the expert reader to adopt the new nomenclature, the corresponding traditional designations are listed in **Figure 1A** and are highlighted in parentheses in the text.

Results

Expression of PDEs in growing *E. coli* cells

High levels of c-di-GMP generally obstruct flagellar motility in various microbes [78,130,142]. As a consequence, PDEs play key roles in regulating cell motility [106,114]. In *E. coli*, the PDE PdeH appears to be the sole contributor to the maintenance of cell motility under laboratory conditions [78]. This is surprising since the genomes of *E. coli* K-12 strains encode more than a dozen additional potential PDEs [77]. One possibility is that most of these components are not expressed during growth under these conditions. Previous studies used microarrays and β -galactosidase reporter assays to demonstrate that, with the exception of *pdeF* (*yfgF*) and *pdeG* (*ycgG*), all genes encoding potential PDEs are actively transcribed [194,195]. To confirm this and to demonstrate that active transcription indeed results in the production of PDEs, chromosomal 3xFlag-tagged constructs were engineered for all potential *pde* genes in the *E. coli* strain MG1655. These were introduced into the wild type and a *pdeH* mutant background, and protein levels were monitored in exponentially growing cells (OD₆₀₀ of 0.5 to 0.8). As shown in **Figure 1C**, most PDEs were readily detected. The only exceptions were PdeF and PdeG, the latter of which was present at low levels in the wild-type background but absent in the *pdeH* strain. This confirmed previous results and indicated that these proteins failed to contribute to cell motility as a result of a lack of expression under these conditions. Rather, most of these PDEs may be present in the cell at high enough concentrations but may not interfere with motility control because of a lack of enzyme activity.

Motile suppressor mutants of a *pdeH* mutant identify activating mutations in alternative PDEs

A *pdeH* mutant is unable to swim effectively toward higher nutrient concentrations in motility plates. To isolate spontaneous motile suppressor mutants, the *pdeH* mutant was inoculated onto the center of motility plates and incubated for an extended period, until visible “flares” were arising and spreading on the plates (**Figure 2A**). It was shown previously that mutations in the gene encoding the motility regulator YcgR can restore motility under these conditions [78]. Likewise, mutations in several genes encoding DGCs required for YcgR activation alleviate the motility block. We reasoned that activating mutations in “alternative” PDEs could also restore motility by countering high levels of c-di-GMP in the *pdeH* mutant. In order to enrich for such rare *pde* gain-of-function mutations, we first designed a tailored screening strain that reduced the likelihood of isolating mutations in known components of c-di-GMP-mediated motility control. To reduce the frequency of loss-of-function mutations in *ycgR*, a second chromosomal copy of *ycgR* was introduced into the *pdeH* screening strain. In addition, the screening strain was equipped with a plasmid carrying a copy of *wspR*, the gene encoding the diguanylate cyclase WspR from *Pseudomonas fluorescens*. Expression of *wspR* from the P_{lac} promoter maintains a threshold level of c-di-GMP that prevents motility even if one of the four active native DGCs is inactivated.

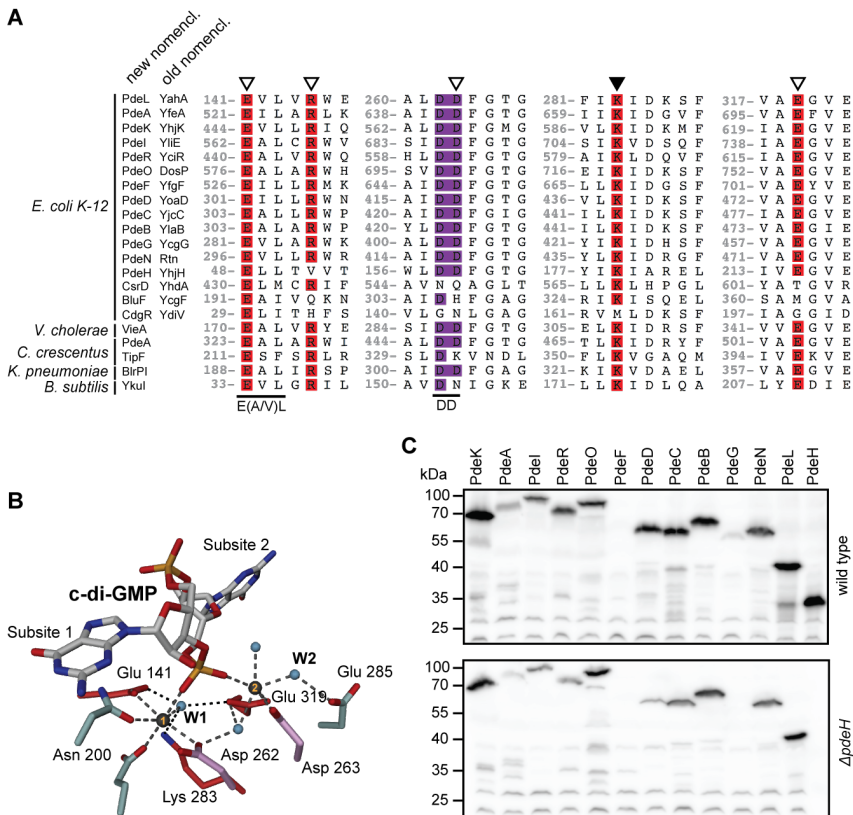


Figure 1 | Conservation of c-di-GMP-specific phosphodiesterases. (A) ClustalW alignment of PdeL with endogenous and exogenous phosphodiesterases and noncatalytic EAL domains. Regions containing residues involved in substrate binding (open triangles) and catalysis (closed triangle) are highlighted. Amino acid numbering refers to the numbering for PdeL. The double-aspartic-acid motif (DD) is displayed in purple, in analogy to panel B. **(B)** Atomic organization of the catalytic site of a PdeL monomer. The two essential metals are displayed as gray spheres. Conserved residues involved in metal coordination or catalysis are displayed in red. The double-aspartic-acid motif (Asp262 and Asp263; shown in purple) is involved in metal ion coordination as well as coordination of the catalytic water (small blue spheres). The same is true for the glutamic acid at position E141, which is part of the conserved E(A/V)L motif. **(C)** Immunoblot analysis of PDEs in *E. coli* wild-type and *pdeH* mutant strains. PDEs were tagged at their C-termini with a 3xFlag-tag and were analyzed with an anti-Flag antibody. Cells were grown in tryptone broth (TB) at 37°C and harvested at an OD₆₀₀ of 0.5–0.8. Note that in both strain backgrounds, all *pde* genes were expressed, with the exception of *pdeF*. PdeG levels were low in the wild type, and the protein seemed to be absent in the *ΔpdeH* mutant.

With this strain, a continuous genetic forward screen was set up. First, activating mutations in one of the *pde* genes were isolated from a pool of spontaneous suppressor mutants. A kanamycin resistance cassette was introduced next to the corresponding *pde* gene on the chromosome. Suppressor mutations linked to this marker were then identified by cotransduction into a clean *pdeH* background and by subsequent sequencing of the neighboring DNA regions. Second, the *pde* gene for which motility suppressor mutants were isolated was deleted from the chromosome. With the resulting mutant strain, a new round of selection for motile suppressor mutants was initiated to isolate mutations in one of the remaining *pde* genes. Successive rounds of selection resulted in the isolation of a total of 16 suppressor mutations in six individual PDEs (**Figure 2B & C**). Closer examination revealed gene fusion events in both *pdeB* and *pdeC*. In the case of *pdeB*, a 5,846-bp deletion between two direct repeats (TTGATGTCATT) resulted in an in-frame fusion of *pdeB* with its upstream gene, *acrB*, encoding a subunit of the Acr multidrug efflux pump. The resulting protein was fused at amino acid 205 of AcrB and position 168 of PdeB, giving rise to a fusion protein of a size similar to that of PdeB. As shown in **Figure 3A**, the overall level of the resulting fusion protein was strongly increased compared to that of the PdeB wild type. This increase likely resulted from the direct coupling of the truncated *pdeB* gene with the promoter of the *acr* operon. We reasoned that motility suppression results either from strong overexpression or from uncoupling of the respective catalytic domain of PdeB from its N-terminal regulatory region. Similarly, an IS element (*ins* mobile element) inserted into the promoter region of *pdeC* (28 bp upstream of the putative transcriptional start site of *pdeC*). As in the case of PdeB, this resulted in a strong upregulation of the overall level of PdeC (**Figure 3B**), indicating a suppression mechanism similar to that described above. Mutations resulting in single amino acid substitutions were identified in *pdeL*, *pdeA*, *pdeI*, and *pdeN*, arguing that the encoded proteins can be activated genetically (**Fig. 2C**). While substitutions in the *pdeA*-, *pdeI*-, and *pdeN*-encoded proteins localized to the EAL domain, to transmembrane regions, or to uncharacterized regions of the protein neighboring the EAL domain, mutations in the *pdeL*-encoded protein localized exclusively within the catalytic domain. This is in line with the observation that the soluble PdeL protein lacks a potential signal input domain and instead harbors a LuxR-type DNA binding domain. Levels of PdeA, PdeI, and PdeN proteins harboring suppressor mutations were unaltered compared to that of the wild type. Also, the cellular concentrations of these enzymes were similar in strains with different levels of c-di-GMP (**Figure 3C-E & 4**). In contrast, levels of several PDEs were different in *E. coli* wild-type, *pdeH*, and *csrA* mutant strains, indicating that their expression might be regulated by c-di-GMP itself (**Figure 3B & F**). In line with this, a subset of the isolated PdeL suppressors revealed higher PdeL protein levels in all genetic backgrounds tested (**Figure 3F**). This was not due to increased protein stability, as suppressor variants and wild-type PdeL showed very similar stabilities upon translation inhibition (**Figure S1**). Together with the finding that all mutations in PdeL mapped to the catalytic domain, this suggested that *pdeL* expression is autoregulated and possibly controlled by the overall cellular level of c-di-GMP. Together, these results indicate that *E. coli* possesses several PDEs that under normal conditions do not contribute to motility control but can be activated genetically to substitute for the role of the primary cellular PDE, PdeH.

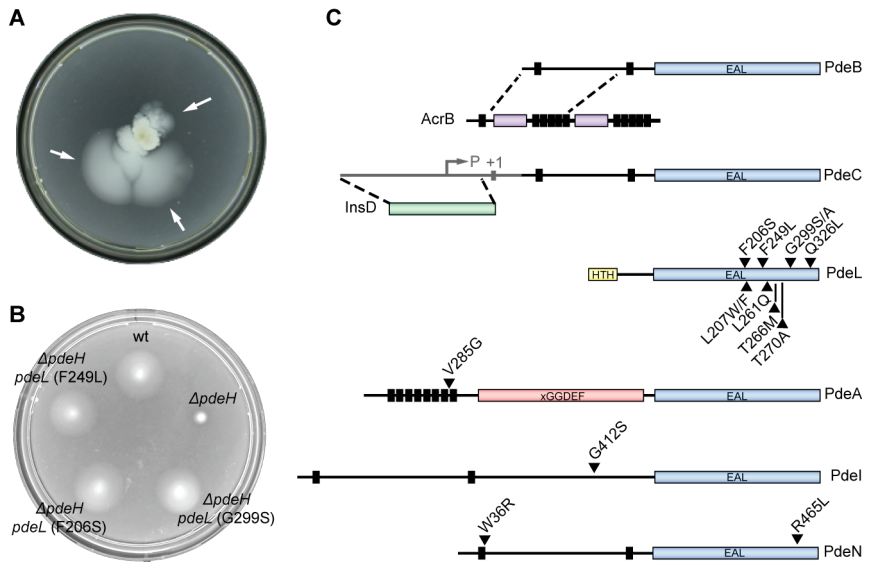


Figure 2 | Isolation of alleles activating *E. coli* phosphodiesterases. (A) Selection for motile suppressor mutants of a non-motile *pdeH* mutant strain on a low- percentage agar plate. Independent suppressors were recovered from motile flares (arrows) after incubation on motility plates for several days at 37°C. (B) Mutations in *pdeL* restore the motility of a *pdeH* mutant. Mutant alleles of *pdeL* are indicated. Motility was examined as described for panel a. wt, wild type. (C) Graphical representation of isolated *pde* suppressor variants. Vertical black bars represent transmembrane helices, c-di-GMP-specific phosphodiesterase do- mains (EAL) are depicted in blue, the LuxR-like DNA binding domain of PdeL is shown in yellow (HTH), and the degenerate cyclase domain (xGGDEF) of PdeA is shown in red. The positions of single amino acid substitutions are marked with black triangles.

Pde suppressor alleles restore motility by reducing intracellular c-di-GMP levels

High levels of c-di-GMP interfere with flagellar motility via the YcgR effector protein. To demonstrate that the *pde* suppressor alleles do indeed reinstate the flagellar motor behavior of a *pdeH* mutant by reducing levels of c-di-GMP, both single-cell trajectories and c-di-GMP concentrations were recorded for a selection of the isolated mutants. Dark-field microscopy tracking and subsequent computational analysis of the recorded trajectories determined the behavior of swimming bacteria. Measured trajectories of an exponentially growing *pdeH* strain revealed swimming velocities of 3.4 to 6.1 $\mu\text{m/s}$ (median, 4.1 $\mu\text{m/s}$), whereas a *pdeH* strain displayed velocities of 6.0 to 12.2 $\mu\text{m/s}$ (median, 8.9 $\mu\text{m/s}$) (Figure 4). Importantly, swimming velocities of all motile suppressor mutants were significantly higher than that of their isogenic *pdeH* strain and were similar to velocities measured for the wild type. To complement these single cell measurements, cellular c-di-GMP concentrations in cell populations of the

same strains were quantified using LC-MS/MS technology [99]. In accordance with earlier observations [78], levels of c-di-GMP were increased 10-fold in the *pdeH* mutant (3.5 μ M) compared to the wild type (0.31 μ M). Importantly, all strains harboring mutations in PDEs showed a significant reduction of the intracellular c-di-GMP pool compared to their isogenic *pdeH* mutant strain. While the reduction of c-di-GMP was moderate in some suppressor mutants, c-di-GMP levels were reduced to levels comparable to that of the wild type or, for one mutant, even below the detection limit (**Figure 4**). Importantly, we observed a strong overall correlation between the reduction of the intracellular c-di-GMP levels and the measured swimming velocities (**Figure 4**).

Together, these findings support the notion that the *pde* suppressor alleles increase the level and/or enzymatic activity of their respective PDE products, lowering the cellular concentration of c-di-GMP in the original *pdeH* mutant and thereby restoring flagellar motor function.

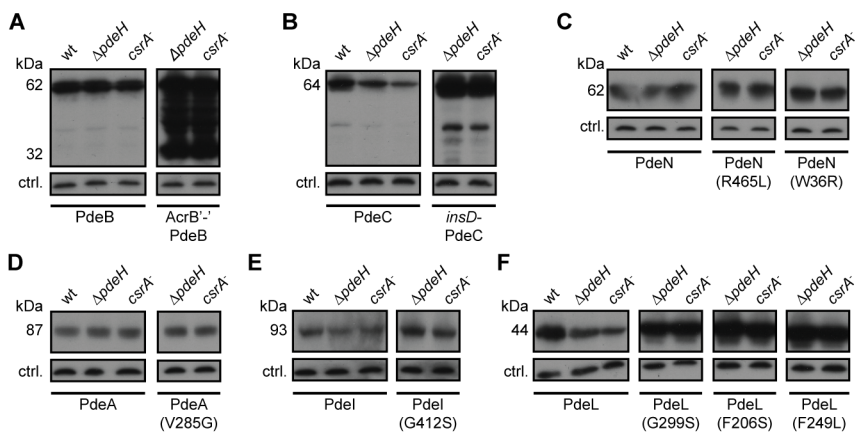


Figure 3 | Expression of mutant phosphodiesterases in *E. coli*. Immunoblot analysis was performed on the wild type and on strains with suppressor variants for detection of PdeB (A), PdeC (B), PdeN (C), PdeA (D), PdeI (E), and PdeL (F) carrying 3xFlag-tags at their C-termini. Proteins were analyzed in the following strains grown to exponential phase: wild type, $\Delta pdeH$ mutant (AB607), and *csrA* mutant (AB958). Suppressor variants of PdeB (A) and PdeC (B) showed strongly increased protein levels indicating derepression of their expression. In contrast, suppressor variants of PdeN, PdeA, and PdeI showed unaltered protein levels in all strain backgrounds tested. Of the 10 PdeL suppressor variants isolated, three were analyzed (G299S, F206S, and F249L). All variants showed increased protein levels in all genetic backgrounds tested. Note that protein levels of PdeC and PdeL differed in different genetic backgrounds.

Pde suppressor alleles reduce poly-GlcNAc levels and cellulose-dependent attachment

The observation that the *pde* suppressor alleles restored motility in a *pdeH* background by reducing the intracellular c-di-GMP concentration prompted us to test if this represents a general cellular response that can also interfere with other c-di-GMP-mediated processes. We have shown previously that poly-

GlcNAc (PGA)-dependent biofilm formation is regulated posttranslationally by c-di-GMP [110]. The *pga* operon encoding the poly-GlcNAc biosynthesis machinery is controlled by the carbon storage regulator CsrA. Inactivation of *csrA* leads to derepression of the *pga* genes and two genes encoding DGCs: *dgcT* (*ycdT*) and *dgcZ* (*ydeH*) [196,197]. As a consequence, a *csrA* mutant strain not only shows constitutive expression of PGA components but also displays a strong increase of the c-di-GMP level (5.35 μ M) compared to that of the wild type (0.31 μ M) (**Figure 5A**). A mutant lacking both CsrA and DgcZ produces significantly less c-di-GMP and shows strongly reduced PGA-dependent attachment [110] (**Figure 5A**). To assay the effect of the *pde* suppressor mutations on PGA-mediated attachment, mutant alleles were introduced into a *csrA* single mutant and a *csrA* *dgcZ* double mutant. As shown in **Figure 5A**, only *pdeC* and two of the *pdeL* alleles were able to effectively reduce attachment in the high-c-di-GMP background (*csrA* mutant). Apparently, in accordance with the capacity of restoring motility, only the most active PDE variants are able to reduce the level of c-di-GMP in this strain to a concentration range below the activation constant (K_{act}) of the PGA biosynthesis machinery (62 nM) [110]. In contrast, when biofilm formation was assayed in the low-c-di-GMP background (*csrA* *dgcZ*), all *pde* alleles showed a significant reduction of biofilm formation. The only suppressor allele that was not able to reduce PGA-dependent biofilm formation was PdeI (G412S) (**Figure 5B**). However, because motile suppressor mutants were isolated at 37°C and biofilm assays were routinely carried out at 30°C, we tested if *pdeI* expression was temperature controlled. As shown in **Figure 5C**, PdeI protein levels were indeed strongly temperature dependent, with the highest concentration reached at 42°C (**Figure 5C**). In line with this observation, the *pdeI* (G412S) allele significantly reduced attachment of the *csrA* *dgcZ* mutant at 37°C (**Figure 5C**).

While *E. coli* forms poly-GlcNAc biofilms in the host and at higher temperatures [198-200], it can form cellulose-based biofilms in the environment and at lower temperatures. Like that of poly-GlcNAc, production of cellulose is also stimulated by c-di-GMP [1]. Many lab-adapted *E. coli* strains, including *E. coli* K-12 MG1655, are deficient in cellulose production. This is due to a single point mutation in the *bcsQ* gene, encoding cellulose synthase. Restoration of the *bcsQ* wild-type sequence results in proficient cellulose production [201]. Introduction of a *bcsQ* wild-type allele into the cellulose-deficient strain MG1655 increased attachment about 2-fold. Deletion of *pdeH* in a *bcsQ* background increased attachment about 4-fold compared to that of the isogenic *bcsQ* strain (**Figure 5D**). Deletion of *pdeH* in the cellulose-deficient MG1655 strain also led to a 4-fold increase in attachment compared to that of the wild type, arguing that other c-di-GMP-dependent systems contribute to biofilm formation in this strain. Importantly, when the three *pdeL* suppressor alleles (encoding G299S, F206S, and F249L mutations) were introduced into the *bcsQ* *pdeH* background, cellulose-dependent attachment was strongly reduced, similar to the pattern observed for poly-GlcNAc-dependent biofilm formation (**Figure 5D**).

These results strongly suggest that genetically activated variants of several PDEs have a profound effect on the cellular c-di-GMP concentration, which eventually becomes manifested in different c-di-GMP-responsive output systems.

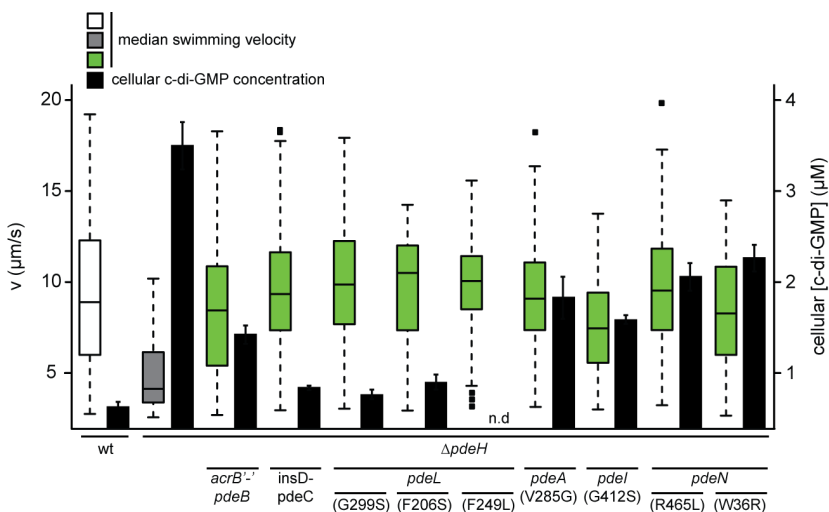


Figure 4 | Swimming velocities of *E. coli* wild-type and phosphodiesterase mutant strains. Velocities of individual cells of the *E. coli* wild type (white), the *pdeH* mutant (gray), and motile suppressor mutants of the *pdeH* mutant (green) were scored. For statistical analysis, the Kruskal-Wallis rank sum test was applied. Swimming velocities of at least 76 single cells are shown as box plots. Boxes show the lower and upper quartiles. Black horizontal lines represent the median velocities. Dashed lines show extreme values, whereas small black squares represent individual outliers. Comparisons of motile suppressor mutants with the parental $\Delta pdeH$ strain all showed statistically significant differences ($P < 0.05$). Motile suppressor mutants showed swimming velocities restored to the levels observed for the wild type. Black bars represent intracellular c-di-GMP concentrations as measured by LC-MS/MS. A mutant lacking PdeH displayed a 10-fold-increased cellular c-di-GMP concentration (3.5 μM) compared to that of the wild type (0.31 μM). Motile suppressor mutants showed reduced intracellular c-di-GMP concentrations compared to their parental strain ($\Delta pdeH$).

PdeL suppressors show increased enzymatic activity

To gain further insight into the suppression mechanisms that caused reduced levels of c-di-GMP, we investigated the specific *in vitro* activity of mutant phosphodiesterases. We chose three representative suppressor mutants of PdeL, since this is the only soluble cytoplasmic enzyme and because it was previously shown to be an active c-di-GMP-specific phosphodiesterase [62,188]. We overexpressed and purified PdeL wild-type and G299S, F206S, and F249L mutant proteins that carried a StrepII tag at the C-terminus. To determine their activities, we developed a novel enzyme-coupled phosphate sensor-based assay that allows for sensitive real-time determination of c-di-GMP-specific phosphodiesterase activity (see the legend to **Figure 6** and Materials and Methods for details). PDE activity was determined at an enzyme concentration of 500 nM, with substrate concentrations ranging from 100 nM to 0.5 μM . While wild-type PdeL had a specific PDE activity (k_{cat}/K_M) of 0.14 $\text{M}^{-1} \text{s}^{-1}$, all three PdeL variants showed significantly increased turnover rates, ranging from 0.21 to 0.26 $\text{M}^{-1} \text{s}^{-1}$ (**Figure 6A**).

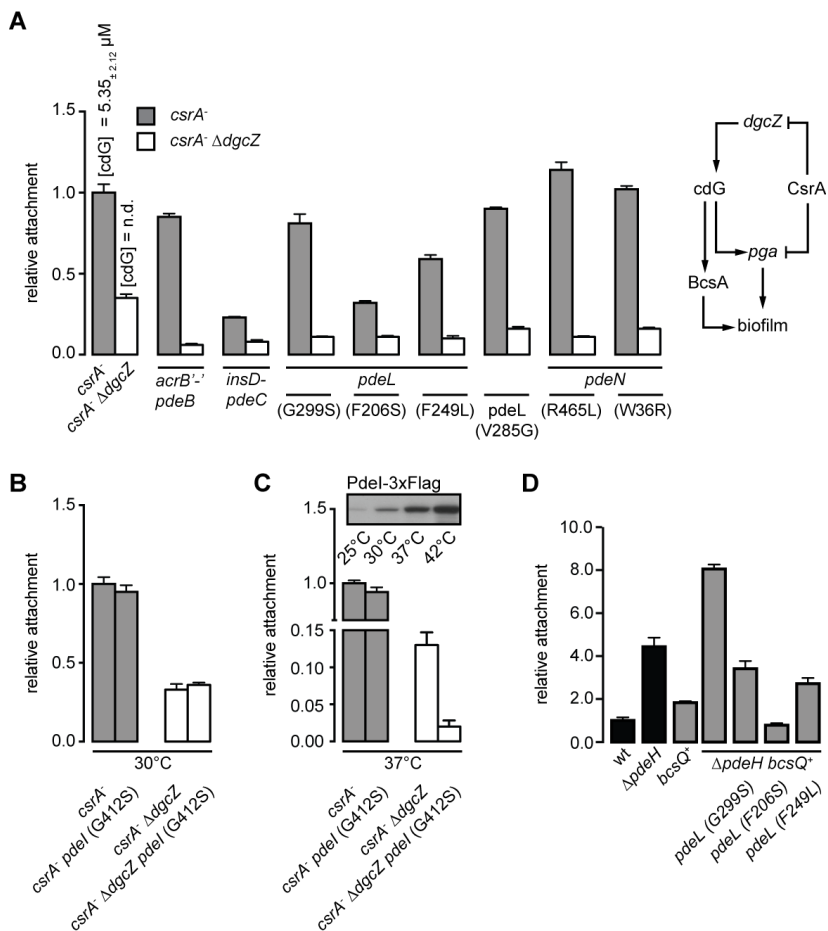


Figure 5 | Surface attachment of *E. coli* wild-type and phosphodiesterase mutant strains. (A) Relative surface attachment of *E. coli* *csrA* and *csrA* Δ *dgcZ* mutant strains harboring individual *pde* suppressor mutations, as indicated. Levels of c-di-GMP (cdG) in both mutant backgrounds are indicated (n.d., not detectable). A schematic of the regulatory network of PGA and cellulose-dependent biofilm control is shown beside the graph. Gray bars and white bars indicate relative levels of biofilm formation in the *csrA* and *csrA* Δ *dgcZ* strain backgrounds, respectively. Biofilm formation was examined at 30°C **(B)** and 37°C **(C)** for strains carrying wild-type *pdeL* and the *pdeL* (G412S) suppressor allele. Temperature-dependent expression of *pdeL* as measured by immunoblot analysis is shown in the inset of panel c. **(D)** Relative attachment of *pdeL* suppressor alleles (G299S, F206S, and F249L) in a cellulose-producing *bcsQ*⁻ Δ *pdeH* background. Black bars indicate strains harboring a single nucleotide polymorphism (SNP) in the *bcsQ* gene, and gray bars represent a “repaired” *bcsQ* gene (*bcsQ*⁻). Attachment is shown relative to that of the cellulose-deficient lab-adapted strain *E. coli* K-12 MG1655 of Blattner et al. [202]. The assay was performed at room temperature.

PdeL suppressors enhance *pdeL* transcription

Strikingly, strains expressing *pdeL* (G299S), *pdeL* (F206S), and *pdeL* (F249L) showed significantly higher PdeL protein levels than that of the isogenic *pdeL* wild-type strain (**Figure 3F**). The observation that PdeL harbors an N-terminal LuxR-type DNA binding domain fused to its catalytic EAL domain led us to investigate whether *pdeL* expression is subject to autoregulation. To test this, we constructed a chromosomal reporter, fusing the entire intergenic region upstream of *pdeL* and downstream of *betT* to the *lacZ* gene. The fusion was engineered in the *lacZ* locus of the chromosome, leaving the original *pdeL* locus intact (**Figure 6B, inset**). β -galactosidase activity was then determined to compare *pdeL* promoter strengths in *pdeH* strains harboring the *pdeL* alleles encoding the G299S, F206S, and F249L substitutions. All strains expressing activated mutant forms showed similar, about 5-fold increases of *pdeL* transcription compared to that in their isogenic strain (**Figure 6B**). This suggested that *pdeL* transcription is autoregulated and that PdeL enzyme activity is coupled to the transcription of its own gene.

PdeL directly regulates its own expression in a c-di-GMP-dependent manner

Promoter activity of *pdeL* could be linked directly to the enzymatic activity of PdeL, possibly through its DNA binding domain. Alternatively, the enzymatic activity of PdeL might influence *pdeL* transcription indirectly by modulating the cellular level of c-di-GMP. To distinguish between these two possibilities, we compared *pdeL* promoter activities in strains expressing a wild-type copy of PdeL but harboring distinct c-di-GMP concentrations. To this end, we used the MG1655 wild-type strain, the *pdeH* mutant strain, and a strain [referred to as the *dgc(4)* strain] lacking four DGCs: DgcE (*yegE*), DgcN (*yfiN*), DgcO (*yddV*), and DgcQ (*yedQ*) [78]. While wild-type MG1655 harbored intermediate cellular levels of c-di-GMP (0.31 μ M), the *pdeH* mutant showed high levels (> 3 μ M), and the *dgc(4)* mutant had very low levels of c-di-GMP as measured by LC-MS/MS (65 nM) (**Figure 6C**). Similar to that in strains harboring PdeL suppressors, *pdeL* promoter activity was increased in a strain lacking the four DGCs.

In contrast, a strain lacking PdeH showed strongly reduced *pdeL* transcription. Together, these observations argued that *pdeL* transcription is controlled negatively by c-di-GMP and that the *pdeL* promoter is highly active when the cellular c-di-GMP concentration is very low. In principle, there are two possibilities to explain this regulatory behavior. Internal c-di-GMP levels could be sensed through an unknown transcription factor that modulates *pdeL* promoter strength accordingly. In this case, the role of PdeL and its enzyme activity in autoregulation would be entirely indirect, through the modulation of the cellular c-di-GMP pool. Alternatively, the role of PdeL could be more direct in that it not only is involved in c-di-GMP homeostasis but also acts as a sensor for the prevailing c-di-GMP concentration and, in response, directly regulates *pdeL* promoter strength, involving its DNA binding domain. To distinguish between these two possibilities, we performed electrophoretic mobility shift assays (EMSAs) to test for binding of purified PdeL to its own promoter region. Due to the exceptional size of the region between *pdeL* and its upstream gene *betT* (874 bp), binding of PdeL to this region had to be tested by using a series of Cy3-labeled DNA probes of various lengths.

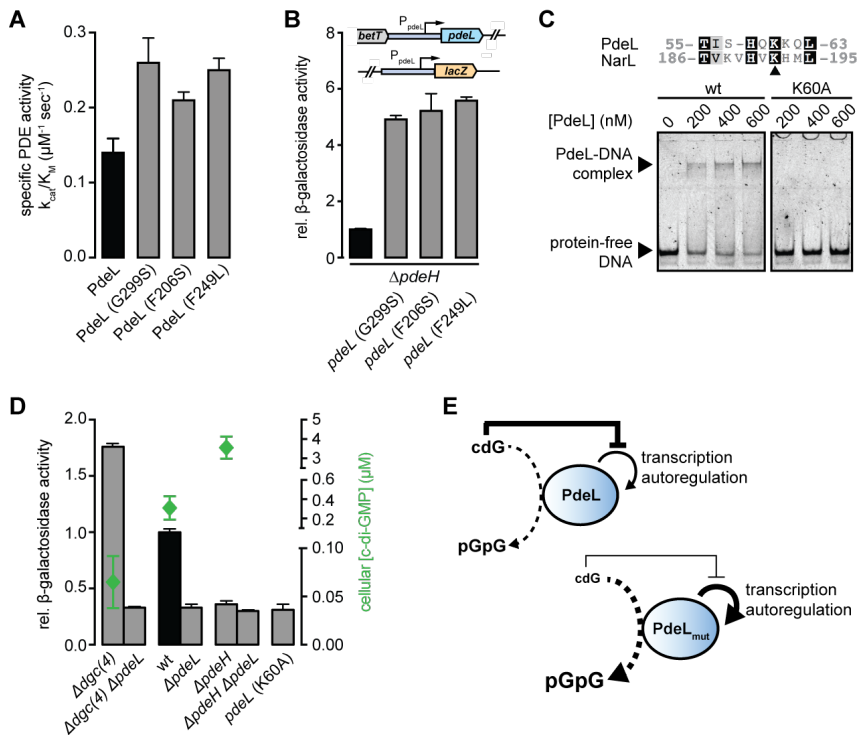


Figure 6 | Enzyme activities and autoregulation of PdeL suppressor variants. **(A)** Specific phosphodiesterase activities of purified wild-type PdeL and mutant PdeL variants. The specific activities (k_{cat}/K_M [$\mu\text{M}^{-1} \text{sec}^{-1}$]) of PDEs were determined using an enzyme-coupled phosphate sensor assay (see Materials and Methods). In our assay, we applied an enzyme concentration of 100 nM and substrate concentrations ranging from 100 nM to 5 μM . All three PdeL mutants showed an increased turnover rate compared to that of the wild type (0.15 $\mu\text{M}^{-1} \text{sec}^{-1}$). **(B)** Relative β -galactosidase activities of *pdeH* mutant strains carrying translational P_{pdeL} -*lacZ* fusions at the native *lacZ* locus. A schematic of the reporter strain is shown at the top. The presence of *pdeL* suppressor alleles increased *pdeL* promoter activity about 5-fold. **(C)** The inset shows a partial alignment of the HTH domain sequence of *E. coli* PdeL and NarL. Lysine 192 of NarL (black arrow) is involved in DNA binding. EMSAs were performed with purified PdeL-StrepII (left panel) and PdeL (K60A)-StrepII (right panel) by using oligonucleotide 4991-7, containing the minimal PdeL binding region. **(D)** c-di-GMP regulates *pdeL* transcription in a PdeL-dependent manner. The promoter activity of *pdeL* was determined for the wild type, a strain exhibiting low levels of c-di-GMP [$\Delta dgc(4)$], and a strain with high levels of c-di-GMP ($\Delta pdeH$). c-di-GMP levels of the respective strains are shown as green diamonds. The graph includes the *pdeL* promoter activity of a strain harboring the *pdeL* (K60A) allele. **(E)** Model of c-di-GMP-dependent *pdeL* transcription control. Enzymatic activity is depicted with a dashed arrow. c-di-GMP negatively regulates *pdeL* transcription through an unknown mechanism. The enhanced enzymatic activity of PdeL suppressor variants (PdeL_{mut}) lowers the cellular levels of c-di-GMP and leads to *pdeL* transcription stimulation.

This analysis yielded a minimal PdeL binding region of 24 bp, located 679 nucleotides upstream of *pdeL*, harboring an imperfect palindromic sequence (5'-TTC AAT AAG TTT AGT CTT ATT TAA) (**Figure 6C**). To corroborate these results, we aimed to construct a DNA binding-deficient mutant of PdeL which harbors an N-terminal LuxR-like helix-turn-helix (HTH) domain. Based on structural information of the LuxR-like domain of the response regulator NarL [203], we identified a conserved lysine at position 60 of PdeL, which in NarL interacts with DNA (**Figure 6C, inset**). As shown in **Figure 6C**, purified PdeL (K60A) failed to bind to the PdeL box as indicated above. Next, we determined *pdeL* promoter activity as a function of c-di-GMP levels in strains lacking PdeL. As shown in **Figure 6D**, *pdeL* promoter activity was strongly reduced in the absence of PdeL, irrespective of the cellular concentration of c-di-GMP. Similarly, when the *pdeL* gene was replaced in the chromosome with a *pdeL* allele encoding the K60A mutation, *pdeL* promoter activity was abolished (**Figure 6D**). Taken together, these experiments strongly argue that PdeL is an enzyme and a transcription factor stimulating its own expression in response to the prevailing c-di-GMP regimen in the cell.

Discussion

A large variety of cellular processes in bacteria are dependent on c-di-GMP and are tuned during growth or behavioral processes by accurately regulated cellular levels of this second messenger. This requires tight and coordinated control of the enzymes producing or degrading c-di-GMP. Many of these enzymes contain N-terminal signal input domains to sense and integrate environmental cues. While some of these signals have been identified and include oxygen, NO, redox, light, and the availability of nutrients [59,61,72,204-206], the vast majority of input signals are unknown. It is thus not surprising that under controlled laboratory conditions, only a subset of these enzymes shows activity and contributes to known c-di-GMP-dependent cellular processes. We showed previously that from a total of 25 potential enzymes involved in c-di-GMP turnover, only four DGCs, DgcO (YddV), DgcQ (YedQ), DgcN (YfiN), and DgcE (YegE), and one PDE, PdeH (YhjH), contribute to the regulation of *E. coli* motility [78]. A major player of this regulation is PdeH (YhjH), a soluble PDE that lacks a signal input domain and is coregulated with other flagellar genes to license cell motility and planktonic cell behavior [193]. In contrast, deletions of any of the remaining 12 candidate PDEs encoded in the genomes of *E. coli* K-12 strains showed no effect on motility control (A. Boehm and U. Jenal, unpublished results). Several possibilities exist to explain this observation. Some of these proteins might not be expressed under laboratory conditions. If present, they might be sequestered to control specific cellular processes, or they might simply lack catalytic activity. Finally, they might require an appropriate stimulus to become operative.

Here we showed that most potential *pde* genes are expressed in *E. coli*, resulting in readily detectable protein levels. This indicated that these PDEs are present in an inactive state. This was corroborated by our findings that several of these components could be activated genetically to interfere with motility and biofilm control by lowering the overall levels of c-di-GMP in the cell. These experiments support the view that bacteria are equipped with an arsenal of sensors that allows bacteria to rapidly integrate a range of environmental signals to modulate the general c-di-GMP pool and thus to optimally adapt to their variable environments. This does not exclude the possibility that bacteria also tune the levels of these enzymes by altering transcriptional or translational control or as a result of differential protein stability. Also, bacteria likely express distinct sets of such sensory components for specific growth phases or environmental niches. This view is supported by the observation that in *E. coli*, several DGCs and PDEs are regulated by the stationary-phase sigma factor, σ^s [194]. Similarly, we found that *pdeI* (*yliE*) expression is strongly temperature controlled and present at high concentrations only at temperatures well above 30°C. This argues that PdeI is part of an enzyme cocktail that is used primarily in the host environment. Finally, we were unable to isolate activating mutations in several of the remaining PDEs, including PdeK (YhjK), PdeR (YciR), PdeO (DosP), and PdeD (YoaD), despite applying strong selective pressure. It is possible that activating mutations in the relevant genes can be isolated in principle and that our genetic screen was not saturated. Likewise, the activities of some of these enzymes might simply be too weak, even in an activated state, to counter the relatively high cellular c-di-GMP levels of the *pdeH* mutant strain. Alternatively, some of these components might be part of a specific spatial or structural

organization that confines them to acting in a functionally restricted manner. This was recently proposed for PdeR (YciR). This enzyme was shown to form a signaling complex together with the diguanylate cyclase DgcM (YdaM) and the transcription factor MlrA. In this complex, PdeR seems to act both as an enzyme and as a local trigger of the transcriptional activity of MlrA, which drives the expression of CsgD, a central biofilm regulator activating the genes for cellulose matrix and curli fibers [80]. While the mechanistic details of the PdeR transcription complex need to be worked out, this regulatory arrangement is consistent with a (locally) limited catalytic function of PdeR, thus offering a plausible explanation for why it was not picked up in our motility screen. Similarly, PdeO (DosP) was recently shown to be part of an RNA degradation complex, in which it seems to locally control RNA turnover in response to oxygen availability [72].

In this study, we used suppression analysis to identify PDE variants in *E. coli* that can substitute for the major PDE PdeH (YhjH). Using this genetic trick allowed us to bypass the requirement of individual input signals that are normally required to unleash the putative PDE activity. The fact that it is possible to isolate activating mutations in PDEs strongly argues that these enzymes exist in two distinct forms, an active and an inactive conformation, and that their activities are tightly controlled, possibly by switching between these two states. The nature of the mutations that lead to enhanced catalytic PDE activity thus reveals details about the specific mechanisms which these enzymes employ to control their own activity. In principle, several mechanisms to activate a PDE are conceivable. (i) Because PDEs are generally active as dimers [61,62], an increase of the protein concentration by overexpression will shift the equilibrium toward the active dimeric state. Consistent with this, overexpression of PDEs (or DGCs) can indeed affect the global c-di-GMP pool of bacterial cells, regardless of their activation state [194,204]. (ii) Signal input domains might obstruct the substrate binding site of the catalytic domain or stabilize the enzyme in an inactive conformation. In this case, enzyme activation could result from a functional uncoupling of the two domains. (iii) Mutations within the enzymatic EAL domain may directly enhance specific catalytic PDE activity or change the equilibrium between putative inactive and active conformations toward the latter. In agreement with such a mechanism, we isolated several suppressor alleles encoding single amino acid changes within the EAL domain in PdeL and PdeN. These mutations likely represent true activating mutations.

Of the PDEs that were able to substitute for PdeH activity, PdeL is the best-characterized enzyme. In our study, we isolated 10 mutations affecting eight individual amino acid residues. Three of these were analyzed in detail and were shown to result in enhanced catalytic activity *in vitro* as well as enhanced *pdeL* expression. In principle, both properties could contribute to the observed suppression phenotype. At low substrate concentrations, i.e., below the observed K_M of about 1 μM , the cellular turnover of c-di-GMP (catalyzed by PdeL) would be increased by a factor of about 10 for the suppressor mutants, as a consequence of a 2-fold increase in specific PDE activity and a 5-fold increase in expression. The increase in specific PDE activity of PdeL mutants is intriguing and warrants a closer analysis. **Figure 7** shows the locations of all identified mutations that map to the two known wild-type PdeL EAL crystal structures [62]. It is striking that none of the mutated sites are part of the active site that is located at the C-terminal

end of the central β -barrel. This enforces the notion that it is not trivial to optimize the catalytic properties of an enzyme through a directed- evolution approach. Rather, the increase in activity may be due to subtle second- or higher-shell effects that are difficult to predict. Alternatively, the mutations may change the thermodynamic equilibrium between (at least) two global conformational states with distinct catalytic activities.

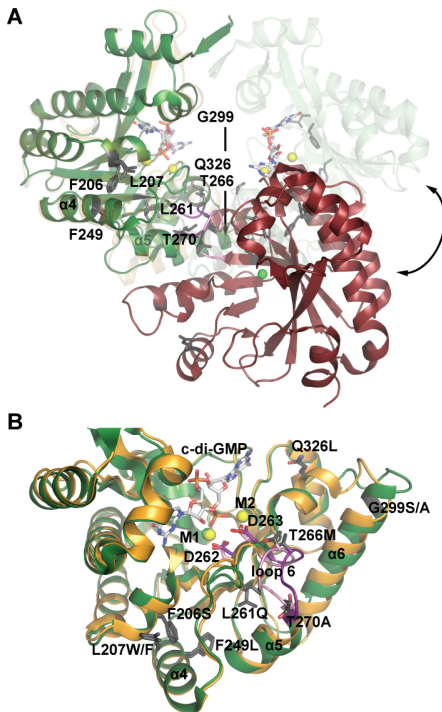


Figure 7 | Model for PdeL phosphodiesterase activation by suppressor mutations. (A) Two distinct EAL dimer structures are shown as obtained recently by X-ray crystallography [62]. The sites of suppressor mutations are shown in grey. Structure of the canonical “open” PdeL EAL dimer as determined in the presence of magnesium (green sphere) (PDB code 4LYK) is shown in orange (protomer A = opaque) and red (protomer B). Structure of the “closed” PdeL EAL dimer as determined in the presence of *c*-di-GMP/ Ca^{2+} (PDB code 4LJ3) is shown in green (protomer A) and light green (protomer B = opaque). Protomer A of open dimer was aligned to protomer A of closed dimer to illustrate the large conformational movement between the two crystalized dimer species (indicated by black arrow). (B) Comparison of the PdeL EAL monomer structures of the “open” and “closed” dimers. Colors are the same as those shown in panel A (green with loop 6 in pink, “open” dimer; orange with magenta loop, “closed” dimer). In addition to the mutation sites (dark gray residues), the substrate *c*-di-GMP, the calcium ions M1 and M2 (yellow), magnesium ion M1 (bright green), and highly conserved metal-coordinating aspartates 262 and 263 at the end of β -strand 5 are highlighted. The latter precedes loop 6 and has been implicated in catalysis regulation [62].

We favor the second scenario, since it was recently shown that the EAL domain of PdeL exhibits exquisite inherent regulatory properties [62]. The domain can adopt two states that differ drastically in their catalytic activity: a virtually inactive monomeric state and a catalytically competent dimeric state. Coupling of a quaternary state to the precise geometry of the active site, and thus to catalytic activity, appears to be mediated by the $\beta 5$ - $\alpha 5$ loop (loop 6) that constitutes a major part of the dimerization interface (Figure 7), as also observed in other EAL structures [207]. Intriguingly, it was also shown that the EAL domain of PdeL can adopt two distinct dimer conformations, both involving similar dimerization interfaces (formed mainly by loop 6 and helices $\alpha 5$ and $\alpha 6$) but showing drastically different

relative monomer arrangements (“open” (**Figure 7A**) and “closed” (**Figure 7B**) dimers) [62]. It has not yet been studied whether both kinds of dimers also exist in solution and, if so, what their relative catalytic activities and the equilibrium constant between them would be.

In light of this structural information, we propose that the fully characterized suppressor mutations (G299S, F206S, and F249L) shift the thermodynamic equilibrium of PdeL from an inactive or lowly active state (EAL domain monomer or dimer of low activity) toward the active state (highly active dimer). Structurally, the shift of the equilibrium would be due to different effects of the suppressor mutations on the two alternative dimerization interfaces (**Figure 7A & B**). Indeed, amino acid 299 is part of dimerization helix α_6 , though the added side chain would not project directly toward the interface. The two phenylalanines, residues 206 and 249, are part of the hydrophobic core that is formed by the packing of helices α_4 and α_5 onto the central β -barrel. Upon mutation at these sites, the two helices may well shift relative to the β -barrel, causing a perturbation of that part of the interface, which is formed by the N-terminus of α_5 and the preceding α_5 - β_5 loop (loop 6). Reassuringly, suppressor mutations F207W/F and L261Q map to the same hydrophobic core, and an increase of activity due to a similar mechanism is predicted. Residues T266 and T270 are part of loop 6 (**Figure 7C**), the part of the structure that changes most between the two PdeL conformations. Thus, differential stabilization of the possibly more active conformation (or destabilization of the inactive conformation) is conceivable.

Our findings suggest that in addition to its enzymatic function, PdeL can also be a transcription factor and a sensor for c-di-GMP. We showed that increased activities of PdeL variants containing suppressor mutations result in increased levels of the respective proteins. The observation that the stability of these activated mutant variants was unaltered, together with the finding that the activity of the *pdeL* promoter was increased in the suppressor strains, strongly argued that PdeL exhibits autoregulation. Transcription of *pdeL* could respond directly to PdeL activity or conformation or could be controlled indirectly through cellular levels of c-di-GMP, which drop as a consequence of increased PdeL activity. The finding that the *pdeL* promoter is strongly upregulated in cells harboring low levels of c-di-GMP but inhibited at high c-di-GMP concentrations strongly argued for the latter. Finally, the observation that c-di-GMP-mediated regulation of *pdeL* promoter strength strictly depended on PdeL itself and on its intact DNA binding domain suggested that PdeL is able to sense cellular levels of c-di-GMP and, in response, tune its own expression. Considering the domain architecture of PdeL, it seems plausible that the EAL domain is involved in sensing c-di-GMP concentrations, while the LuxR-type DNA binding domain is likely required for transcriptional autoregulation. While the exact mechanism and physiological significance of this feedback control remain to be elucidated, it is notable that a similar mechanism was described recently, in which PdeR plays a role both as an enzyme and as a sensor for c-di-GMP [80]. This example illustrates that an active phosphodiesterase can adopt additional functions to control gene expression in response to substrate availability. Thus, PdeL and PdeR are conceptually very similar in that both proteins “measure” c-di-GMP via an unknown mechanism and in turn regulate gene expression. But while PdeR engages in a signaling complex together with an independent transcription factor, PdeL apparently has evolved more independence by recruiting and directly coupling a DNA binding domain

to its catalytic domain. Proteins coupling metabolite availability to gene expression control are common in bacteria and were termed trigger enzymes [149]. It will be interesting to clarify the regulatory details and similarities of these systems and to analyze how widespread this phenomenon is among phosphodiesterases.

Author contribution

AR, CH, SO, AB, UJ and TD conceived and designed the experiments. AR, CH and SO performed the experiments. AR, AM, TS and UJ analyzed the data. AR, TS and UJ wrote the paper.

Author information

Correspondence should be addressed to urs.jenal@unibas.ch.

Supplemental material

Supplemental materials are available in the online version of the publication.

Acknowledgements

This project was initiated by our fellow friend and scientist colleague Dr. Alexander Böhm who passed away on November 27th, 2012 and to whom we dedicate this work [208]. We thank Prof. Volkhard Kaever from the Medizinische Hochschule Hannover for c-di-GMP measurements. The Fellowship For Excellence (FFE) International PhD Program supported this work. Swiss National Science Foundation provided funding to Urs Jenal under grant number 310030B_147090.

Materials & Methods

Bacterial strains, plasmids, and growth conditions

The bacterial strains and plasmids used in this study are listed in Table S1 in the supplemental material. *E. coli* K-12 MG1655, obtained from Blattner et al. [202], and its derivatives were grown as indicated in the relevant sections. When needed, antibiotics were included at the following concentrations: 30 µg/ml chloramphenicol for plasmids, 20 µg/ml chloramphenicol for chromosomal chloramphenicol resistance cassettes, 12.5 µg/ml tetracycline, 50 µg/ml kanamycin, 100 µg/ml ampicillin for plasmids, and 30 µg/ml ampicillin for chromosomal ampicillin resistance cassettes.

DNA work

(i) **PCR amplification.** Each PCR mixture contained the following: 1x polymerase buffer (NEB), a mix containing a 0.1 mM concentration of each deoxynucleoside triphosphate (dNTP), 0.3 µM forward primer, 0.3 µM reverse primer, 10-20 pg template DNA, and 0.7 µL *Taq* polymerase (NEB). For colony PCR, a single colony was picked up with a pipette tip and resuspended in the PCR mixture.

(ii) **Gel electrophoresis.** Five microliters of PCR product was mixed with DNA loading dye, loaded into a 1 % agarose gel supplemented with a 1:20,000 dilution of RedSafe DNA stain (iNtRON), and separated using 1x Tris-borate-EDTA (TBE) buffer. DNA was analyzed under UV light.

(iii) **Sequencing.** Linear DNA was purified using NucleoSpin extract II (Macherey-Nagel). Sequencing reactions were carried out by Microsynth AG (Balgach, Switzerland). The sequences obtained were assembled and analyzed using 4Peaks (mekentosj).

(iv) **Plasmid preparation.** Plasmid DNA was purified using a Gen-Elute plasmid miniprep kit (Sigma) according to the commercial protocol.

(v) **TSS transformation.** Transcription start site (TSS) transformation of plasmid DNA was carried out as previously described [209].

(vi) **Electroporation.** For electroporation of purified linear DNA with a Bio-Rad GenPulser cuvette (1 mm diameter), the following electroporation settings were applied: 400 Ω, 1.75 kV, and 25 µF.

P1 phage lysate preparation and transduction

P1 phage lysate preparations and transductions were carried out essentially as described by Miller [210].

λ-RED recombineering

(i) **Chromosomal gene deletions and modifications.** Gene deletions were carried out essentially as described by Datsenko and Wanner [211], with the use of a comprehensive mutant library (Keio collection [[212]]) and P1-mediated transduction. Chromosomal 3xFlag-tags were constructed according to the published method of Uzzau et al. ([213]). For unmodified strains, AB330 was used (**Table S1**), whereas pKD46 was used for construction of 3xFlag-tagged versions of the motile suppressor mutants. Kanamycin resistance markers used for selection during strain construction were removed by site-

specific recombination using pCP20, generating a short, “Frt” scar sequence which replaced the deleted gene or cotransduced kanamycin resistance marker [211].

(ii) Construction of *lacZ* promoter fusions. The construction of chromosomal *lacZ* promoter fusions was constructed via λ -RED-mediated recombination essentially as described above. AB989 (**Table S1**) was used as a template for construction of the reporter fusion. AB989 contains $P_{rha-ccdB}$ and a flanking kanamycin resistance cassette which is inserted upstream of the native *lacZ* locus. The donor PCR fragment harboring the promoter of interest was designed to site-specifically excise $P_{rha-ccdB}$ and integrate upstream of the *lacZ* open reading frame (ORF), generating a merodiploid translational fusion. Selection of successful integration events was achieved through growth at 30°C on minimal medium plates provided with 0.2 % rhamnose supplemented with 0.5 μ g/ml biotin. The fusion was transduced into strains of interest via P1 transduction.

Immunoblotting

Cells were grown with shaking in tryptone broth (TB) at 37°C until an optical density at 600 nm (OD_{600}) of 0.5-0.8. An equivalent of 1 mL of cells at an OD_{600} of 1.0 was pelleted and resuspended in 100 μ L SDS Laemmli buffer. For detection of 3xFlag-tagged PdeA and its derivatives, the cells were resuspended in 30 μ L SDS loading dye. Cells were lysed by boiling the sample at 98°C for 15 min. Eight microliters of the total cell extract was loaded onto a 12.5 % SDS-polyacrylamide gel, and proteins were transferred by use of a Bio-Rad wet blot system. Proteins were detected with a 1:10,000 dilution of mouse anti-Flag monoclonal antibody (Sigma) and a 1:10,000 dilution of horseradish peroxidase (HRP)-conjugated rabbit anti-mouse secondary antibody (DakoCytomation, Denmark). Proteins were visualized by use of an enhanced chemiluminescence (ECL) detection reagent (PerkinElmer Life Sciences) on a photo film (Fuji) or gel imager (GE ImageQuant LAS 4000).

Suppressor screen

The strains used for the genetic forward screen of individual PDEs are listed in **Table S1** in the supplemental material. Each strain was transformed with *pwspR*. For each screen, 300 TB swarm plates supplemented with tetracycline were prepared, among which 100 were supplemented with 5 μ M isopropyl- β -D-thiogalactopyranoside (IPTG) and 100 were supplemented with 20 μ M IPTG. Single colonies of the screening strain harboring *pwspR* were applied to screening plates. The screening plates were incubated at 37°C. Over the course of a week, all plates displaying motile suppressor mutants showed visible flares spreading from the center of inoculation. The motile suppressor mutants were isolated and pooled in a liquid LB culture. A pool lysate was prepared and transduced into AB607 ($\Delta pdeH$). Transductants were picked up and placed on TB swarm plates supplemented with kanamycin and 20 mM sodium citrate. After incubation at 37°C for 3 to 4 h, the motile suppressor mutants that appeared were restreaked, and the ORF of the PDE of interest was sequenced.

Video tracking

Bacterial swimming speed measurements were carried out essentially as described by Boehm et al. ([78]). Briefly, bacteria were grown in TB at 37°C to an OD₆₀₀ of 0.5-0.8. Cells were diluted 1:100 into fresh TB and applied to a coverslip that was attached to a glass slide with two-sided adhesive tape. Two videos of 30 sec each were recorded at 15 fps with a video microscope and dark-field optics at a magnification of 40x. The acquired videos were imported into ImageJ 1.43 (NIH), and trajectories were calculated with the “2D particle tracker” plug-in. Velocities and statistical data were computed via a custom-made R script.

C-di-GMP measurements

C-di-GMP measurements were performed according to the published procedure of Spangler et al. ([99]). Briefly, *E. coli* cells were grown in 5 mL TB at 37°C until an OD₆₀₀ of 0.5-0.8. The culture was pelleted and washed in 300 µL ice-cold distilled H₂O. After washing, the cell pellet was resuspended in 300 µL ice-cold extraction solvent (acetonitrile/methanol/distilled H₂O, 40/20/20 [vol/vol/vol]). After incubating on ice for 15 min, the samples were boiled at 100°C for 15 min. After pelleting, the supernatant was transferred to a safe-lock tube, and the extraction procedure was repeated twice with 200 µL extraction solvent. Biological triplicates were performed for each tested bacterial strain. Measurements were performed in collaboration with the group of Volkhard Kaever (Institute of Pharmacology, Hannover, Germany) via high-pressure liquid chromatography–tandem mass spectrometry (HPLC-MS/MS). Measured values were mathematically converted into intracellular c-di-GMP concentrations (µM) per CFU.

Attachment assay

Attachment assays were carried out as described by Boehm et al. ([214]). Briefly, 5 µL of a shaking overnight culture grown in TB at 37°C was used to inoculate 200 µL TB provided in a 96-well microtiter plate (Falcon, NJ). The plate was incubated statically at 30°C for 24 h. For quantification of cellulose-dependent attachment, cells were incubated statically in TB at room temperature for 24 h. After recording of the OD₆₀₀ of the total biomass, the planktonic phase of the culture was discarded and the wells were washed with deionized water from a hose. The total attached biomass was stained with 300 µL 0.3% crystal violet (0.3 % [vol/vol] in distilled H₂O, 5 % [vol/vol] 2-propanol, 5 % [vol/vol] methanol) for 20 min. Subsequently, the plate was washed, and the remaining crystal violet-stained biomass was dissolved in 20 % acetic acid for 20 min and quantified by measuring the OD₆₀₀. Attachment was normalized to the initially measured total biomass.

Protein purification

(i) Strep II purification. C-terminally Strep II-tagged wild-type and mutant variants of *pdeL* were cloned into a pET28a vector (Novagen) between the NcoI and NotI restriction sites. Proteins were overexpressed from plasmids in BL21-AI cells grown at 30°C in 2 L of LB medium. At an OD₆₀₀ of 0.6, the culture was

induced with 0.1 % L-arabinose. Cells were harvested at 4 h post induction by centrifugation at 3,500 rpm for 30 min at 4°C. The cell pellet was resuspended in 8 mL buffer A (100 mM Tris-HCl, pH 8.0, 250 mM NaCl, 5 mM MgCl₂, 0.5 mM EDTA, 1 mM dithiothreitol [DTT]) including a tablet of Complete mini EDTA-free protease inhibitor (Roche) and a spatula tip of DNase I (Roche). Cells were lysed in a French press and the lysate cleared at 4°C in a table-top centrifuge for 40 min at full speed. The cleared supernatant was loaded onto 1 mL Strep-Tactin Superflow Plus resin (Qiagen). The supernatant was reloaded another two times before washing with a total of 60 ml buffer A. Protein was eluted as 500 µL aliquots with a total of 10 mL elution buffer A containing 2.5 mM D-desthiobiotin. Fractions with the highest protein concentrations were pooled.

(ii) Heparin purification. A 1 mL HiTrap heparin HP column (GE Healthcare) was washed with 10 mL distilled H₂O followed by equilibration with 10 mL buffer A. The eluate from the StrepII purification was loaded three times. After loading, the column was washed with 10 ml buffer A followed by a washing step with 10 mL buffer B (100 mM Tris-HCl, pH 8.0, 300 mM NaCl, 5 mM MgCl₂, 0.5 mM EDTA, 1 mM DTT). The protein was eluted in 500 µL fractions with a total of 10 mL buffer C (100 mM Tris-HCl, pH 8.0, 1 M NaCl, 5 mM MgCl₂, 0.5 mM EDTA, 1 mM DTT). The fractions containing the highest protein concentrations were pooled and dialyzed overnight against 1.5 L of dialysis buffer (100 mM Tris-HCl, pH 8.0, 250 mM NaCl, 5 mM MgCl₂, 0.5 mM EDTA, 1 mM DTT). The final protein concentration was recorded at 280 nm, and the content of copurified nucleotides was determined through the 260/280 nm ratio.

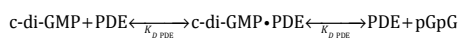
C-di-GMP hydrolysis assay and data fitting (phosphate sensor assay)

PdeL-catalyzed conversion of c-di-GMP to the linear pGpG dinucleotide was measured indirectly by a novel alkaline phosphatase (AP) phosphate sensor online assay. In this assay, the terminal phosphate of the pGpG product is cleaved by the coupling enzyme AP (20 U/µL; 5 U in assay mixture; Roche), and the phosphate concentration is determined from the fluorescence increase through binding of phosphate to the phosphate sensor (0.5 µM in assay mixture; Life Technologies).

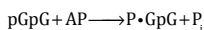
Dialysis buffer was used as the assay buffer. The assay was performed at a protein concentration of 100 nM and substrate concentrations ranging from 100 nM to 5 M, in a final volume of 300 µL in a 5-mm by 5-mm cuvette (Hellma Analytics). Progress curves were recorded with a Jasco FP-6500 fluorescence spectrophotometer at 20°C. The instrument settings were as follows: bandwidth (excitation), 5 nm; bandwidth (emission), 5 nm; excitation wavelength, 430 nm; emission wavelength, 468 nm; response, 1 s; sensitivity, low; and data pitch, 2 s.

The measured progress curves of fluorescence increases were fitted to the following scheme:

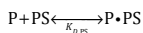
(i)



(ii)



(iii)



with the measured relative fluorescence units (RFU) originating from the uncomplexed (RFU1) and complexed (RFU2) sensors, as follows:

$$RFU = RFU1 + RFU2 = sc \times PS \times sc \times gain \times P \cdot PS$$

By a sufficiently large concentration of AP, it was ensured that reaction 2 was not rate limiting. The equilibrium dissociation constant for PS ($K_{d,PS}$) was obtained by phosphate titration in the absence of enzymes. Fitting of the data with this kinetic model was done with a custom-built Python script using NumPy and SciPy libraries. The corresponding differential equations were integrated with the assumption that product formation is the rate-determining step. The kinetic parameters of the PDE ($K_{d,PDE}$ and k_{cat}) as well as the scaling parameters (sc and $gain$) were refined globally for each series of experiments measured with various substrate concentrations. An observed slight background increase with time was taken into account by addition of a linear term with locally refined parameters. Fitted progress curves as well as individual K_m and k_{cat} values are documented in **Figure S2** and **Table S2** in the supplemental material.

Electrophoretic mobility shift assay (EMSA)

Cy3-labeled DNA probes were generated via either oligonucleotide annealing or PCR, using *E. coli* MG1655 as the template. Oligonucleotides used are indicated in the oligonucleotide list in **Table S1** in the supplemental material. DNA (10 nM) was incubated with purified PdeL-StrepII (0, 200, 400, or 600 nM) for 10 min at room temperature in 10 μ L buffer (50 mM Tris-HCl, pH 8.0, 50 mM NaCl, 10 mM MgCl₂, 10% glycerol, 1 mM DTT, 0.01 % Triton X-100, 0.1 mg/mL bovine serum albumin [BSA], and 25 μ g/ml DNA). After electrophoresis on 8 % polyacrylamide gels, DNA-protein complexes were analyzed using a Typhoon FLA 7000 imager (GE Healthcare).

β -galactosidase reporter assay

Strains were grown in TB overnight at 37°C. The next day, cultures were diluted 1:1,000 in fresh medium and grown with shaking at 37°C to an OD₆₀₀ of 0.8. An equivalent of 1 mL of culture at an OD₆₀₀ of 1.0

was pelleted and resuspended in 1 mL Z-buffer (75 mM Na_2HPO_4 , 40 mM NaH_2PO_4 , 1 mM KCl, 1 mM MgSO_4 ; pH 7.0). 100 μL of 0.1 % SDS was added together with 20 μL chloroform. The samples were vortexed for 20 sec and then left on the bench to sediment until samples cleared up. Two hundred microliters of each sample was transferred to a 96-well plate. Twenty-five microliters of a 4 mg/ml σ -nitrophenyl- β -D-galactopyranoside (σ NPG) solution (dissolved in Z-buffer) was added as the substrate. The β -galactosidase activity was measured in a plate reader at 405 nm (20 reads; fastest interval) and determined as the initial slope of the curve in the linear range. Experiments were carried out as biological triplicates.

Strains, plasmids and oligonucleotides

Table S1A

Strain	Genotype	Source
MG1655	<i>E. coli</i> K-12	Blattner et al.
AB607	$\Delta pdeH::frr$	A. Böhm
AB958	<i>csrA::Tn5Δ(kan)::frr</i>	A. Böhm
AB959	<i>csrA::Tn5Δ(kan)::frr ΔdgcZ::frr</i>	A. Böhm
AB330	λ cI857 Δ (<i>cro-bioA</i>)	A. Böhm
AB989	λ cI857 Δ (<i>cro-bioA</i>) <i>kan::P_{hta}-ccdB-lacZ</i>	A. Böhm
BL21 (AI)	<i>FompT hsdS_B (r_B m_B) gal dcm araB::T7RNAP-tetA</i>	Life technologies
AB1928	<i>pdeB-3xflag::kan</i>	this study
AB1925	<i>pdeL-3xflag::kan</i>	this study
AB1985	<i>pdeC-3xflag::kan</i>	this study
AB1923	<i>pdeR-3xflag::kan</i>	this study
AB2161	<i>pdeO-3xflag::kan</i>	this study
AB1926	<i>pdeH-3xflag::kan</i>	this study
AB1989	<i>pdeF-3xflag::kan</i>	this study
AB1924	<i>pdeA-3xflag::kan</i>	this study
AB1987	<i>pdeK-3xflag::kan</i>	this study
AB1927	<i>pdeI-3xflag::kan</i>	this study
AB1922	<i>pdeN-3xflag::kan</i>	this study
AB1986	<i>pdeD-3xflag::kan</i>	this study
AB1988	<i>pdeG-3xflag::kan</i>	this study
AB2023	<i>pdeB-3xflag::kan ΔpdeH::frr</i>	this study
AB2024	<i>pdeL-3xflag::kan ΔpdeH::frr</i>	this study
AB2025	<i>pdeC-3xflag::kan ΔpdeH::frr</i>	this study
AB2026	<i>pdeR-3xflag::kan ΔpdeH::frr</i>	this study
AB2162	<i>pdeO-3xflag::kan ΔpdeH::frr</i>	this study
AB2027	<i>pdeF-3xflag::kan ΔpdeH::frr</i>	this study
AB2028	<i>pdeA-3xflag::kan ΔpdeH::frr</i>	this study
AB2029	<i>pdeK-3xflag::kan ΔpdeH::frr</i>	this study
AB2032	<i>pdeI-3xflag::kan ΔpdeH::frr</i>	this study
AB2030	<i>pdeN-3xflag::kan ΔpdeH::frr</i>	this study
AB2031	<i>pdeD-3xflag::kan ΔpdeH::frr</i>	this study
AB2033	<i>pdeG-3xflag::kan ΔpdeH::frr</i>	this study
AB2077	<i>pdeB-3xflag::kan csrA::Tn5Δ(kan)::frr</i>	this study
AB2078	<i>pdeL-3xflag::kan csrA::Tn5Δ(kan)::frr</i>	this study
AB2079	<i>pdeC-3xflag::kan csrA::Tn5Δ(kan)::frr</i>	this study
AB2080	<i>pdeR-3xflag::kan csrA::Tn5Δ(kan)::frr</i>	this study
AB2163	<i>pdeO-3xflag::kan csrA::Tn5Δ(kan)::frr</i>	this study

AB2081	<i>pdeH-3xflag::kan csrA ::Tn5Δ(kan)::frit</i>	this study
AB2082	<i>pdeF-3xflag::kan csrA ::Tn5Δ(kan)::frit</i>	this study
AB2083	<i>pdeA-3xflag::kan csrA ::Tn5Δ(kan)::frit</i>	this study
AB2084	<i>pdeK-3xflag::kan csrA ::Tn5Δ(kan)::frit</i>	this study
AB2085	<i>pdeI-3xflag::kan csrA ::Tn5Δ(kan)::frit</i>	this study
AB2086	<i>pdeN-3xflag::kan csrA ::Tn5Δ(kan)::frit</i>	this study
AB2087	<i>pdeD-3xflag::kan csrA ::Tn5Δ(kan)::frit</i>	this study
AB2088	<i>pdeG-3xflag::kan csrA ::Tn5Δ(kan)::frit</i>	this study
AB2038	<i>acrB'-pdeB-3xflag::kan ΔpdeH::frit</i>	this study
AB2034	<i>pdeC (IS ins.)-3xflag::kan ΔpdeH::frit</i>	this study
AB2035	<i>pdeL (G299S)-3xflag::kan ΔpdeH::frit</i>	this study
AB2036	<i>pdeL (F206S)-3xflag::kan ΔpdeH::frit</i>	this study
AB2037	<i>pdeL (F249L)-3xflag::kan ΔpdeH::frit</i>	this study
AB3062	<i>pdeL (L207W) ΔbetI::kan ΔpdeH::frit</i>	this study
AB3063	<i>pdeL (L207F) ΔbetI::kan ΔpdeH::frit</i>	this study
AB3057	<i>pdeL (L261Q) ΔbetI::kan ΔpdeH::frit</i>	this study
AB3058	<i>pdeL (T266M) ΔbetI::kan ΔpdeH::frit</i>	this study
AB3059	<i>pdeL (T270A) ΔbetI::kan ΔpdeH::frit</i>	this study
AB3061	<i>pdeL (G299A) ΔbetI::kan ΔpdeH::frit</i>	this study
AB3060	<i>pdeL (Q326L) ΔbetI::kan ΔpdeH::frit</i>	this study
AB2039	<i>pdeA (V285G)-3xflag::kan ΔpdeH::frit</i>	this study
AB2040	<i>pdeN (R465L)-3xflag::kan ΔpdeH::frit</i>	this study
AB2041	<i>pdeN (W36R)-3xflag::kan ΔpdeH::frit</i>	this study
AB2145	<i>pdeI (G412S)-3xflag::kan ΔdeoR::frit ΔpdeH::frit</i>	this study
AB2089	<i>acrB'-pdeB-3xflag::kan csrA ::Tn5Δ(kan)::frit</i>	this study
AB2093	<i>pdeC (IS ins.)-3xflag::kan csrA ::Tn5Δ(kan)::frit</i>	this study
AB2090	<i>pdeL (G299S)-3xflag::kan csrA ::Tn5Δ(kan)::frit</i>	this study
AB2091	<i>pdeL (F206S)-3xflag::kan csrA ::Tn5Δ(kan)::frit</i>	this study
AB2092	<i>pdeL (F249L)-3xflag::kan csrA ::Tn5Δ(kan)::frit</i>	this study
AB2094	<i>pdeA (V285G)-3xflag::kan csrA ::Tn5Δ(kan)::frit</i>	this study
AB2095	<i>pdeN (R465L)-3xflag::kan csrA ::Tn5Δ(kan)::frit</i>	this study
AB2096	<i>pdeN (W36R)-3xflag::kan csrA ::Tn5Δ(kan)::frit</i>	this study
AB2146	<i>pdeI (G412S)-3xflag::kan ΔdeoR::frit csrA ::Tn5Δ(kan)::frit</i>	this study
AB2109	<i>acrB'-pdeB-3xflag::kan csrA ::Tn5Δ(kan)::frit ΔydeH::frit</i>	this study
AB2110	<i>pdeL (G299S)-3xflag::kan csrA ::Tn5Δ(kan)::frit ΔdgcZ::frit</i>	this study
AB2111	<i>pdeL (F206S)-3xflag::kan csrA ::Tn5Δ(kan)::frit ΔdgcZ::frit</i>	this study
AB2112	<i>pdeL (F249L)-3xflag::kan csrA ::Tn5Δ(kan)::frit ΔdgcZ::frit</i>	this study
AB2113	<i>pdeC (IS1 ins.)-3xflag::kan csrA ::Tn5Δ(kan)::frit ΔdgcZ::frit</i>	this study
AB2114	<i>pdeA (V285G)-3xflag::kan csrA ::Tn5Δ(kan)::frit ΔdgcZ::frit</i>	this study
AB2115	<i>pdeN (R465L)-3xflag::kan csrA ::Tn5Δ(kan)::frit ΔdgcZ::frit</i>	this study
AB2116	<i>pdeN (W36R)-3xflag::kan csrA ::Tn5Δ(kan)::frit ΔdgcZ::frit</i>	this study

AB2147	<i>pdeI (G412S)-3xflag::kan ΔdeoR::frt csrA::Tn5Δ(kan)::frt ΔdgcZ ::frt</i>	this study
AB2117	<i>ΔpdeH::frt ΔpdeL::frt ΔpdeA::frt ΔpdeR::frt ΔpdeN::frt ΔpdeC::frt</i> <i>λ-att::(bla lacIQ P_{lac}::ycgR) Δaes::kan p_{wsp}R</i>	this study
AB2118	<i>ΔpdeH::frt ΔpdeA::frt ΔpdeL::frt ΔpdeR::frt ΔpdeN::frt ΔpdeC::frt</i> <i>λ-att::(bla lacIQ P_{lac}::ycgR) ΔbetI::kan p_{wsp}R</i>	this study
AB2119	<i>ΔpdeH::frt ΔpdeL::frt ΔpdeA::frt ΔpdeR::frt ΔpdeN::frt ΔpdeC::frt</i> <i>λ-att::(bla lacIQ P_{lac}::ycgR) ΔmalK::kan p_{wsp}R</i>	this study
AB2120	<i>ΔpdeH::frt ΔpdeL::frt ΔpdeA::frt ΔpdeB::frt ΔpdeC::frt ΔpdeN::frt</i> <i>λ-att::(bla lacIQ P_{lac}::ycgR) ΔtrpC::kan p_{wsp}R</i>	this study
AB2121	<i>ΔpdeH::frt ΔpdeL::frt ΔpdeA::frt ΔpdeR::frt ΔpdeN::frt ΔpdeC::frt</i> <i>λ-att::(bla lacIQ P_{lac}::ycgR) ΔosmC::kan p_{wsp}R</i>	this study
AB2122	<i>ΔpdeH::frt ΔpdeL::frt ΔpdeA::frt ΔpdeR::frt ΔpdeN::frt ΔpdeC::frt</i> <i>λ-att::(bla lacIQ P_{lac}::ycgR) ΔpurM::kan p_{wsp}R</i>	this study
AB2123	<i>ΔpdeH::frt ΔpdeL::frt ΔpdeI::frt ΔpdeR::frt ΔpdeN::frt ΔpdeC::frt</i> <i>λ-att::(bla lacIQ P_{lac}::ycgR) ΔptsI::kan p_{wsp}R</i>	this study
AB2124	<i>ΔpdeH::frt ΔpdeL::frt ΔpdeA::frt ΔpdeR::frt ΔpdeN::frt ΔpdeC::frt</i> <i>λ-att::(bla lacIQ P_{lac}::ycgR) ΔdctA::kan p_{wsp}R</i>	this study
AB2125	<i>ΔpdeH::frt ΔpdeL::frt ΔpdeA::frt ΔpdeR::frt ΔpdeN::frt ΔpdeC::frt</i> <i>λ-att::(bla lacIQ P_{lac}::ycgR) ΔdeoR::kan p_{wsp}R</i>	this study
AB2126	<i>ΔpdeH::frt ΔpdeL::frt ΔpdeA::frt ΔpdeR::frt ΔpdeC::frt</i> <i>λ-att::(bla lacIQ P_{lac}::ycgR) ΔfruB::kan p_{wsp}R</i>	this study
AB2127	<i>ΔpdeH::frt ΔpdeL::frt ΔpdeA::frt ΔpdeR::frt ΔpdeN::frt ΔpdeC::frt</i> <i>λ-att::(bla lacIQ P_{lac}::ycgR) ΔmanX::kan p_{wsp}R</i>	this study
AB2128	<i>ΔpdeH::frt ΔpdeL::frt ΔpdeA::frt ΔpdeR::frt ΔpdeN::frt ΔpdeC::frt</i> <i>λ-att::(bla lacIQ P_{lac}::ycgR) ΔicdC::kan p_{wsp}R</i>	A. Böhm
AB1868	<i>ΔpdeH::frt ΔpdeL::frt ΔpdeA::frt ΔpdeB::frt</i> <i>λ-att::(bla lacIQ P_{lac}::ycgR) ΔlacZ 4787(::<rrnb-3)< i=""></rrnb-3)<></i>	A. Böhm
AB1374	<i>ΔpdeH::frt ΔpdeL::frt ΔpdeA::frt</i> <i>λ-att::(bla lacIQ P_{lac}::ycgR)</i>	A. Böhm
AB3142	<i>ΔpdeH::frt λ-att::(bla lacIQ P_{lac}::ycgR)</i>	A. Böhm
AB2531	<i>pdeL-3xflag::frt kan:: P_{pdeL}-lacZ</i>	this study
AB2844	<i>ΔdgcE::frt ΔdgcN::frt ΔdgcO::frt ΔdgcQ::frt (Δ4) pdeL-3xflag::frt kan:: P_{pdeL}-lacZ</i>	this study
AB2834	<i>ΔpdeH::frt pdeL-3xflag::frt kan:: P_{pdeL}-lacZ</i>	this study
AB2569	<i>ΔpdeL::frt kan:: P_{pdeL}-lacZ</i>	this study
AB2842	<i>ΔdgcE::frt ΔdgcN::frt ΔdgcO::frt ΔdgcQ::frt (Δ4) ΔpdeL::frt kan:: P_{pdeL}-lacZ</i>	this study
AB2854	<i>ΔpdeH::frt ΔpdeL::frt kan:: P_{pdeL}-lacZ</i>	this study
AB2378	<i>ΔpdeH::frt pdeL (G299S)-3xflag::frt kan:: P_{pdeL}-lacZ</i>	this study
AB2942	<i>ΔpdeH::frt pdeL (F206S)-3xflag::frt kan:: P_{pdeL}-lacZ</i>	this study
AB2945	<i>ΔpdeH::frt pdeL (F249L)-3xflag::frt kan:: P_{pdeL}-lacZ</i>	this study
AB3000	<i>bcsQ⁺</i>	this study
AB3143	<i>bcsQ⁺ ΔpdeH::frt</i>	this study

AB3144	<i>bcsQ⁺ ΔpdeH::frrt pdeL (G299S)-3xflag::kan</i>	this study
AB3145	<i>bcsQ⁺ ΔpdeH::frrt pdeL (F206S)-3xflag::kan</i>	this study
AB3146	<i>bcsQ⁺ ΔpdeH::frrt pdeL (F249L)-3xflag::kan</i>	this study

Table S1B

Plasmid	Genotype	Comments	Source
pCP20	FLP ⁺ (<i>amp</i>) (<i>cat</i>)	Temperature sensitive replication and thermal induction of FLP recombinases	Cherepanov et al.
pSUB11	<i>3xflag::kan</i>	<i>3xflag</i> -tag template for generation of chromosomal <i>3xflag::kan</i> constructs	Uzzau et al.
pKD46	λ-RED ⁺ (<i>amp</i>)	Arabinose inducible expression of λ-RED genes	Datsenko et al.
pKD45	<i>kan::P_{ma}ccdB</i>	Rhamnose inducible CcdB toxin with adjacent kan-cassette	Datsenko et al.
<i>pwspR</i>	<i>wspR</i> in pME6032 (<i>tetR</i>)	IPTG inducible expression of <i>wspR</i> from <i>P. fluorescens</i>	J. Malone
pAR1	<i>pdeL-strepII</i> in pET28a (<i>kan</i>)	PdeL-StrepII overexpression plasmid	this study
pAR2	<i>pdeL (G299S)-strepII</i> in pET28a (<i>kan</i>)	PdeL (G299S)-StrepII overexpression plasmid	this study
pAR54	<i>pdeL (F206S)-strepII</i> in pET28a (<i>kan</i>)	PdeL (F206S)-StrepII overexpression plasmid	this study
pAR55	<i>pdeL (F249L)-strepII</i> in pET28a (<i>kan</i>)	PdeL (F249L)-StrepII overexpression plasmid	this study

Table S1C

Oligonucleotide	Sequence	Purpose
1639-yhjH_test_fwd	cctaacgtccgcgctttctcgg	PCR, seq.
1640-yhjH_test_rev	tgactaatgaacggagataatccctcacc	PCR, seq.
3262-yhjH_3xFlag_P1	CACGCCCGGCACCGATAGAAACGCTGAA TACGGCGGTTCTGGCGCTAttgactacaagg accatgacgg	C-ter 3xFlag-tag
3263-yhjH_3xFlag_P2	gttcgtctctcatattctctgtgccagtcctaaag atagTACATATGAATATCCTCCTTAG	
1658_yhjH_test_fwd_new	tcatgattcgccaatcacggc	PCR, seq.
1659_yhjH_test_rev_new	cgcgtggcaaatgaccatcg	PCR, seq.
1674-yahA_upstream_fwd	ttgtttttttggcattgctataattgg	PCR, seq.

1674-yahA_upstream_fwd	ttgtttttatggcattgctataattgg	PCR, seq.
1675-yahA_rev	aatggcatattaacgggatctatcagg	PCR, seq.
2978-yahA_3xFLAG_P1	ACCGGGTAATAAAATTTATCTCTGAATGG GTAATGAAAGCAGGTGGTttcgactacaaag accatgacgg	C-ter 3xFlag-tag
2979-yahA_3xFLAG_P2	TACTGCATCGGGAGAATTAAtcgetgccaa ctcccgatgcgctgTACATATGAATATCCT CCTTAG	C-ter 3xFlag-tag
3158_rtn_test_fwd	ccgctcttgatccaggctatagccg	PCR, seq.
3159_rtn_test_rev	agcagtatgcgcacaatcatctgcaacg	PCR, seq.
3220_rtn_seq_550_fwd	CGCTCTGAATCTCAACCTGACGCC	seq.
3268_rtn_3xFLAG_P1	TTTTGTTCGCTGGCTAAAGAAACCGTATA CGCCGACGTGGTtcgactacaaagaccatgacgg	C-ter 3xFlag-tag
3269_rtn_3xFLAG_P2	tagccgaatccggcatgctttcactatgaataaagggTA CATATGAATATCCTCCTTAG	C-ter 3xFlag-tag
2362_yfgF_fwd	cgctgtggacggctactacattaaggc	PCR, seq.
2363_yfgF_rev	gacactgctgttcccgatgac	PCR, seq.
3395_yfgF_3x_FLAG_P1	TAATTGATACGCTGAATGAAATCGAACCC CATTCCGCAAAGTGCCctcgactacaaagaccat gacgg	C-ter 3xFlag-tag
3396_yfgF_3x_FLAG_P2	ACACCAGAAATCGCCGCTTAAactttgacgg gccgcagagaaaTACATATGAATATCCTCCT TAG	C-ter 3xFlag-tag
3475_yfgF_test_seq_1	GGTTACAGGGTCTTTACTCCCCGGCG TAAC	seq.
3476_yfgF_test_seq_2	GTCAATTATATGGCTGTACTGGCAACCC GTCAGAG	seq.
3477_yfgF_test_seq_3	CATTTTTTCTGATGGCCAGCCGATT ACCG	seq.
1749-yfeA_up_fwd	ggttttttctctctcttttggccg	PCR, seq.
1750-yfeA_down_rev	TAGCGCTATATGGGATAAATCCCCG	PCR, seq.
1751-yfeA_435_fwd	ATGCAGCATGTATCTTGTGGGGAGC	seq.
1752-yfeA_1021_fwd	TCCTACCCAACCTTCGTGCGTTGG	seq.
1857-yfeA_test_rev	aggcgtcgcattctcagatggctc	PCR, seq.
3266-yfeA_3xFLAG_P1	GCAAGGGTATTTGATTGGTCGCCCCGA GCCATTAGCTGATtcgactacaaagaccatgacgg	C-ter 3xFlag-tag
3267-yfeA_3xFLAG_P2	ttcttcagatggttcaacccttaagttagcgtcttatgggata TACATATGAATATCCTCCTTAG	C-ter 3xFlag-tag
3164-ycgG_test_fwd	ttctaccatgctctctgtagatccagc	PCR, seq.

3165-ycgG_test_rev	gctgtctataattacaccgcactatggcc	PCR, seq.
3393_ycgG_3x_FLAG_P1	GGTCAA AATTATCCTTTCTAAACCGAA GGTGAAGGTTGTGGTTGAGttcgactacaaa gaccatgacgg	C-ter 3xFlag-tag
3394_ycgG_3x_FLAG_P2	taattagctgtctataattacaccgcactatggccttactgatc aaTACATATGAATATCCTCCTTAG	C-ter 3xFlag-tag
3520_ycgG_test_seq_1	GGACATTATCCCTATACCGAGAAGG TTCCTCC	seq.
3521_ycgG_test_seq_2	GGCTACTCAGGGCTTTCTTATCTTCAT GACCTG	seq.
3276_yddU_3xFLAG_P1	AGAAAATCCAGGCTGGATGAGCAGCGT GTTACCGCTGAAAATCttcgactacaagacca tgacgg	C-ter 3xFlag-tag
3277_yddU_3xFLAG_P2	tcgtagctgaaatcacagltttaagtgacagtgctcagttaa atgTACATATGAATATCCTCCTTAG	C-ter 3xFlag-tag
3335_yddU_test_fwd	GGCGTATTCAATTCGATCTCCAGATC AGGG	PCR, seq.
3336_yddU_test_rev	GTGGGGCCATAACACTGGTGATGAAATTC	PCR, seq.
3337_yddU_seq_1_rev	GGAAGACTGACTAAGCGGGATAATCCGG	seq.
3338_yddU_seq_2_rev	GCCGTTACCGCCATTTCTGCGAATATAATC	seq.
3339_yddU_seq_3_rev	CAGCGAAACATGCGATTCGTTGAGTAC	seq.
3340_yddU_seq_4_rev	GACTCATCCCCTCAACACGGCCTTTAC	seq.
2360_yhjK_fwd	ccagcaggcgaagattacgcac	PCR, seq.
2361_yhjK_rev	ccagcaggcgaagattacgcac	PCR, seq.
2371_yhjK_fwd_2	CAGCAGCGAAAGATTACGCAC	PCR, seq.
2372_yhjK_rev_2	gctgtcaggacctgaaagtaaaggc	PCR, seq.
3391-yhjK_3x_FLAG_P1	CGCCCACTCCCTATTGAAATCTTCGAA GAGAGTTACCTGGAAAGAAAAGttcgactac aaagaccatgacgg	C-ter 3xFlag-tag
3392_yhjK_3x_FLAG_P2	ggctgcacaaaccgactttttaagtttgaatcagttt ggggTACATATGAATATCCTCCTTAG	C-ter 3xFlag-tag
1649-yliE_test_fwd	gatggtttacgcatgcgctgg	PCR, seq.
1650-yliE_test_rev	aaaccgagtcggcgtaagctgtgc	PCR, seq.
3272-yliE_3xFLAG_P1	GCCATTTCTCCGCTGGGATAAAAAGTG GAAAATTAGTAAAAGAGttcgactacaaag accatgacgg	C-ter 3xFlag-tag
3273-yliE_3xFLAG_P2	agactgactgtaagtacgaacttattgattcggacatcgt TACATATGAATATCCTCCTTAG	C-ter 3xFlag-tag
3517_yliE_test_seq_1	GATTTTAACCCATCGAAACGACCGT GGTCGGTG	seq.

3518_yliE_test_seq_2	CGATCGCGGAAATGAAAGATGCCGA AATTG	seq.
3519_yliE_test_seq_3	GTCTATCAACCGATCGTTGATATTA CACCCGC	seq.
2539-ylaB_fwd	gcttggtcaaatgacaatgatcgtttcc	PCR, seq.
2540-ylaB_seq1_fwd	CACAAGGGAAAAGATGCGCTGCAGG	seq.
2541-ylaB_seq2_fwd	GGCTACAAAAACACCCGGTGAGC	seq.
2543-ylaB_rev	atggcggattcagatcaatcatcg	PCR, seq.
2588-ylaB_seq_rev	CACAAACATCGCTGCCAGCAGG	seq.
3274-ylaB_3xFLAG_P1	TTACCGAAAAGAAGATTCTTACGCTG GGCCGAGCAACATTTGtgcactacaagaac catgacgg	C-ter 3xFlag-tag
3275-ylaB_3xFLAG_P2	GAATATCCTCCTTAGGATGGAGCAAT TACCCGCGCGGA	C-ter 3xFlag-tag
3270-yjcC_3xFLAG_P1	GTTAACGCGCGGCAAttgcactacaagaac catgacgg	C-ter 3xFlag-tag
3271-yjcC_3xFLAG_P2	cggcagttgatcgactccagcattatcgccacgcct gtaTACATATGAATATCCTCCTTAG	C-ter 3xFlag-tag
3283_yjcC_test_fwd	GTGGTAGGGTAGCCATCAAACAATT CCTCTG	PCR, seq.
3284_yjcC_test_rev	GCAACATATCGCAACACATCACGTTT ATATCGCC	PCR, seq.
3285_yjcC_seq_1	CTGAACGCTATCAGGGCAAGTTT GCACTC	seq.
3286_yjcC_seq_2	CGCGCCCTCGAAAAACATCAACTTTGTC	seq.
3162-yoaD_test_fwd	cgcttctcgtctgtaataattccc	PCR, seq.
3163-yoaD_test_rev	gaagccaatgattatcggttgatctgg	PCR, seq.
3397_yoaD_3x_FLAG_P1	GCCCCCCGGCATAATGGACATATCA CGCCCATATGCCGTTACGTTgcactacaaa gaccatgacgg	C-ter 3xFlag-tag
3398_yoaD_3x_FLAG_P2	gttcgaattgtaagagcaaccggcgacgatgaagatga gtaaTACATATGAATATCCTCCTTAG	C-ter 3xFlag-tag
3473_yoaD_test_seq_1	GCTGGGGTACATGGAGATGATTAACAT CGAC	seq.
3474_yoaD_test_seq_2	GATCTCAATCAGTACTGGTTTAGCGCTC ACCCG	seq.
3160-yciR_test_fwd	aaccgggactccgctgtaaccg	PCR, seq.
3161-yciR_test_rev	gggcatcaaatcagacatcaagacatcc	PCR, seq.
3264-yciR_3xFLAG_P1	CGCCTTCGAACGCTGGTATAAACGCTA TCTGAAGCGCGCAAttgcactacaagaacatgacgg	C-ter 3xFlag-tag

3265-yciR_3xFLAG_P2	caacggctaattatcatccaggaatcacgatataataatgacgg gaTACATATGAATATCCTCCTTAG	C-ter 3xFlag-tag
4697-yahA-strepII_NcoI_fwd.	CAAAAAAACCATGGCTAATTCATGTGATTTT CGTG	<i>pdeL-strepII</i>
4698-yahA-strepII_NotI_rev.	CAAAAAAAGCGGCCGCTTACTTTTCGAACT GCGGGTGGCTCCAACCACCTGCTTTCATTA CCCATTC	<i>pdeL-strepII</i>
4398-PyahA-lacZ (transl.)_fwd.	TCGCTGTCTGTCTCCGGAAGTGTGAGGC CATGGTGGCCTTGTTATTGCATAAAAACCGC GCC	P_{pdeL} -lacZ
4399-PyahA-lacZ (transl.)_rev.	CGTTGTA AACGACGCCAGTGAATCCGTA ATCATGGTCATCAGAAAAACAGAAAATCA CATGAATTCATGAACACACCTTTATCTTTT ATC	P_{pdeL} -lacZ
7335-bcsQ-kan-ccdB_fwd.	CTGCCTGATCCC CGGATAGGCTATATCTTCC AGAATGATATTGTGGCGTTCAGAGAAGCTC GTCAAGAAG	bcsQ repair
7336-bcsQ-kan-ccdB_rev.	TAGCGCAACCCAGCGTCACGCCAGTCCTG GCCATCCAGCATCGCTCTGCCCGATATTA TCGTGAGGATG	bcsQ repair
7337-bcsQ-repair_fwd.	CTGCCTGATCCC CGGATAGGCTATATCTTCC CAGAATGATATTGTGGCG	bcsQ repair
7338-bcsQ-repair_rev.	TAGCGCAACCCAGCGTCACGCCAGTCCTG GCCATCCAGCATCGCTC	bcsQ repair
7339-bcsQ-repair_SOE_fwd.	CCACGCCTCCC CGCACCCCTGCAATCCC AGTACGGCCATTCAACAATC	bcsQ repair
7340-bcsQ-repair_SOE_rev.	GATTGGTGAATGGCCGTACTGGGATTGCAG GGGGTGGGGGAGGCGTGG	bcsQ repair
8034-bcsQ_test_fwd	GTTTTTATGTTCTGCGCGAATACGCTGCCAG	PCR, seq.
8035-bcsQ_test_rev	GTAACGGAAAGTCAAAAAGTGAGCAAATTC CCGCTCTGCGG	PCR, seq.
4991-yahA-EMSA-20	GTGCGAATGTTCAATAAGTTTAG	EMSA
4997-yahA-pal-3-rev	ATGCGTCATTTCAAATGATCAGC	EMSA

Chapter 4 | PROJECT 3

Stay or go? A bistable molecular switch facilitating bacterial lifestyle transitions

Alberto Reinders, Shogo Ozaki, Johanna Rueher, Benjamin Sellner, Matteo Sangermani,
Tilman Schirmer and Urs Jenal

Adapted from:
'Stay or go? A bistable molecular switch facilitating bacterial lifestyle transitions'
Manuscript under preparation

Abstract

Bacteria preferentially colonize surfaces and air-liquid interfaces as matrix embedded communities called biofilms. Biofilms exhibit specific physiological properties, including general stress tolerance, increased antibiotic recalcitrance and tolerance against phagocytic clearance. Together this largely accounts for increased biofilm persistence, chronic infections and infection relapses. One of the principle regulators of biofilm formation is c-di-GMP, a bacterial second messenger controlling various cellular processes. Cellular levels of c-di-GMP are controlled by two antagonistic enzyme families, diguanylate cyclases and phosphodiesterases. But despite the identification and characterization of an increasing number of components of the c-di-GMP network in different bacterial model organisms, details of c-di-GMP mediated decision-making have remained unclear. In particular, how cells shuttle between specific c-di-GMP regimes at the population and single cell level is largely unknown and moreover how these transitions are deterministically made in time and space, given that bacterial networks of diguanylate cyclases and phosphodiesterases show a high degree of complexity.

Here we describe a novel mechanism regulating c-di-GMP mediated biofilm formation in *E. coli*. This mechanism relies on the bistable expression of a key phosphodiesterase that acts both as catalyst for c-di-GMP degradation and as a transcription factor promoting its own production. Bistability results from two interconnected positive feedback loops operating on the catalytic and gene expression level. Based on genetic, structural and biochemical analyses we postulate a simple substrate-induced switch mechanism through which this enzyme can sense changing concentration of c-di-GMP and convert this information into a bistable c-di-GMP response. This mechanism may explain how cellular heterogeneity of small signaling molecules is generated in bacteria and used as a bet hedging strategy for important lifestyle transitions.

Introduction

To maintain their own integrity and fitness, all living organisms need to be able to effectively change the cellular program in order to take over specialized functions or to respond to changes in the environment. To provide directionality to key cellular decisions such as changing cell shape and/or behavior, the respective regulatory networks need to be deterministic and robust. For example, stem cells need to stably maintain their replicative program but at the same time be capable to rapidly induce cell differentiation in response to external signals [215,216]. This is mainly achieved through positive feedback regulation and mutual cross-inhibition of master regulators activating downstream feedforward regulatory cascades [217]. Thus, although differentiation of cells is not terminal, reversion of this highly coordinated and robust process becomes harder, the more differentiation has proceeded [218].

In analogy, bacteria can transit between two different forms of behavior, a motile single cell and a sessile, community-based lifestyle called biofilm [161,162,219]. These two lifestyles are fundamentally different with respect to gene expression patterns and the overall physiological state of the cell [220-223]. Consequently, both the transition between and the stable maintenance of these two physiological states come with substantial costs. Thus, the decision to transit from single cell to community behavior requires fine-tuned regulatory processes that integrate environmental signals and – in response – establish robust and stable programs at the right time and space. While several aspects of cellular control mechanisms of this switch have been uncovered, it has remained unclear which factors contribute to the directionality and stability of this important bi- or multimodal program [224].

One of the central regulators of this physiological adaptation is the second messenger c-di-GMP. Discovered as a small signaling molecule stimulating cellulose production in *Gluconacetobacter xylinus* [1], c-di-GMP controls important behavioral processes such as motility [78], virulence [225], biofilm formation [110] or cell-cycle regulation [9]. Planktonic cells are associated with low intracellular c-di-GMP concentrations [78,79], whereas sessile communities generally display high levels of c-di-GMP [128]. Most bacteria harbor large arrays of enzymes that synthesize (diguanylate-cyclases, DGC) or degrade c-di-GMP (phosphodiesterases PDE) to adjust their internal concentration of the second messenger in response to specific intrinsic or extrinsic signals [59,61,72-75]. The internal c-di-GMP concentration is then sensed by downstream effectors, which ultimately elicit a cellular function (see reviews [54,219]). The co-occurrence of multiple DGCs and PDEs, combined with hypersensitive downstream effectors (nM affinities) poses the problem of stochastic noise and network stability [161,162]. While in eukaryotic cells, compartmentalization can potentially shield cellular components from such effects, bacteria cannot rely on physical barriers. Thus, there is a necessity for systems that buffer stochastic fluctuations and establish precise threshold concentrations of c-di-GMP to initiate rapid program switch. We postulate that in order to install stable programs, cells harbor specialized enzymes with the ability to “sense” the prevailing c-di-GMP levels and are equipped with feedback control and

non-linear behavior. In principle such a cellular component could generate populations with bistable c-di-GMP steady states, where intermediate levels would be highly unstable [226].

Here we characterize the c-di-GMP-specific phosphodiesterase and transcription factor PdeL from *Escherichia coli* K-12. We show that PdeL is feedback regulated both on the transcriptional and on the enzymatic level and that these properties install bistable c-di-GMP regimes in *E. coli* cells. PdeL transcription is under superordinate control by the central metabolic regulator Cra, which binds to the *pdeL* promoter region to recruit PdeL. PdeL stimulates its own expression in a c-di-GMP-dependent manner. This positive feedback loop on the transcriptional level is assisted by a double-negative feedback loop at the enzymatic level where c-di-GMP inhibits PdeL activity and PdeL itself negatively contributes to the c-di-GMP pool. As a consequence, PdeL shows high catalytic and transcription activity at low c-di-GMP levels, while the protein is catalytically and transcriptionally inert when c-di-GMP levels are high. We present structural, biochemical and genetic evidence that PdeL catalysis and transcription are directly interlinked through a c-di-GMP-driven non-linear conformational switch of PdeL. This system generates bistable populations with a high degree of cellular memory that buffers against noise in c-di-GMP distribution and establishes self-sustained heritable regimes of a potent small signaling molecule.

Results

Cra and PdeL are activators of *pdeL* transcription

To understand the determinants of *pdeL* auto-regulation, we set out to dissect the regulatory elements of the *pdeL* promoter region (**Figure 1A**). This region contains a σ^{70} -dependent promoter, 341 bp upstream of the *pdeL* start codon [227], a binding site for the central metabolic regulator Cra (catabolite repressor activator) [227,228], and a palindromic binding site for PdeL 675 bp upstream of the *pdeL* start codon [79]. We first confirmed that Cra binds with high affinity ($K_D = 49$ nM) to a site 114 bp upstream of the *pdeL* promoter, which shows strong similarity to other Cra binding sites [228] (**Figure 1A, B & S1A, B**). EMSA experiments with different DNA fragments and oligonucleotides spanning the promoter region revealed an additional binding site for PdeL in the immediate vicinity of the Cra binding site (**Figure 1A & B**). PdeL binding to this site was dependent on the presence of Cra, indicating that Cra is able to recruit PdeL to this site upstream of the promoter. We thus termed this binding site Cra-dependent PdeL-box (CDB). Titration experiments revealed that PdeL binds to this DNA site with an affinity similar to Cra ($K_D = 76$ nM) (**Figure S1C, D**). In contrast, PdeL binds to the upstream Cra-independent binding site (CIB) with significantly lower affinity ($K_D = 573$ nM) (**Figure 1B & S1E, F**). While c-di-GMP negatively impacts *pdeL* transcription [79], *in vitro* binding of PdeL to the CDB and CIB sites was not modulated by c-di-GMP (**Figure 1B**).

Strains lacking Cra or PdeL showed strongly reduced *pdeL* promoter activity as compared to wild type (**Figure 1C**), arguing that both proteins help stimulating *pdeL* transcription. Scrambling of the Cra- or PdeL-boxes (**Figure S1G, H**), resulted in a similar reduction of *pdeL* promoter activity (**Figure 1C**). The observation that the *cra* deletion had a stronger effect as compared to the *pdeL* mutant, together with the observation that Cra is required for PdeL binding to the CDB site indicated that Cra acts upstream of PdeL in stimulating *pdeL* transcription. Scrambling one half-site of the CIB palindrome significantly reduced *pdeL* transcription 2.5-fold (**Figure 1C**).

A previous study had shown that the histone-like protein H-NS binds to the intergenic region of *pdeL* [229]. After recognition of a specific nucleation consensus sequence [230-232], H-NS is described to polymerize across AT-rich DNA-stretches thus facilitating bending or bridging of DNA [233]. The *pdeL* promoter region has a relatively high AT content (66%) and contains several putative H-NS recognition sequences, one of which overlaps the 5'-palindrome half-site of the CIB (**Figure 1A & S5**). EMSA analyses showed that PdeL competes with H-NS for binding to the CIB (**Figure 1D**). In agreement with H-NS acting as a transcriptional silencer of *pdeL* [234], an *hns* mutant showed strong derepression of *pdeL* transcription (**Figure 1C**).

Together these data indicated that Cra, PdeL and H-NS are critical regulatory elements of the *pdeL* promoter. The data suggested that H-NS acts as a transcriptional silencer, possibly by protecting large regions of the *pdeL* promoter region.

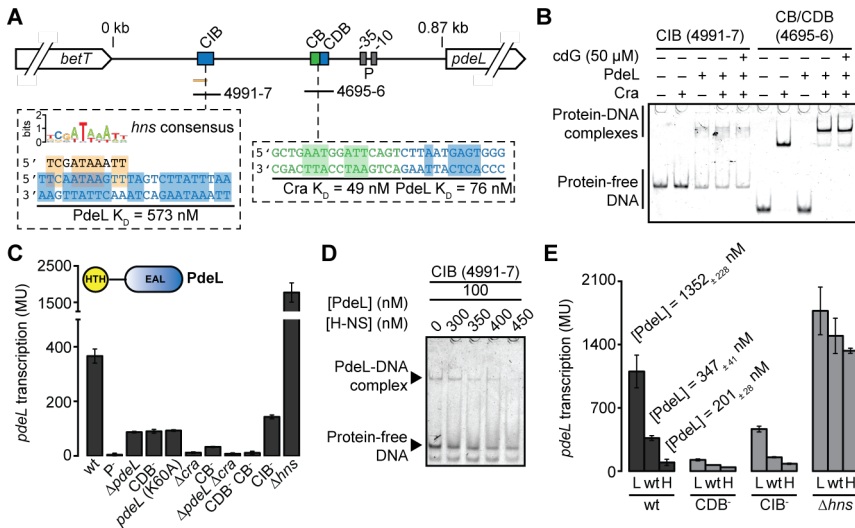


Figure 1 | Regulation of *pdeL* transcription. (A) Schematic representation of *pdeL* intergenic region (not to scale). Minimal binding regions for PdeL- and Cra-binding are shown in blue and green respectively. Palindromes or bases, which were identified to be crucial for transcription factor binding are highlighted in blue or green boxes respectively. Binding affinities for Cra and PdeL to respective binding boxes are shown as determined by EMSA (see Figure S1). H-NS recognition sequence is shown as web logo. Putative H-NS-recognition site overlapping with CIB is highlighted in orange. (B) Electrophoretic mobility shift assay (EMSA) of 5' Cy3 labeled oligonucleotides, co-incubated with purified Cra-StrepII and PdeL-StrepII. (CDB = Cra-dependent PdeL-box; CB = Cra-box; CIB = Cra-independent PdeL-box). The position of the labeled oligonucleotides (4991-7 & 4695-6) within the intergenic region is depicted in (A). (C) β -galactosidase activity of merodiploid translational *P_{pdeL}-lacZ* promoter fusion. Transcription factor recognition sequences were randomized to abolish binding. Mutations abolishing binding of PdeL to CIB were chosen to not affect H-NS recognition sequence. Inset shows domain architecture of PdeL. (D) Competition of PdeL and HNS for CIB as determined by EMSA. Increasing H-NS-StrepII concentrations were titrated to a fixed PdeL-StrepII concentration of 100 nM. (E) Effect of c-di-GMP on *pdeL* transcription. *pdeL* transcription was probed in strains with different c-di-GMP regimes (L = low c-di-GMP levels, which correspond to a Δ *pdeH* strain with 65 μ M IPTG induction of plasmid-borne *P_{lac}-pdeH*. H = high c-di-GMP levels, which correspond to a Δ *pdeH* strain with uninduced *P_{lac}-pdeH*). Cellular PdeL protein levels – as determined by SRM LC-MS/MS – are shown above corresponding bars. c-di-GMP-dependent *pdeL* transcription is shown in CDB⁻ and CIB⁻ promoter mutation as well as in an *hns* mutant background.

Cra and PdeL mediate c-di-GMP-dependent transcription of *pdeL*

PdeL autoregulates transcription of the *pdeL* gene in response to the cellular levels of c-di-GMP [79] (Figure 1E). While *pdeL* transcription is maximal at low c-di-GMP concentration, it is strongly reduced at increased c-di-GMP levels. As a result, PdeL protein levels change roughly 6.7-fold from 201 nM \pm 28 nM – 1352 \pm 228 nM in strains with c-di-GMP levels ranging from 0 – ca. 7.6 μ M (Figure S4). This c-di-GMP mediated response was not only dependent on PdeL itself, but was also impacted when the PdeL binding sites in the *pdeL* promoter region were mutated (Figure 1E). While scrambling the CDB site abolished

pdeL transcription, mutation of the CIB strongly diminished the dynamic range of *pdeL* promoter strength. These data suggested that the CDB is the primary control element of c-di-GMP-dependent *pdeL* transcription, while the distal CIB serves as an auxiliary site to enhance the dynamic range of c-di-GMP control. The c-di-GMP mediated control of *pdeL* transcription is completely abolished in an *hns* mutant (Figure 1E), arguing that H-NS acts as a silencer to gauge *pdeL* transcription to a range in which c-di-GMP has the maximal dynamic range effect on *pdeL* transcription.

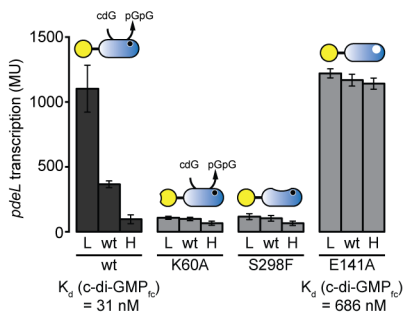


Figure 2 | PdeL is a c-di-GMP sensor. *PdeL* transcription was measured via a chromosomal merodiploid translational P_{pdeL} -*lacZ* reporter fusion in strains with different c-di-GMP regimes (L = low c-di-GMP levels, which correspond to a $\Delta pdeH$ strain with 65 μ M IPTG induction of plasmid-borne P_{lac} -*pdeH*. H = high c-di-GMP levels, which correspond to a $\Delta pdeH$ strain with uninduced P_{lac} -*pdeH*, wt = wild type background with respective PdeL mutant variant and empty vector). This was performed for various mutant PdeL alleles: K60A = DNA-binding-deficient, S298F = dimerization-deficient and E141A = c-di-GMP binding-deficient. For wild type, as well as variant E141A the binding affinity of fluorescein-labeled c-di-GMP (c-di-GMP_{ic}) to PdeL_{EAL} was determined in the presence of Mg²⁺.

PdeL is a c-di-GMP sensor

We previously showed that PdeL acts as a sensor for c-di-GMP by translating the intracellular c-di-GMP concentration into *pdeL* expression [79] (Figure 1E). To understand this link, we genetically dissected the properties of PdeL needed for c-di-GMP-dependent *pdeL* transcription.

In our previous study [79], we introduced a DNA-blind PdeL mutant (K60A), which showed baseline *pdeL* expression, thus concluding that PdeL regulates its own expression. In line with these results a *pdeL* (K60A) allele remained transcriptionally insensitive to c-di-GMP (Figure 2). In agreement with our previously published data [79], this reinforces that PdeL itself is strictly required for c-di-GMP-dependent *pdeL* autoregulation by binding to its own promoter region.

In a previous study focusing on structural and biochemical characterization of the EAL-domain of PdeL it was shown that c-di-GMP drives PdeL dimerization [62]. Moreover, a crucial serine (S298) was identified as a key residue for dimerization. Mutation of this serine to a bulky aromatic amino acid fully abrogated dimerization and consequently enzyme activity [62]. Interestingly, mutation of S298 to phenylalanine (S298F) rendered the *pdeL* promoter irresponsive to c-di-GMP (Figure 2) arguing that c-di-GMP-dependent transcription requires either the enzymatic activity of PdeL, its ability to dimerize or both. To further address this, we focused on the highly conserved glutamate as part of the name-giving EAL-motif, which was reported to be crucial for substrate binding [80]. Interestingly, alanine-substitution

of this particular glutamate (E141A) lead to derepressed and *c*-di-GMP-independent *pdeL* transcription (Figure 2).

Given that – compared to the *c*-di-GMP blind E141A variant – a dimerization deficient PdeL mutant shows wild-type-like substrate binding constants [62] these results suggest that absent *c*-di-GMP-dependent *pdeL* transcription of a dimerization mutant is a consequence of impaired dimerization, rather than absent enzymatic activity. From this we conclude that *c*-di-GMP is sensed by binding to the active site of PdeL and thereby inducing dimerization to regulate *pdeL* transcription.

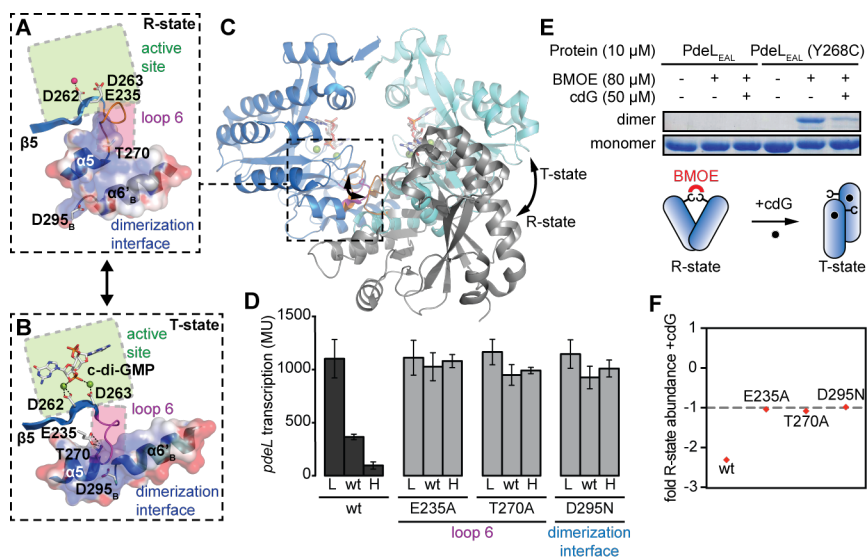


Figure 3 | Characterization of PdeL dimer species. (A) Zoom of active site (green), loop 6 (loop itself shown in orange, region in magenta) and dimerization helices in canonical “open” dimer configuration (R-state) of PdeL EAL-domain as crystallized in apo in presence of Mg²⁺ (PDB: 4LYK). Dimerization helices $\alpha 5$ and $\beta 6'_B$ are shown with electrostatic potential area. (B) Zoom of non-canonical “closed” dimer configuration, crystallized in presence of Ca²⁺ and *c*-di-GMP (PDB: 4LJ3). Coloring is analogous to (A), with loop 6 shown here in magenta. (C) Overlay of T-state dimer (blue hues) and protomer B of the R-state configuration (grey), depicting large quaternary rearrangements and positioning of loop 6. (D) *c*-di-GMP-dependent *pdeL* Promoter activity of PdeL point mutations in the dimerization interface and loop 6. (L = low *c*-di-GMP levels, H = high *c*-di-GMP levels as introduced in Figure 1 & 2). Note that both D295N and T270A were isolated as a motile suppressor allele (see Figure S2). (E) *In vitro* cysteine-crosslink of PdeL_{EAL} (Y268C)-StrepII with bismaleimidoethane (BMOE) (see Figure S3). Crosslinks were performed with Ca²⁺ to prevent *c*-di-GMP hydrolysis and in absence or presence of 50 μ M *c*-di-GMP. As a negative control for Y268C-specific crosslink wild type PdeL_{EAL}-StrepII was included. (F) Quantification of *in vitro* cysteine-crosslinks of PdeL mutant variants as described in (E). Graph shows ratio of band intensity between cysteine-crosslink in presence and absence of excess *c*-di-GMP, plotted as fold change.

Two dimer configurations of PdeL drive c-di-GMP-dependent *pdeL* transcription

Given that both DNA-binding and dimerization of PdeL are prerequisites for *pdeL* transcription and that substrate binding induces dimerization, it is tempting to hypothesize that substrate-induced dimerization of the EAL-domain facilitates dimerization of the associated HTH-domains and therefore DNA binding. However, the observation that a dimerization-deficient mutant showed wild-type like binding to DNA (data not shown) lead us to test alternative hypotheses for how c-di-GMP-dependent PdeL autoregulation. Structural studies with the EAL-domain of PdeL revealed that PdeL can adopt two different dimer configurations [62]. In its apo form, PdeL_{EAL} crystalized as a canonical “open” EAL-dimer (**Figure 3A & C**), whereas in its c-di-GMP-bound form, PdeL formed a non-canonical “closed” EAL-dimer configuration (**Figure 3B & C**). For simplicity reason the canonical dimer configuration is termed R-state (relaxed) and the non-canonical configuration T-state (tight) throughout this study. Formation of the T-state requires the two dimerization helices $\alpha 5_A$ and $\alpha 6'_B$ to face each other via their positively charged N-termini. In order to enable this conformation, intercalation of the negatively charged D295_B residue is strictly required (**Figure 3A-C**). Moreover formation of the two dimer configurations comes along with large structural movements in a highly conserved loop region, which connects strand $\beta 5$ and $\alpha 5$ of the EAL TIM-barrel structure and is commonly termed loop 6 (**Figure 3A-C**) [62]. Loop 6 was shown to play a central role in PDE enzyme activity and to impact dimerization and the formation of higher oligomers [64]. In PdeL a striking feature of loop 6 is its ability to adopt two different conformations, which are attributed to the T- and R-state [62]. Alternative conformations of loop 6 are directed by (i) the dimer configuration, (ii) occupancy of the active site and (iii) E235, the so-called “anchoring glutamate”, which interacts either with active-site residue D263 (R-state) or with T270 (T-state), a central residue within loop 6 (**Figure 3A & B**). Thus, it appears that there is a loop 6-mediated bidirectional communication between the active site and the dimerization interface of PdeL.

As a matter of fact, mutating the anchoring glutamate (E235A) lead to derepressed and c-di-GMP-independent *pdeL* transcription (**Figure 3D**) arguing that destabilization of loop 6 favors a transcriptionally active species of PdeL. Based on the PdeL_{EAL} structure, mutating the T-state interaction partner of the anchoring glutamate (T270) or the residue stabilizing the T-state conformation of dimerization helices $\alpha 5$ and $\alpha 6'$ (D295), should in principle phenocopy the effect of an E235A. This was confirmed by gain of function *pdeL* alleles (T270A & D295N), which were isolated in a selection screen for motile suppressors of a non-motile $\Delta pdeH$ strain (see [79] and **Figure S2**). Reassuringly, these mutations indeed fully abrogated c-di-GMP-dependent *pdeL* transcription control (**Figure 3D**).

Thus, c-di-GMP seems to be sensed via the active site and this information translated via the conserved loop 6 to the dimerization interface in order to dictate the dimer configuration of PdeL, which in turn determines transcriptional activity of PdeL.

C-di-GMP determines PdeL dimer-species configuration

The previous section suggested that PdeL can shuttle between a transcriptionally inert T-state and a transcriptionally active R-state dimer. Since *pdeL* transcription is a function of c-di-GMP levels, we postulated that c-di-GMP drives the switch between the two PdeL dimer configurations. In order to test this substrate-dependent regulation we performed cysteine cross-link assays with the catalytic domain of PdeL in presence and absence of c-di-GMP. These experiments were based on a cysteine substitution in residue Y268, which exclusively show close steric proximity to the R-state dimer (**Figure S3**). Bismaleimidoethane-mediated (BMOE) oxidation of Y268C revealed that in absence of c-di-GMP the R-state variant is predominantly cross-linked (**Figure 3E**). Further, in line with our transcriptional data, mutations of crucial loop 6 residues or the aspartic acid intercalating between loop $\alpha 5_A$ and $\alpha 6'_B$ renders PdeL insensitive to a substrate-induced R- to T-state switch (**Figure 3F**).

These data evoke a model where PdeL can adopt two alternative conformations, the equilibrium of which is determined by the concentration of its substrate. While low c-di-GMP concentrations favor the transcriptionally active R-state, PdeL switches into the inert T-state at high substrate concentrations.

PdeL enzyme activity scales with c-di-GMP concentrations

The isolated motile-suppressor mutant alleles of PdeL were isolated in a strain background displaying high c-di-GMP levels ($\Delta pdeH$). Under such conditions, wild type PdeL does not show high enough activity to suppress this phenotype. Characterization of several motile suppressor alleles ([79] & **Figure S2**) showed enhanced enzymatic activity as well as derepressed *pdeL* transcription indicating that the suppressor mutations lock PdeL in a state in which c-di-GMP can no longer regulate PdeL and therefore display high activity even at high c-di-GMP levels. Together with the previous results we hypothesized that the c-di-GMP-driven equilibrium shift from the R-state to the T-state not only switches PdeL off as a transcription factor but also as an enzyme.

To test this, we measured turnover rates of PdeL as a function of increasing substrate concentrations (**Figure 4A**). Indeed, we determined substrate concentration-dependent turnover rates that were nicely fitted with a substrate inhibition Michaelis-Menten model, thus confirming that PdeL activity negatively scales with increasing c-di-GMP levels.

PdeL enzyme activity scales with PdeL concentrations

In the previous sections, we showed that c-di-GMP drives *pdeL* transcription by determining the equilibrium between an enzymatically and transcriptionally inert T-state and highly active R-state configuration. As a consequence, within a c-di-GMP concentration range between 0 – 7.6 μ M (**Figure S4**), PdeL protein levels inversely scale between 201 – 1352 nM (**Figure 1E**). Although this feature is commonly observed in transcription factors that regulate their own expression in response to a ligand [235] this autoregulation is particularly interesting given that PdeL is a *bona fide* c-di-GMP-specific

phosphodiesterase. Thus, increasing PdeL levels could in principle also impact PdeL enzyme activity and by that have substantial implications on the feedback loop itself as well as on general cell physiology. To address this question, we determined turnover rates of PdeL as a function of PdeL concentration. PdeL turnover rates showed a non-linear apparent k_{cat} , with half-maximal activation at ca. 1.5 μM PdeL concentration (**Figure 4B**). From this we concluded that one reason for building up PdeL levels is a net increase in PdeL enzyme activity.

Since our data reinforces the notion that there is bidirectional communication between the dimer configuration and the active site via loop 6, we hypothesized that – in addition to substrate controlled dimer-state equilibrium – PdeL itself can drive the equilibrium between the inert T-state and highly active R-state. To test this, we measured enzyme activity of the D295N R-lock variant as a function of protein concentrations. We could clearly show that – compared to wild type – an R-lock mutant shows a protein concentration-independent k_{cat} , which is comparable to the highest k_{cat} values measured for wild type PdeL (**Figure 4B**).

This argues that in addition to substrate-regulated T- to R-state equilibrium, the dimer configurations of PdeL are a function of PdeL levels itself therefore possibly strongly enhancing the equilibrium shift from a transcriptionally and enzymatically inert T-state to a highly active R-state.

PdeL controls the global c-di-GMP pool

Determination of PdeL enzyme activity revealed that PdeL activity is a function of substrate concentration (**Figure 4A**) as well as the PdeL concentration itself (**Figure 4B**). Moreover, since PdeL levels are determined via the cellular c-di-GMP levels (**Figure 1E**), these properties allow PdeL to show maximal activity at low c-di-GMP concentrations. As a consequence, PdeL might be an important component to adjust the cellular c-di-GMP pool in response to c-di-GMP changes. To test this, we compared the cellular c-di-GMP levels of a $\Delta pdeH$ and a $\Delta pdeH \Delta pdeL$ background in which we tuned the levels of c-di-GMP by expressing plasmid-borne $P_{lac-pdeH}$. To assess the effect of PdeL on increasing and decreasing c-di-GMP levels, we pre-established initially low or initially high levels of c-di-GMP by either fully (**Figure 4C**) or not inducing (**Figure 4D**) $P_{lac-pdeH}$ over night. While PdeL did not seem to accelerate a decrease in c-di-GMP, PdeL showed a strong buffering effect at rising c-di-GMP levels, leading to a maximal difference in cellular c-di-GMP concentration of ca. 2 μM (**Figure 4D**).

These data clearly show that – depending on the initial c-di-GMP concentration – PdeL significantly contributes to the global c-di-GMP pool. PdeL functions as a buffer for increasing c-di-GMP concentrations, while we could not observe a PdeL-driven boost when c-di-GMP levels decrease. It might nevertheless be that under the conditions tested such an effect is masked by the overriding PDE activity of PdeH.

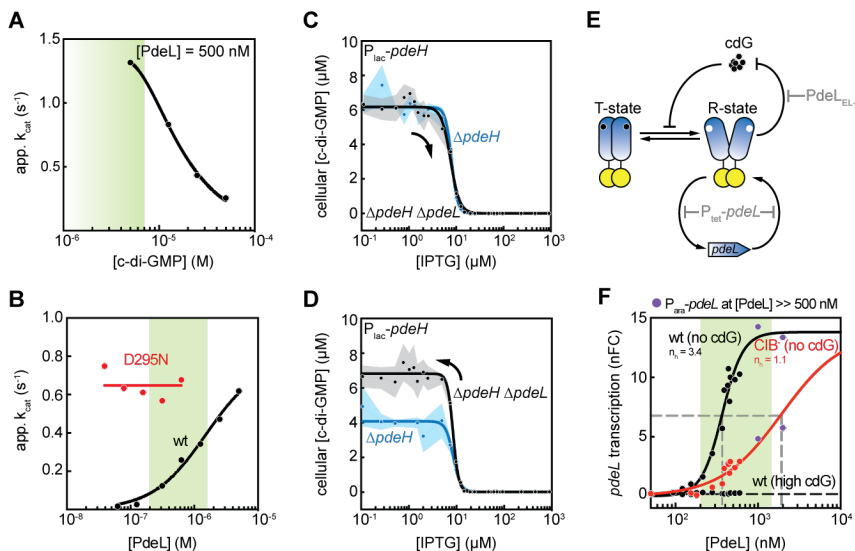


Figure 4 | Properties of PdeL enzyme activity, effect of PdeL on global c-di-GMP pool and cooperativity of *pdeL* transcription. (A) Apparent k_{cat} at 37°C of 500 nM PdeL-StrepII as a function of increasing substrate concentrations. Enzyme activity was measured with FPLC as published in [62]. Data points were fitted with a Michaelis-Menten substrate inhibition model. Green area depicts physiologically relevant c-di-GMP concentration range (see (B)). (B) Apparent k_{cat} of PdeL-StrepII at 37°C as a function of PdeL concentration (wt = black, motile suppressor and R-lock mutant D295N = red). Enzyme activity was measured with phosphate sensor method as previously published in [79]. Data points were fitted with a simple Michaelis-Menten model. Green area depicts physiologically relevant PdeL concentration range (see **Figure 1E**). Cellular c-di-GMP concentration were measured by nucleotide extraction from cell extracts and subsequent quantification by LC-MS/MS. Measurements were performed in a $\Delta pdeH$ strain expressing plasmid-borne $P_{lac-pdeH}$. To establish a c-di-GMP history with initial high levels of c-di-GMP, plasmid was not induced during overnight growth at 37°C in TB medium (C), whereas plasmid was induced with 65 μ M IPTG to generate initially low levels of c-di-GMP (D). Experiments were performed in a $\Delta pdeH$ strain (blue) and a $\Delta pdeH \Delta pdeL$ strain (black). Before sampling, overnight cultures were diluted back 1:500 and grown for 4.5 h in TB medium at 37°C (final OD_{600} of ca. 0.4). Experiments were performed as biological triplicates. Data points show mean of replicates and standard deviations are shown in grey and blue area. Curves show Michaelis-Menten fit with hill coefficient. (E) Schematic of feedback loops determining *pdeL* transcription. PdeL is in an equilibrium between T- and R-state. Upper loop = double-negative enzymatic feedback loop where high c-di-GMP levels shift the equilibrium towards the enzymatically and transcriptionally active R-state. Enzymatic feedback loop can be opened by a catalytically inactive PdeL_{EL} mutant (PdeL (D263N) (K283R)), which is still able to sense c-di-GMP. Lower loop = transcriptional feedback loop. Chromosomal construct of $P_{tet-pdeL}$ ($P_{tet-pdeL}$) opens transcriptional feedback loop. (F) Cooperative behavior of PdeL-dependent *pdeL* transcription shown as fold change compared to lowest measured value (nFC). Experiment was performed in a $\Delta pdeH$ background with chromosomal $P_{tet-pdeL}$ or $P_{ara-pdeL}$ (violet data points) and plasmid borne $P_{lac-pdeH}$. Black curve = full induction of $P_{lac-pdeH}$ to generate background devoid of c-di-GMP. Stippled black curve = no induction of $P_{lac-pdeH}$ to generate high c-di-GMP levels. Red curve = $P_{pdeL-lacZ}$ reporter strain with mutated CIB measured in absence of c-di-GMP. Data points were fitted with a Michaelis-Menten fit with hill-coefficient. Data points of stippled black curve were fitted with horizontal line. Stippled grey line shows K_{half} of Michaelis-Menten fits. Black curve K_{half} = 317 nM, red curve K_{half} = 693 nM. Green area depicts physiologically relevant cellular PdeL concentration (see **Figure 1E**).

***PdeL* expression is highly cooperative and requires the Cra-independent PdeL-box**

At this stage, the data allow us to place PdeL in the center of two interlinked positive feedback loops. (i) a double-negative enzymatic feedback where c-di-GMP inhibits PdeL enzyme activity and PdeL negatively affects the c-di-GMP pool and (ii) a positive transcriptional feedback loop where increasing PdeL levels enhance *pdeL* transcription (**Figure 4E**). When present in noisy systems, positive feedback loops can give rise to bistability [236-239], especially when these feedback loops show strong non-linear or cooperative behavior. The observation that *pdeL* transcription is driven by two intricate positive feedback loops suggests that *pdeL* transcription shows cooperative behavior.

We tested whether the *pdeL* promoter responds in a cooperative manner to increasing PdeL levels. To do so we measured *pdeL* transcription as a function of PdeL levels by driving PdeL from a chromosomal tetracycline-inducible promoter ($P_{tet-pdeL}$). To exclude the c-di-GMP effect on *pdeL* transcription we performed this experiment in a strain devoid of c-di-GMP (full $P_{lac-pdeH}$ induction in a $\Delta pdeH$ background). We observed that *pdeL* transcription reacts in a highly cooperative manner ($n_H = 3.4$) to increasing levels of PdeL, with a half-maximal activation constant of 368 nM PdeL (**Figure 4F**).

To address the source of cooperativity we focused on the distal Cra-independent PdeL-box (CIB). We previously described and characterized the palindromic and Cra-independent low-affinity binding box for PdeL (CIB), which – when mutated – significantly reduced *pdeL* transcription (**Figure 1C**). The observation that a CIB⁻ strain still responded to c-di-GMP but reduced the overall dynamic range of *pdeL* transcription (**Figure 1E**), argued that c-di-GMP control goes via the CDB and that the CIB serves as an enhancing auxiliary element. We therefore asked to what extent the CIB contributes to *pdeL* expression as a function of PdeL levels. Again, we expressed PdeL from our previously introduced $P_{tet-pdeL}$ construct in a strain background devoid of c-di-GMP and measured the *pdeL* promoter response. Interestingly the *pdeL* CIB⁻ promoter responded in a non-cooperative manner ($n_H = 1.1$) with a half-maximal activation constant (K_{half}) of 693 nM (**Figure 4F**). Interestingly, the activation constant is 25-fold higher than the determined *in vitro* K_D for PdeL binding to the CDB (**Figure 1A & 51C, D**) suggesting that other cellular factors such as H-NS might possibly occlude the CDB thus resulting in weaker binding *in vivo*.

From this we concluded that the upstream PdeL binding-box serves as an auxiliary element to generate a cooperative, switch-like *pdeL* promoter activation in response to increasing PdeL levels.

***PdeL* transcription is bistable**

In the previous section, we showed that the *pdeL* promoter reacts in a cooperative manner to PdeL levels. In the light of positive feedback regulation, this property might be the framework for bistable expression of *pdeL*. A hallmark of bistability is hysteresis, which describes the discrepancy in activation energies depending on the initial resting state of a system [239-241]. This feature ultimately endows a system with intrinsic memory and can lead to the establishment of bistable and bimodal populations [242].

To test this, we performed hysteresis experiments *in vivo*. In order to modulate c-di-GMP levels we made use of the previously described P_{lac} -*pdeH* expression system, which we introduced in a $\Delta pdeH$ background. Either not inducing or fully inducing the plasmid over-night allowed us to pre-establish a history with high or low levels of c-di-GMP respectively. In these two backgrounds, we finely tuned the c-di-GMP levels and measured *pdeL* transcription as a function of c-di-GMP in exponential growing cells. In this experiment, we saw a remarkable hysteresis window with a window size of ca. 5 log, within a c-di-GMP concentration range of 0.1 nM and ca. 5 μ M (**Figure 5A**). Interestingly, after 4.5 h growth, *pdeL* on-kinetics did not reach the maximal possible transcription level in absence of c-di-GMP.

Although c-di-GMP-dependent *pdeL* regulation shows strong hysteresis it might nonetheless be that the memory quickly collapses over time, which would argue against a highly stable system. We thus re-performed the hysteresis experiment after 8 h of continuous cultivation in exponential phase. The *pdeL* on-kinetics curve now reached maximal *pdeL* transcription levels at c-di-GMP concentrations as high as 0.3 μ M (**Figure 5B**), thus converging towards the off-kinetics curve, yet showing a still significantly present hysteresis window.

This experiment reinforces that c-di-GMP-dependent *pdeL* transcription not only shows strong transcriptional memory but can maintain this memory over long timescales, thus confirming the strong bistable nature of *pdeL* transcription.

Enzymatic feedback loop is not required for *pdeL* bistability

At this point we aimed to dissect the requirements for bistable c-di-GMP-dependent *pdeL* transcription. As previously described, *pdeL* transcription depends on two intricate self-amplifying feedback loops (**Figure 4E**). We therefore asked, which of the two feedback loops has the greatest contribution or is even essential for the establishment of bistability. To open the enzymatic feedback loop we made use of a PdeL variant, which has a mutation in the conserved double-aspartic acid motif (D263N) as well as the conserved catalytic base (K283R), both residues which are essential for enzymatic activity (**Figure S4**). In fact, the individual mutations render PdeL catalytically inactive. Transcriptionally however the individual mutations show an inverse behavior. While both individual mutations abrogate c-di-GMP-dependent *pdeL* transcription control, D263N shows basal and K283R derepressed *pdeL* transcription. Surprisingly, combination of both mutations fully restored c-di-GMP-dependent *pdeL* transcription control, while still being catalytically inactive. Although a mechanistic explanation is hard to reconcile, this particular mutant can be exploited to study c-di-GMP-dependent *pdeL* transcription in absence of PdeL catalytic activity, thus opening the enzymatic feedback loop (**Figure 4E**). For simplicity, the PdeL (D263N) (K283R) mutant will be termed PdeL_{EL-} (EL- = enzymatic loop) throughout this study. Re-performing the hysteresis experiment with PdeL_{EL-} after 8 h continuous cultivation in exponential phase (**Figure 5C**), showed a hysteresis pattern resembling wild type (**Figure 5C**) with still significantly present hysteresis window.

From this we concluded that bistability of *pdeL* does not depend on the enzymatic feedback loop. Rather the enzymatic feedback loop adds a strong time component to the persistence of hysteresis by contributing to steady-state levels of c-di-GMP.

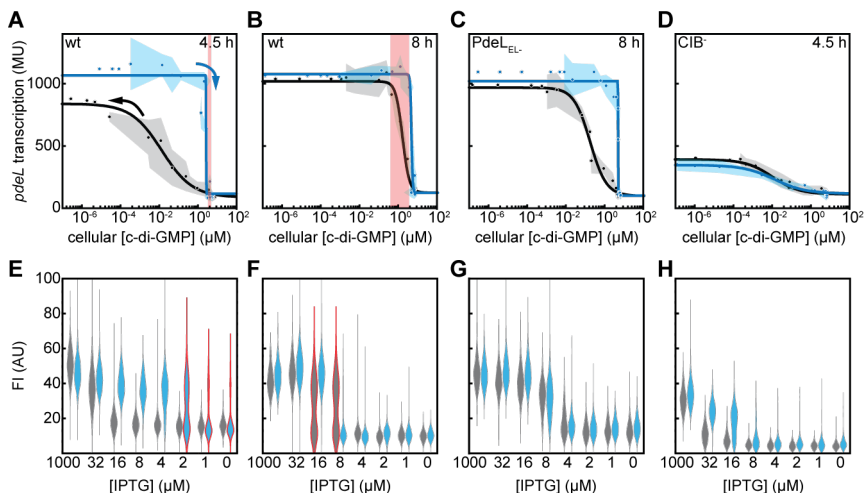


Figure 5 | Bistability and bimodality of *pdeL*. Hysteresis experiment showing *pdeL* transcription as a function of cellular c-di-GMP levels. Strain background is $\Delta pdeH P_{lac-pdeH}$. black curve represents strain background grown over night with no induction of plasmid-borne *pdeH* = initial high c-di-GMP levels. Blue curve represents strain background grown over night with full induction of plasmid-borne *pdeH* = low initial c-di-GMP levels. Through gradual expression of *pdeH*, black curve shows *pdeL* on-kinetics due to reduction of c-di-GMP levels and blue curve shows *pdeL* off-kinetics due to increasing c-di-GMP levels. Curves were fitted with Michelis-Menten model with Hill-coefficient. **(A)** Experiment performed in a wild type strain after 4.5 h exponential growth and **(B)** 8 h continuous cultivation. Red area depicts c-di-GMP concentration range in which bimodality was observed on single-cell level. **(C)** Hysteresis experiment performed with enzymatic feedback loop-deficient $PdeL_{EL-}$ variant after 4.5 h exponential growth. **(D)** Experiment performed analogous to **(A)** with a strain with mutated CIB after 4.5 h exponential growth. **(E-H)** Quantification of single cell fluorescence of a *pdeL*-[RBS-*mCherry*]₂ reporter fusion in a $\Delta pdeH$ background. Hysteresis experiment was performed analogous to **(A-D)** by tuning $P_{lac-pdeH}$ in a strain where $P_{lac-pdeH}$ was previously fully induced (blue) or not induced (black) over night. Histograms shown as violin plots. Conditions where bimodality was observed on single cell level are outlined red.

CIB is required for *pdeL* bistability

The previous section showed that *pdeL* bistability is still present in absence of the enzymatic feedback loop. Moreover, considering that the transcriptional feedback loop reacts highly cooperative to increasing PdeL levels (**Figure 4E**) and cooperativity is often the basis for bistable systems, we focused on the contribution of the CIB on *pdeL* bistability. We previously showed that cooperative *pdeL*

transcription is dependent on the CIB (**Figure 4F**). Thus, we asked whether an intact CIB is a prerequisite for bistability. To test this, we performed a hysteresis experiment after 4.5 h exponential growth in a CIB-strain background. In addition to the previously observed overall lower *pdeL* transcription (**Figure 1C & E**), *pdeL* CIB⁻ transcription showed no apparent hysteresis (**Figure 5D**), confirming that transcription hysteresis and thus establishment of bistability requires the auxiliary CIB.

Bistable expression of *pdeL* generates bimodal populations

The behavior of individuals within a clonal population will ultimately determine how a population will adapt to environmental changes, which in this particular case are changes in c-di-GMP levels. It is mostly observed that bistable systems also manifest in bimodality on the single-cell level [243]. These properties help to establish life-strategies such as bet-hedging and/or division of labor, which significantly contribute to the fitness of a whole population [236,243,244]. In the previous section, we observed strong and time-dependent bistability of *pdeL* expression on the population level. To address how this translates to individual cells we re-performed the hysteresis experiment on the single-cell level by measuring fluorescence of a transcriptional *pdeL*-[RBS-*mCherry*]₂ fusion.

Here we observed that while *pdeL* on-kinetics showed a unimodal – yet switch-like – behavior, down-kinetics showed clear bimodal population split at c-di-GMP concentrations of ca. 2 μ M (**Figure 5E**). In contrast, after 8 h *pdeL* transcription showed bimodal behavior during *pdeL* on-kinetics (**Figure 5F**) at a c-di-GMP concentration, which coincides with the hysteresis window seen at the population level (**Figure 5B**). In line with this observation, a *pdeL* CIB⁻ promoter mutant that does not show bistability on population levels (**Figure 5D**) is monomodal on the single cell level (**Figure 5H**).

Thus, c-di-GMP-dependent and bistable *pdeL* transcription establishes bimodality, which depends on time and the c-di-GMP history of the cells, both of which depend on a functional transcriptional feedback loop.

The enzymatic feedback loop is required for *pdeL* bimodality

On the population level, we clearly saw that the enzymatic feedback loop is not required to establish bistability (**Figure 5C**) but rather determines the half-life of the transcription memory by contributing to the global c-di-GMP pool (compare **Figure 5B & C**). In the light of PdeL being a candidate for the establishment of bimodal c-di-GMP regimes, we asked, whether the enzymatic feedback loop is required to establish bimodal *pdeL* expression and consequently bimodal c-di-GMP regimes. We therefore determined single cell *pdeL* expression after 8 h continuous cultivation in exponential phase of a PdeL_{EL}-variant, which lost its ability to degrade c-di-GMP in response to the prevailing c-di-GMP levels. Strikingly we found that – although showing strong bistability on the population level (**Figure 5C**) – a PdeL variant with inactive enzymatic feedback loop fully loses its ability to establish bimodal populations (**Figure 5G**).

These data suggest that initial c-di-GMP heterogeneity is sensed by PdeL_{EL}- and amplified into a bistable *pdeL* promoter response. As PdeL_{EL}- is catalytically inactive, it cannot amplify the initial c-di-GMP heterogeneity into discrete bimodal c-di-GMP regimes within a population. Thus, within the two positive feedback loops that drive c-di-GMP-dependent *pdeL* transcription, PdeL enzyme activity is dedicated to establish bimodal c-di-GMP regimes.

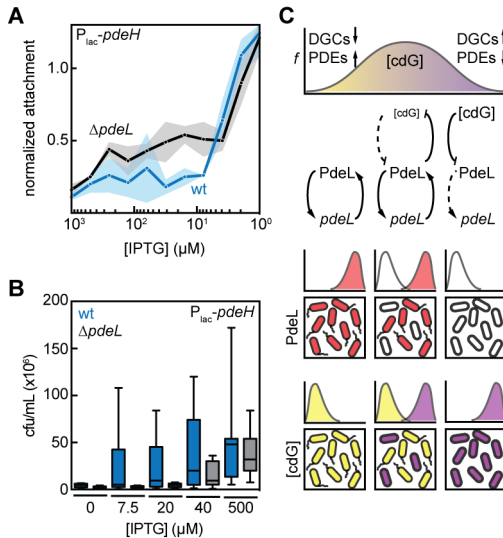


Figure 6 | Effect of PdeL on c-di-GMP-dependent processes. (A) Crystal-Violet-based staining of attached biomass during gradual expression of plasmid-borne $P_{lac-pdeH}$. Biofilm formation of a $\Delta pdeH$ background (blue) and $\Delta pdeH \Delta pdeL$ background (black), both with constitutive chromosomal *pgaA-D* expression ($P_{const-pgaA-D}$). In order to start with low c-di-GMP levels strains were grown over night with full induction of plasmid-borne $P_{lac-pdeH}$. (B) Quantification of planktonic cells escaping a pre-formed biofilm. A *csrA* $\Delta pdeH$ (black) and *csrA* $\Delta pdeH \Delta pdeL$ (blue), equipped with plasmid-borne $P_{lac-pdeH}$ were incubated for 8 h static at 30°C to form a biofilm. After washing, fresh medium supplemented with increasing amounts of IPTG was added to the pre-formed biofilm and incubated static at 30°C for 3 h. Escaped planktonic cells were quantified by dot-spotting serial dilutions and determination of cfu/mL. Black bars represent median cfu/mL, error-bars show upper and lower quartile. (C) Schematic showing the effect of PdeL on global c-di-GMP and related phenotypes. A clonal population experiences

noise in the intracellular c-di-GMP levels. Large changes in the cellular c-di-GMP concentration are governed by the action of upstream cyclases (DGCs) and phosphodiesterases (PDEs) and either buffered or accelerated by PdeL the enzymatic action of PdeL itself. A strong net decrease in c-di-GMP levels leads to strong upregulation of PdeL (red cells) and concomitant contribution of PdeL to decreasing c-di-GMP levels. As a consequence, most cells will show phenotypes associated with low c-di-GMP levels (yellow) such as motility (= flagellated cells). Respectively a strong net increase in c-di-GMP levels will inhibit both enzymatic and transcriptional activity of PdeL. This will generate a population with the majority of cells showing phenotypes associated with high c-di-GMP levels (purple) such as biofilm formation (depicted as thicker cell outline). In the case of noise-induced intermediate c-di-GMP levels, PdeL will act as a decision maker and establish a bimodal population.

PdeL is a gatekeeper for motile-sessile lifestyle transcription

The dissection of the feedback loops driving c-di-GMP-dependent *pdeL* transcription, showed that PdeL is in the center of two positive feedback loops, which sense c-di-GMP but at the same time affect the c-di-GMP pool itself (Figure 4E). This suggests that within a certain c-di-GMP concentration window, PdeL can have a substantial impact on the global c-di-GMP pool and therefore on c-di-GMP-related cellular

processes. To test this, we looked at the effect of PdeL on the formation of biofilms and the escape from preformed biofilms, which both are processes known to be regulated by c-di-GMP [128]. To this end we chose to test the effect of PdeL on poly-GlcNAc-dependent (PGA) biofilm formation, since it was previously described that this system is post-translationally regulated by c-di-GMP with an activation constant of 62 nM [110]. In order to test the effect of PdeL on biofilm entry we took advantage of our P_{lac} -*pdeH* expression system to tune c-di-GMP in strain backgrounds, with initially low c-di-GMP levels. In order to uncouple the translation of the *pga* operon from the upstream BarA-UvrY/CsrA-cascade [245], we expressed the *pga* operon from a weak constitutive promoter. While the wild type strain showed a sharp and steep response to increasing c-di-GMP levels, the *pdeL* mutant prematurely increased biofilm formation at already much lower c-di-GMP levels compared to wild type (**Figure 6A**). Apparently, one role of PdeL is to buffer c-di-GMP noise and to prevent premature entry into biofilm mode. Since PdeL is a phosphodiesterase it could in principle also confer an advantage to cells trying to escape from an existing biofilm. We thus designed an experiment in which we compared the ability of a *csrA* Δ *pdeH* and a *csrA* Δ *pdeH* Δ *pdeL* to escape from a preformed biofilm upon reduction of c-di-GMP levels through induction of plasmid-borne PdeH. While escape rates remained low over a range of c-di-GMP levels (PdeH induction), a strain harboring *pdeL* displayed significantly higher escape rates even at relatively low PdeH induction (**Figure 6B**).

Thus, PdeL not only buffers against premature entry into biofilms as c-di-GMP levels increase in response to DGC activity, but it also promotes cellular escape from biofilms as c-di-GMP levels drop in response to PDE activity. These results provide physiological relevance to PdeL as a cellular component facilitating rapid and robust lifestyle switches.

Discussion

Binary switches between alternative cellular programs are key features of natural systems contributing to cellular homeostasis or population fitness in fluctuating environments. The second messenger c-di-GMP directs a series of important cellular processes in bacteria including motility, virulence and biofilm formation. But how are c-di-GMP dependent programs regulated considering that this cellular network might exhibit considerable internal noise and is highly sensitive and complex? Is the internal noise in this network a basis for “all-or-nothing” phenotypes? Are these decisive phenotypes beneficial in nature? And if so how are stochastic fluctuations amplified or buffered to drive deterministic and robust lifestyle-decisions? Here we identify the phosphodiesterase PdeL as a central element of c-di-GMP homeostasis in *E. coli*. We demonstrated that PdeL activity and expression respond to c-di-GMP and by coupling enzymatic and transcriptional feedback provides bistable c-di-GMP regimes and rapid responses at c-di-GMP threshold levels.

Based on our genetic and biochemical data we propose the following working model: PdeL is recruited to the *pdeL* promoter region by the Cra regulator at metabolic conditions that favor gluconeogenesis [246]. When intracellular c-di-GMP levels are high, PdeL adopts the non-canonical T-state dimer configuration. In this static conformation, the active sites of both protomers are occupied with substrate thereby shifting PdeL into a conformation that is both catalytically and transcriptionally inert. When cellular levels of c-di-GMP drop, the fully loaded and inert T-state is destabilized, thereby shifting the equilibrium to the canonical R-state dimer configuration, which is highly active both as an enzyme and as a transcription factor. This model is supported by the observations that mutations, which generally abolish either substrate binding such as E141A or the stabilization of loop 6 or the dimerization helices in the T-state conformation (E235A, T270A, D295N) lead to derepressed and c-di-GMP-irresponsive *pdeL* transcription (Figure 3D & F).

We conclude that relieving the T-state through reduction of the c-di-GMP regime initiates an equilibrium shift from an inert to a catalytically and transcriptionally highly active PdeL species. This will have two effects: (i) derepression of the catalytic activity of PdeL enhanced decrease of c-di-GMP and (ii) substantially increase in PdeL levels. The latter is of great importance, since apart from the substrate-mediated effect on *pdeL* transcription we observed that *pdeL* transcription and PdeL enzyme activity is a function of PdeL levels itself. Since it is not conceivable, how increasing PdeL levels might positively affect an equilibrium between to dimer species, we suggest that increasing PdeL levels will allow PdeL to bind to the upstream low affinity Cra-independent PdeL-box (CIB) therefore inducing tetramerization of PdeL with a PdeL dimer bound to the Cra-dependent PdeL-box (CDB). We suggest that tetramerization will further shift the equilibrium towards the R-state, resulting in maximal transcriptional and catalytic activity. This is corroborated by the observation that loss of the CIB impairs maximal promoter response. In addition, tetramerization might aid to displace the general gene silencer H-NS off the intergenic region of *pdeL*. In fact, the intergenic region of *pdeL* displays several regions strongly resembling the consensus recognition sequence of H-NS, one of which we showed overlaps with

the CIB and for which both H-NS and PdeL compete (**Figure S5**). Thus, occupation of the CIB at increasing PdeL levels likely induces tetramerization of PdeL, eventually facilitating a robust ON-state of *pdeL* transcription and catalytic activity.

In this study, we show that placing an enzyme – which at the same time is a transcription factor – in the center of two interconnected positive feedback loops (**Figure 4E**), allows to sense the prevailing c-di-GMP concentration and translate this information into autoregulation. As a c-di-GMP specific phosphodiesterase PdeL will feed back into the global c-di-GMP pool and concomitantly impose robust c-di-GMP regimes. While it is unclear whether the commitment of such a component is to generate stochasticity or to amplify already existing fluctuation, it appears that coupling of a transcription factor with an enzyme is a smart way to fulfill either of the two tasks (**Figure 6C**). This might have implication in both the establishment of environmental biofilm structures as well as survival in the host environment. The need to stably reside in either of the two states becomes evident when microscopically observing *E. coli* macrocolonies. These structures are highly organized displaying vegetative, flagellated cells at the nutrient-rich bottom and curli and cellulose expressing cells in the upper – nutrient limiting – layers [201]. Here, PdeL could be a key player to maintain low c-di-GMP levels in the lower nutrient rich areas. Moreover, it has been observed that these structures are not homogeneous. In fact, one can frequently find curli-ON and flagellated curli-OFF cells side-by-side even in the upper layers of such macrocolonies. This might have two implications: (i) According to the cross-sections of the macrocolonies it appears that flagella of cells trapped within these structures serve as a scaffold for secreted curli fibers and cellulose. (ii) Moreover, in line with our observations, that *pdeL* facilitates cell-dispersal from mature biofilms its bistable nature might be beneficial in order to maintain regions with flagellated cells at the surface of these structures to allow for occasional single-cell dispersal.

We postulate that PdeL is a central module to allow for bet hedging and division of labor in fluctuating environments. Thus, during its voyage through the host, including the shedding into the non-host environment, *E. coli* encounters ever-changing environments to which the phenotypic heterogeneity within a population strongly contributes in terms of survival. Therefore, nature must have selected for modules that drive phenotypic heterogeneity such as PdeL.

Thinking of PdeL as a transcription factor it is hard to reconcile that – with PdeL levels fluctuating between ca. 200 and 1000 molecules per cell – PdeL is solely required for c-di-GMP-dependent autoregulation. It is more likely that PdeL engages into two major tasks: (i) autoregulation according to the metabolic- and c-di-GMP-status, which eventually affects the global c-di-GMP pool to facilitate robust lifestyle transitions in a bistable and bimodal manner and (ii) c-di-GMP-dependent regulation of secondary genes involved in either of the two major lifestyles. These two properties could be inextricably linked, since full activation of PdeL activity to affect the global c-di-GMP pool, might need saturation of all PdeL binding sites on the *E. coli* chromosome. The use of ChIP-Seq and proteomics to unravel and characterize the complete PdeL-regulon will be the aim of future work.

Author contribution

AR, SO, JR, BS, MS, TS and UJ conceived and designed the experiments. AR, SO, JR and BS performed the experiments. AR, SO, JR, BS, MS, TS and UJ analyzed the data. AR and UJ wrote the manuscript.

Author information

Correspondence should be addressed to urs.jenal@unibas.ch.

Supplemental material

For supplemental materials see in Chapter 5.

Acknowledgements

We thank Prof. Volkhard Kaever and Annette Garbe from the Medizinische Hochschule Hannover for c-di-GMP measurements and Fabienne Hamburger for technical support. Moreover, we thank the Proteomics Core Facility (PCF) of the Biozentrum, University of Basel for absolute protein concentration quantification. The Fellowships For Excellence (FFE) International PhD Program supported this work.

Materials & Methods

Bacterial strains and growth conditions

The bacterial strains and plasmids used in this study are listed in **Table S1**. *E. coli* K-12 MG1655 from Blattner et al. [202] and its derivatives were grown as indicated in the dedicated methods sections. When needed antibiotics were present at following concentrations: 30 µg/mL chloramphenicol for plasmids and 20 µg/mL chloramphenicol for chromosomal chloramphenicol resistance cassettes, 50 µg/mL kanamycin, 100 µg/mL ampicillin for high copy plasmids and 30 µg/mL for low or single-copy plasmids.

P1 phage lysate preparation and transduction

P1 phage lysate preparation and transduction were carried out as described in [210].

Gene deletions and λ -RED-mediated recombineering

Chromosomal gene deletions and modifications: Gene deletions were essentially carried out either as described by Datsenko et al. [211] or with the use of a comprehensive mutant library (“Keio collection” [212]) and P1 mediated transduction. Chromosomal 3xflag-tagging of genes was carried out according to the published method by Uzzau et al. [213]. For unmodified strains AB330 (see strain list **Table S1**) was used, whereas pKD46 was used for construction of strains already harboring chromosomal modifications. Selection markers were removed by site-specific recombination using pCIP20 [211].

Construction of promoter-lacZ fusions: Construction of chromosomal promoter-*lacZ* fusions were carried out via λ -RED-mediated recombination as described above. AB989 (see strain list **Table S1**) was used as a recipient strain. The donor PCR fragment harboring the promoter of interest was designed to site-specifically excise $P_{tha-ccdB}$ and integrate upstream of the native *lacZ* ORF to generate a merodiploid translational fusion. Successful integration events were selected through growth on rhamnose minimal plates.

Electrophoretic mobility shift assay (EMSA)

5' Cy3-labeled input DNA was generated either via oligonucleotide annealing or PCR. For oligonucleotides used see **Table S1**. 10 nM of the input DNA and purified proteins were incubated for 10 min at room temperature in buffer consisting of 50 mM Tris-HCl pH 8.0, 50 mM NaCl, 10 mM MgCl₂, 10 % glycerol, 1 mM DTT, 0.01 & Triton X-100, 0.1 mg/mL BSA and 25 µg/mL λ -DNA. As indicated in the figures, samples were incubated in the presence or absence of 2 mM CaCl₂ and 50 µM c-di-GMP. Samples were run on 8 % polyacrylamide gel. DNA-protein complexes were analyzed using Typhoon FLA 7000 (GE healthcare).

β -galactosidase reporter

Strains were grown in TB medium o/n at 37°C. The next day cultures were diluted back 1:500 into fresh medium and grown at 37°C until desired OD₆₀₀. 500 µL of the culture were mixed with 380 µL Z-buffer

(75 mM Na₂HPO₄, 40 mM NaH₂PO₄, 1 mM KCl, 1 mM MgSO₄), 100 µL 0.1 % SDS and 20 µL chloroform. Samples were vortexed for 10 sec and left on the bench for 15 min. 200 µL sample were transferred into a clear 96-well plate (Falcon). As substrate 25 µL 4 mg/mL *o*-nitrophenyl-*b*-D-galactopyranoside (*o*NPG) solution (dissolved in Z-buffer) were added. The initial velocity of the color reaction was determined at a wavelength of 420 nm.

Protein purification

All strepII-tagged proteins were purified using the same method. Pde^{LEAL} variants were purified by a single StrepII-tag affinity purification, whereas for full-length PdeL and other transcription factors a heparin purification step was added.

StrepII purification: All proteins were cloned into a pET28a vector (Novagen) between NcoI and NotI restriction sites. Proteins were overexpressed in BL21 (AI) cells grown at 30°C in 2 L LB medium. For overexpression of mutant protein variants, the corresponding wild type version of the gene was deleted in the overexpression strain. At an OD₆₀₀ of 0.6 the culture was induced with 0.1 % L-arabinose. Cells were harvested 4 h post induction by centrifugation at 5000 rpm for 30 min at 4°C. The cell pellet was resuspended in 7 mL Buffer A (100 mM Tris-HCl pH 8.0, 250 mM NaCl, 5 mM MgCl₂, 0.5 mM EDTA, 1 mM DTT) including a tablet of c0mplete mini EDTA-free protease inhibitor (Roche) and a spatula tip of DNaseI (Roche). Cells were lysed by 4 passages of french press and the lysate cleared at 4°C in a tabletop centrifuge set at full-speed for 40 min. The cleared supernatant was loaded on 1 mL StrepTactin Superflow Plus resin (QIAGEN). The supernatant was reloaded another two times before washing with a total of 50 mL Buffer A. The column was washed with 10 mL Buffer B (100 mM Tris-HCl pH 8.0, 50 mM NaCl, 5 mM MgCl₂, 0.5 mM EDTA, 1 mM DTT). 500 µL aliquots of proteins were eluted with Buffer B supplemented with 2.5 mM d-Desthiobiotin.

Heparin Purification: A 1 mL HiTrap Heparin HP column (GE healthcare) was washed with 10 mL H₂O_{dest.}, followed by an equilibration with 10 mL Buffer B. The eluate from the StrepII-tag affinity purification was loaded three times. After loading the column was washed with 10 mL Buffer A followed by a washing step with 10 mL Buffer C (100 mM Tris-HCl pH 8.0, 350 mM NaCl, 5 mM MgCl₂, 0.5 mM EDTA, 1 mM DTT). The protein was eluted in 500 µL fractions with a total of 10 mL Buffer D (100 mM Tris-HCl pH 8.0, 2 M NaCl, 5 mM MgCl₂, 0.5 mM EDTA, 1 mM DTT). The fractions containing the highest protein concentration were pooled and dialyzed o/n at 4°C against 1.5 L Dialysis Buffer (100 mM Tris-HCl pH 8.0, 250 mM NaCl, 5 mM MgCl₂, 0.5 mM EDTA, 1 mM DTT). Pde^{LEAL} variants used for cysteine crosslink assays were dialyzed against CXA Buffer (100 mM Tris-HCl pH 7.2, 250 mM NaCl, 2 mM EDTA). The final protein concentration was recorded at 280 nm and the content of co-purified nucleotide contaminants determined as a ration of 260/280 nm.

Immunoblotting

Cells were grown in TB medium at 37°C until desired OD₆₀₀. An equivalent of 1 mL of an OD₆₀₀ of 1.0 was pelleted and resuspended in 100 µL SDS Laemmli buffer. Cells were lysed by boiling the sample at

98°C for 10 min. 8 μ L of the total cell extract were loaded onto a 12.5 % SDS-polyacrylamide gel and proteins transferred using a BioRad® wet blot system. Proteins with 3xflag-tag were detected with a 1:10.000 dilution of monoclonal mouse α -Flag monoclonal antibody (Sigma) and a 1:10.000 dilution of polyclonal rabbit α -mouse horseradish-peroxidase (HRP) secondary antibody (DakoCytomation, DK). Proteins were visualized with enhanced chemiluminescence (ECL) detection reagent (Perkin Elmer Life Science) and imaged in a gel imager (GE ImageQuant LAS 4000).

C-di-GMP hydrolysis assay

Phosphate Sensor assay: Phosphate sensor assay was essentially performed as described in [79]. Briefly: Conversion of c-di-GMP into pGpG was measured indirectly by a coupled alkaline phosphatase (AP)/phosphate sensor online assay. The terminal phosphate of the pGpG product is cleaved by the coupling enzyme AP (20 U/ μ L, Roche), and the phosphate concentration is determined from the fluorescence increase through binding of phosphate to the phosphate sensor (0.5 μ M; Life Technologies). PdeL and c-di-GMP concentrations were used as shown in the individual experiments. Fluorescence increase was detected by excitation at 430 nm and emission at 468 nm.

FPLC assay: Assay was performed as described in [62]. Enzymatic activity was assayed offline by FPLC-based steady-state nucleotide quantification following incubation for varying durations. Enzymatic reactions were carried out at 20°C in 100 mM Tris-HCl pH 8.0, 250 mM NaCl, 5 mM MgCl₂, 0.5 mM EDTA, 1 mM DTT and 50 M thiamine pyrophosphate as FPLC standard. PdeL and c-di-GMP concentrations were used as described in the result section. The reaction was started by addition of enzyme to a total reaction volume of 600 μ L. Samples volumes of 100 μ L were withdrawn and the reaction was stopped at different time points by addition of 10 μ L of 100 mM and subsequent heating at 98°C for 10 min.

The samples were then analyzed using ion-exchange chromatography (1-mL- Resource-Q column) after addition of 890 μ L of 5 mM ammonium bicarbonate (NH₄ CO₃) to increase the volume to 1 mL. 500 μ L of this was then loaded onto the column. The column was washed thoroughly and the bound nucleotides were eluted with a linear NH₄CO₃ gradient (5 mM to 1 M) over 17 column volumes. The amount of pGpG product was determined by integration of the corresponding absorption (253 nm) peak after normalization of the data with respect to the internal thiamine pyrophosphate standard.

Cysteine crosslink assay

10 μ M PdeL_{EAL}-3xFlag-StrepII variants purified in CXA Buffer (100 mM Tris-HCl pH 7.2, 250 mM NaCl, 2 mM EDTA) were incubated for 10 min at room temperature in presence of 10 mM CaCl₂ either in presence or absence of 50 μ M c-di-GMP. Proteins were crosslinked for 1 h at room temperature with an 8-fold molar excess (80 μ M) of bismaleimidoethane (BMOE) (ThermoFisher Scientific). Crosslink reaction was quenched for 15 min at room temperature by addition of 50 mM DTT. Samples were supplemented with SDS Laemmli buffer and proteins denature by heating at 98°C for 5 min. Samples were loaded on a 12.5 % SDS-polyacrylamide gel and detected by staining with Coomassie Brilliant Blue.

Microscopy

Fluorescence and differential interference contrast (DIC) microscopy was performed on a DeltaVision Core (Applied Precision, USA) microscope equipped with an Olympus 100X/1.30 Oil objective and an EDGE/sCMOS CCD camera. Cells were placed on a PBS pad solidified with 1% agarose. Exposure time for microscopy picture was 0.05 sec for bright field (POL) and 0.3 s for mCherry. For both settings, the ND filter was set to 100% transmission.

Analysis of microscopy images

Cell outlines of images were determined by open source software-package Oufiti [247]. Outlines were used to compute mean single cell fluorescence by our custom made program WHISIT [248].

C-di-GMP measurements

C-di-GMP measurements were performed according to the published procedure by Spangler et al. [99]. In brief: *E. coli* cells were grown in 24 mL TB medium at 37°C until an OD₆₀₀ of 0.5. Cells were pelleted and washed in 300 µL ice-cold H₂O_{dest.}. After washing the cell pellet was resuspended in 300 µL ice-cold extraction solvent (acetonitrile/methanol/H₂O_{dest.}, 40/20/20 v/v/v). After pelleting, the supernatant was transferred into a 2 mL safe-lock tube and the extraction procedure repeated twice with 200 µL extraction solvent. Biological triplicates were performed. Measurements were performed in collaboration with the group of Prof. Volkhard Kaever (Institute of Pharmacology, Hannover) via HPLC-MS/MS. Measured values were mathematically converted into cellular c-di-GMP concentration. Constants of *E. coli* cell volume and cfu/mL needed for calculation were experimentally determined.

Absolute protein concentration determination via selected reaction-monitoring (SRM) LC-MS analysis

600 µL of an *E. coli* culture grown in TB to an OD₆₀₀ of ca. 0.5 were pelleted and washed twice with 1 mL ice-cold PBS. Cells were lysed in 1 % sodium deoxycholate (SDC), 100 mM Tris pH 8.5 by sonication. Proteins were denatured by heating at 95°C for 10 min. Protein alkylation was performed with chloroacetamide. Protein digestion was performed by subsequent treatment with Lys-C (enzyme/protein ratio 1:200) and trypsin (enzyme/protein ratio 1:50). Peptides were acidified with TFA and desalted using PreOmics (ThermoFisher) cartridges.

To each peptide samples an aliquot of a heavy reference peptide mix was spiked into each sample at a concentration of 20 fmol of heavy reference peptides per 1µg of total endogenous protein mass. The heavy peptide mix contained 10 chemically synthesized proteotypic peptides (JPT Peptide Technologies GmbH) of the two target proteins (5 peptides each) that showed the highest MS1 responses in a previous large-scale study [249]. In a first step, selected reaction-monitoring (SRM) assays [250] were generated from a mixture containing 500 fmol of each reference peptide and shotgun LC-MS/MS analysis on a Q-Exactive HF platform. The setup of the µRPLC-MS system was as described previously [251]. Chromatographic separation of peptides was carried out using an EASY nano-LC 1000 system

(Thermo Fisher Scientific), equipped with a heated RP-HPLC column (75 μm x 37 cm) packed in-house with 1.9 μm C18 resin (Reprosil-AQ Pur, Dr. Maisch). Peptides were analyzed per LC-MS/MS run using a linear gradient ranging from 95% solvent A (0.1% formic acid) and 5% solvent B (99.9% acetonitrile, 0.1% formic acid) to 45% solvent B over 60 minutes at a flow rate of 200 nL/min. Mass spectrometry analysis was performed on Q-Exactive HF mass spectrometer equipped with a nanoelectrospray ion source (both Thermo Fisher Scientific). Each MS1 scan was followed by high-collision-dissociation (HCD) of the 10 most abundant precursor ions with dynamic exclusion for 20 seconds. Total cycle time was approximately 1 sec. For MS1, $3e6$ ions were accumulated in the Orbitrap cell over a maximum time of 100 ms and scanned at a resolution of 120,000 FWHM (at 200 m/z). MS2 scans were acquired at a target setting of $1e5$ ions, accumulation time of 50 ms and a resolution of 30,000 FWHM (at 200 m/z). Singly charged ions and ions with unassigned charge state were excluded from triggering MS2 events. The normalized collision energy was set to 27%, the mass isolation window was set to 1.4 m/z and one microscan was acquired for each spectrum.

The acquired raw-files were searched against a decoy database using the MaxQuant software (Version 1.0.13.13) containing normal and reverse sequences of the predicted SwissProt entries of *E. coli* (www.ebi.ac.uk, release date 2016/05/02), retention time standard peptides and commonly observed contaminants (in total 10402 sequences) generated using the SequenceReverser tool from the MaxQuant software (Version 1.0.13.13). The precursor ion tolerance was set to 10 ppm and fragment ion tolerance was set to 0.02 Da. The search criteria were set as follows: full tryptic specificity was required (cleavage after lysine or arginine residues unless followed by proline), 3 missed cleavages were allowed, carbamidomethylation (C) was set as fixed modification and arginine (+10 Da), lysine (+8 Da) and oxidation (M) were set as a variable modification. The resulting msms.txt file was converted to a spectral library panel with the 5 to 10 best transitions for each peptide using an in-house software tool. This was then imported into the SpectroDive program (Version 7.5, Biognosys, Schlieren, Switzerland) and a transition list for quantitative SRM analysis was generated. Here, all samples were analyzed on a TSQ-Vantage triple-quadrupole mass spectrometer coupled to an Easy-nLC (Thermo Fisher, Scientific). In each injection, an equivalent of 1.5 μg of peptides including heavy peptide references was loaded onto a custom-made main column (Reprosil C18 AQ, 3 μm diameter, 100 \AA pore, 0.75 x 300 mm) and separated using the same gradient mentioned above. The mass spectrometer was operated in the positive ion mode using ESI with a capillary temperature of 275 $^{\circ}\text{C}$, a spray voltage of +2200 V. All of the measurements were performed in an unscheduled mode and a cycle time of 2 sec. A 0.7 FWHM resolution window for both Q1 and Q3 was set for parent- and product-ion isolation. Fragmentation of parent-ions was performed in Q2 at 1.2 mTorr, using collision energies calculated with the SpectroDive software (version 7.5). Each condition was analyzed in biological quadruplicates. All raw-files were imported into SpectroDive for absolute peptide and protein quantification.

Attachment assay

Attachment assays were carried out as described by Böhm et al [214]. Briefly: 200 μ L TB medium provided in a clear 96-well microtiter plate (Falcon) were inoculated 1:40 with an o/n culture grown at 37°C. The plate was incubated statically at 37°C for 24 h unless indicated differently. After recording the OD₆₀₀ of the total biomass, the planktonic phase of the culture was discarded and the wells washed with H₂O_{dest.} from a hose. The remaining attached biomass was stained with 200 μ L 0.3 % crystal violet (0.3 % (w/v) in 5 % (v/v) 2-propanol, 5 % (v/v) methanol) for 20 min. The plate was washed with H₂O_{dest.} from a hose and the stained biofilm dissolved in 20 % acetic acid for 20 min. Intensity of crystal violet stain was quantified at 600 nm and normalized to the initially measured total biomass.

Biofilm escape assay


Cells harboring pAR81 (see plasmid list **Table S2**) were given 7 h time at 30°C to attach to 96-well microtiter plate supplemented with TB medium supplemented with ampicillin. Plate was gently washed with deionized water from a hose and dried for 20 min. Fresh medium supplemented with IPTG to induce plasmid-borne P_{lac}-*pdeH* was added to the wells and incubated for 3 h at 30°C. After incubation, 10 μ L of the planktonic phase were isolated to determine cfu/mL by spotting serial dilutions in LA plates supplemented with ampicillin.

Motility assay

A single colony was picked onto a TB swarmer plate (0.3 % agar). Plates were incubated at 37°C for 3-4 h. Swarm halos were recorded with a NIKON Coolpix990 and swarm radius quantified via ImageJ (NIH, USA).

Strains, plasmids and oligonucleotides

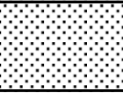
Table S1



Strain	Genotype	Source	Used in
MG1655	<i>E. coli</i> K-12	Blattner et al.	
BL21 (AI)	<i>F ompT hsdS_B (r_B m_B) gal dcm araB::T7 RNAP-tetA</i>	Life techn.	
AB330	λ cI857 Δ (<i>cro-bioA</i>)	A. Böhm	
AB989	λ cI857 Δ (<i>cro-bioA</i>) <i>kan::P_{pha}-ccdB-lacZ</i>	A. Böhm	
AB2986	<i>kan::P_{pdeL}-lacZ</i> (merodiploid translational fusion)	this study	
AB2727	<i>kan::P_{pdeL, P1}-lacZ</i> (merodiploid translational fusion)	this study	
AB2569	Δ <i>pdeL::frt kan::P_{pdeL, P1}-lacZ</i> (merodiploid translational fusion)	Reinders et al. J. Bact. 2015	
AB2402	<i>kan::P_{pdeL, CDB}-lacZ</i> (merodiploid translational fusion)	this study	
AB2609	<i>pdeL (K60A)-3xflag::frt kan::P_{pdeL}-lacZ</i> (merodiploid translational fusion)	Reinders et al. J. Bact. 2015	Figure 1C
AB2809	Δ <i>cra::frt kan::P_{pdeL, P1}-lacZ</i> (merodiploid translational fusion)	this study	
AB2400	<i>kan::P_{pdeL, CIB}-lacZ</i> (merodiploid translational fusion)	this study	
AB2789	Δ <i>pdeL::frt Δcra::frt kan::P_{pdeL, P1}-lacZ</i> (merodiploid translational fusion)	this study	
AB2401	<i>kan::P_{pdeL, CIB & CDB}-lacZ</i> (merodiploid translational fusion)	this study	
AB3292	<i>kan::P_{pdeL, CIB}-lacZ</i> (merodiploid translational fusion)	this study	
AB2830	Δ <i>hns::frt pdeL-3xflag::frt kan::P_{pdeL}-lacZ</i> (merodiploid translational fusion)	this study	
AB2377	Δ <i>pdeH::frt kan::P_{pdeL}-lacZ</i> (merodiploid translational fusion)	this study	
AB2986	<i>kan::P_{pdeL}-lacZ</i> (merodiploid translational fusion)	this study	
AB3340	Δ <i>pdeH::frt kan::P_{pdeL, CDB}-lacZ</i> (merodiploid translational fusion)	this study	
AB2402	<i>kan::P_{pdeL, CDB}-lacZ</i> (merodiploid translational fusion)	this study	
AB3335	Δ <i>pdeH::frt P_{pdeL, CIB}-pdeL-3xflag::frt kan::P_{pdeL, CIB}-lacZ</i> (merodiploid translational fusion)	this study	Figure 1E
AB3292	<i>kan::P_{pdeL, CIB}-lacZ</i> (merodiploid translational fusion)	this study	
AB2923	Δ <i>pdeH::frt Δhns::frt pdeL-3xflag::frt kan::P_{pdeL}-lacZ</i> (merodiploid translational fusion)	this study	
AB2830	Δ <i>hns::frt pdeL-3xflag::frt kan::P_{pdeL}-lacZ</i> (merodiploid translational fusion)	this study	
AB2377	Δ <i>pdeH::frt kan::P_{pdeL}-lacZ</i> (merodiploid translational fusion)	this study	
AB2986	<i>kan::P_{pdeL}-lacZ</i> (merodiploid translational fusion)	this study	
AB2847	Δ <i>pdeH::frt pdeL (K60A)-3xflag::frt kan::P_{pdeL}-lacZ</i> (merodiploid translational fusion)	this study	
AB2609	<i>pdeL (K60A)-3xflag::frt kan::P_{pdeL}-lacZ</i> (merodiploid translational fusion)	Reinders et al. J. Bact. 2015	Figure 2
AB2848	Δ <i>pdeH::frt pdeL (S298F)-3xflag::frt kan::P_{pdeL}-lacZ</i> (merodiploid translational fusion)	this study	
AB2521	<i>pdeL (S298F)-3xflag::frt kan::P_{pdeL}-lacZ</i> (merodiploid translational fusion)	this study	

AB2849	<i>ΔpdeH::frit pdeL (E141A)-3xflag ::frit kan ::P_{pdel}-lacZ (merodiploid translational fusion)</i>	this study	
AB2731	<i>pdeL (E141A)-3xflag ::frit kan ::P_{pdel}-lacZ (merodiploid translational fusion)</i>	this study	
AB2377	<i>ΔpdeH::frit kan ::P_{pdel}-lacZ (merodiploid translational fusion)</i>	this study	
AB2986	<i>kan ::P_{pdel}-lacZ (merodiploid translational fusion)</i>	this study	
AB2851	<i>ΔpdeH::frit pdeL (E235A)-3xflag ::frit kan ::P_{pdel}-lacZ (merodiploid translational fusion)</i>	this study	
AB2519	<i>pdeL (E235A)-3xflag ::frit kan ::P_{pdel}-lacZ (merodiploid translational fusion)</i>	this study	Figure 3D
AB3383	<i>ΔpdeH::frit pdeL (T270A)-3xflag ::frit kan ::P_{pdel}-lacZ (merodiploid translational fusion)</i>	this study	
AB3381	<i>pdeL (T270A)-3xflag ::frit kan ::P_{pdel}-lacZ (merodiploid translational fusion)</i>	this study	
AB3449	<i>ΔpdeH::frit pdeL (D295N)-3xflag ::frit kan ::P_{pdel}-lacZ (merodiploid translational fusion)</i>	this study	
AB3447	<i>pdeL (D295N)-3xflag ::frit kan ::P_{pdel}-lacZ (merodiploid translational fusion)</i>	this study	
AB607	<i>ΔpdeH::frit</i>	Boehm et al. Cell 2010	Figure 4C, D
AB2271	<i>ΔpdeH::frit ΔpdeL::frit</i>	this study	
AB3455	<i>ΔpdeH::frit frit::P_{tet}-tetR-pdeL kan ::P_{pdel}-lacZ (merodiploid translational fusion)</i>	this study	Figure 4F
AB3508	<i>ΔpdeH::frit frit::P_{tet}-tetR-pdeL kan ::P_{pdel}-lacZ (merodiploid translational fusion)</i>	this study	
AB2377	<i>ΔpdeH::frit kan ::P_{pdel}-lacZ (merodiploid translational fusion)</i>	this study	Figure 5A, B
AB2939	<i>ΔpdeH::frit pdeL (D263N) (K283R)-3xflag ::frit kan ::P_{pdel}-lacZ (merodiploid translational fusion)</i>	this study	Figure 5C
AB3335	<i>ΔpdeH::frit P_{pdel}-lacZ (merodiploid translational fusion)</i>	this study	Figure 5D
AB3431	<i>ΔpdeH::frit pdeL-[RBS_{synth}-mCherry]::frit</i>	this study	Figure 5E, F
AB3496	<i>ΔpdeH::frit pdeL (D263N) (K283R)-[RBS_{synth}-mCherry]::frit</i>	this study	Figure 5G
AB3499	<i>ΔpdeH::frit P_{pdel}-lacZ-[RBS_{synth}-mCherry]::frit</i>	this study	Figure 5H
AB3299	<i>ΔpdeH::frit frit::P_{const. weak}-pgaA-D</i>	this study	Figure 6A
AB3302	<i>ΔpdeH::frit ΔpdeL::frit frit::P_{const. weak}-pgaA-D</i>	this study	
AB2996	<i>ΔpdeH::frit csrA::Tn5Δ(kan)::frit</i>	this study	Figure 6B
AB2997	<i>ΔpdeH::frit ΔpdeL::frit csrA::Tn5Δ(kan)::frit</i>	this study	
MC1655	E. coli K-12	Blattner et al.	
AB607	<i>ΔpdeH::frit</i>	Boehm et al. Cell 2010	
AB2137	<i>ΔpdeH::frit pdeL (G2995)-3xflag ::frit</i>	Reinders et al. J. Bact. 2015	Figure S1A
AB2202	<i>ΔpdeH::frit pdeL (F206)-3xflag ::frit</i>	Reinders et al. J. Bact. 2015	

AB2203	<i>ΔpdeH::frit pdeL (F249L)-3xflag::frit</i>	Reinders et al. J. Bact. 2015	
AB3368	<i>ΔpdeH::frit pdeL (T270A)-3xflag::frit</i>	this study	
AB2377	<i>ΔpdeH::frit kan::P_{pdeL}-lacZ (merodiploid translational fusion)</i>	this study	
AB2986	<i>kan::P_{pdeL}-lacZ (merodiploid translational fusion)</i>	this study	
AB2378	<i>ΔpdeH::frit pdeL (G299S)-3xflag::frit</i> <i>kan::P_{pdeL}-lacZ (merodiploid translational fusion)</i>	this study	
AB2535	<i>pdeL (G299S)-3xflag::frit kan::P_{pdeL}-lacZ (merodiploid translational fusion)</i>	this study	
AB2942	<i>ΔpdeH::frit pdeL (F206S)-3xflag::frit</i> <i>kan::P_{pdeL}-lacZ (merodiploid translational fusion)</i>	this study	Figure S1D
AB2940	<i>pdeL (F206S)-3xflag::frit kan::P_{pdeL}-lacZ (merodiploid translational fusion)</i>	this study	
AB2945	<i>ΔpdeH::frit pdeL (F249L)-3xflag::frit</i> <i>kan::P_{pdeL}-lacZ (merodiploid translational fusion)</i>	this study	
AB2943	<i>pdeL (F249L)-3xflag::frit kan::P_{pdeL}-lacZ (merodiploid translational fusion)</i>	this study	
AB3383	<i>ΔpdeH::frit pdeL (T270A)-3xflag::frit</i> <i>kan::P_{pdeL}-lacZ (merodiploid translational fusion)</i>	this study	
AB3381	<i>pdeL (T270A)-3xflag::frit kan::P_{pdeL}-lacZ (merodiploid translational fusion)</i>	this study	
AB2377	<i>ΔpdeH::frit kan::P_{pdeL}-lacZ (merodiploid translational fusion)</i>	this study	
AB2986	<i>kan::P_{pdeL}-lacZ (merodiploid translational fusion)</i>	this study	
AB2846	<i>ΔpdeH::frit pdeL (D263N)-3xflag::frit</i> <i>kan::P_{pdeL}-lacZ (merodiploid translational fusion)</i>	this study	
AB2520	<i>pdeL (D263N)-3xflag::frit kan::P_{pdeL}-lacZ (merodiploid translational fusion)</i>	this study	
AB2907	<i>ΔpdeH::frit pdeL (K283R)-3xflag::frit</i> <i>kan::P_{pdeL}-lacZ (merodiploid translational fusion)</i>	this study	Figure S4
AB2905	<i>pdeL (K283R)-3xflag::frit kan::P_{pdeL}-lacZ (merodiploid translational fusion)</i>	this study	
AB2939	<i>ΔpdeH::frit pdeL (D263N) (K283R)-3xflag::frit</i> <i>kan::P_{pdeL}-lacZ (merodiploid translational fusion)</i>	this study	
AB2937	<i>pdeL (D263N) (K283R)-3xflag::frit</i> <i>kan::P_{pdeL}-lacZ (merodiploid translational fusion)</i>	this study	

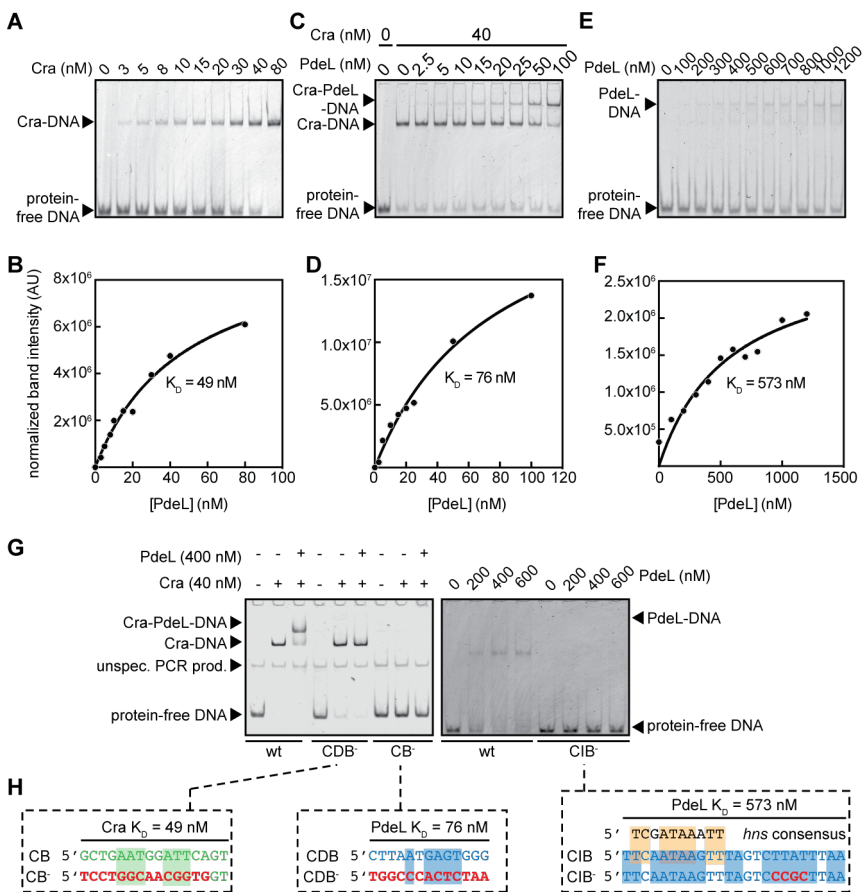
Table S2

Plasmid	Genotype	Source	Used in
pKD46	λ RED ⁺ (<i>amp</i>)	Datsenko et al.	
pCP20	FLP ⁺ (<i>amp</i>)	Cherepanov et al.	
pET28a	pBR332 lacI P ₁₇ (<i>kan</i>) 6xHis expression vector	Novagen	
pARI	<i>pdeL-strepII</i> in pET28a (<i>kan</i>)	Reinders et al. J. Bact. 2015	Figure 1B
pARI9	<i>cra-strepII</i> in pET28a (<i>kan</i>)	this study	

pAR28	<i>hns-strepII</i> in pET28a (<i>kan</i>)	this study	Figure 1D
pAR81	P_{lac} -RBS _{synth} - <i>pdeH</i> -3xflag in pNDM220 (<i>amp</i>)	this study	Figure 1E
pNDM220	<i>repA parR parM</i> P_{lac} (<i>amp</i>)	Gotfredsen et al.	
pAR81	P_{lac} -RBS _{synth} - <i>pdeH</i> -3xflag in pNDM220 (<i>amp</i>)	this study	Figure 2
pNDM220	<i>repA parR parM</i> P_{lac} (<i>amp</i>)	Gotfredsen et al.	
	6xhis- <i>pdeL</i> _{EAL} in pET28a (<i>kan</i>)	David Hinnen	
	6xhis- <i>pdeL</i> _{EAL} (E141A) in pET28a (<i>kan</i>)	David Hinnen	
pAR81	P_{lac} -RBS _{synth} - <i>pdeH</i> -3xflag in pNDM220 (<i>amp</i>)	this study	Figure 3D
pNDM220	<i>repA parR parM</i> P_{lac} (<i>amp</i>)	Gotfredsen et al.	
pAR202	<i>pdeL</i> _{EAL} -3xflag- <i>strepII</i> in pET28a (<i>kan</i>)	this study	Figure 3E
pAR205	<i>pdeL</i> _{EAL} (Y268C)-3xflag- <i>strepII</i> in pET28a (<i>kan</i>)	this study	
pAR202	<i>pdeL</i> _{EAL} -3xflag- <i>strepII</i> in pET28a (<i>kan</i>)	this study	Figure 3F
pAR205	<i>pdeL</i> _{EAL} (Y268C)-3xflag- <i>strepII</i> in pET28a (<i>kan</i>)	this study	
pAR211	<i>pdeL</i> _{EAL} (Y268C) (E235A)-3xflag- <i>strepII</i> in pET28a (<i>kan</i>)	this study	
pAR210	<i>pdeL</i> _{EAL} (Y268C) (T270A)-3xflag- <i>strepII</i> in pET28a (<i>kan</i>)	this study	
pAR212	<i>pdeL</i> _{EAL} (Y268C) (D295N)-3xflag- <i>strepII</i> in pET28a (<i>kan</i>)	this study	
pAR1	<i>pdeL</i> - <i>strepII</i> in pET28a (<i>kan</i>)	Reinders et al. J. Bact. 2015	
pAR201	<i>pdeL</i> (D295N)- <i>strepII</i> in pET28a (<i>kan</i>)	this study	Figure 4C, D, F
pAR81	P_{lac} -RBS _{synth} - <i>pdeH</i> -3xflag in pNDM220 (<i>amp</i>)	this study	
pAR81	P_{lac} -RBS _{synth} - <i>pdeH</i> -3xflag in pNDM220 (<i>amp</i>)	this study	Figure 5A-H
pAR81	P_{lac} -RBS _{synth} - <i>pdeH</i> -3xflag in pNDM220 (<i>amp</i>)	this study	Figure 6A, B
pAR19	<i>cra-strepII</i> in pET28a (<i>kan</i>)	this study	Figure S1A-D, G
pAR1	<i>pdeL</i> - <i>strepII</i> in pET28a (<i>kan</i>)	Reinders et al. J. Bact. 2015	Figure S1AC-G
pAR81	P_{lac} -RBS _{synth} - <i>pdeH</i> -3xflag in pNDM220 (<i>amp</i>)	this study	Figure S2D
pNDM220	<i>repA parR parM</i> P_{lac} (<i>amp</i>)	Gotfredsen et al.	
pAR81	P_{lac} -RBS _{synth} - <i>pdeH</i> -3xflag in pNDM220 (<i>amp</i>)	this study	Figure S4
pNDM220	<i>repA parR parM</i> P_{lac} (<i>amp</i>)	Gotfredsen et al.	
pAR3	<i>pdeL</i> (D263N)- <i>strepII</i> in pET28a (<i>kan</i>)	this study	
pAR52	<i>pdeL</i> (K283R)- <i>strepII</i> in pET28a (<i>kan</i>)	this study	
pAR62	<i>pdeL</i> (D263N) (K283R)- <i>strepII</i> in pET28a (<i>kan</i>)	this study	

Chapter 5 | SUPPLEMENTALS

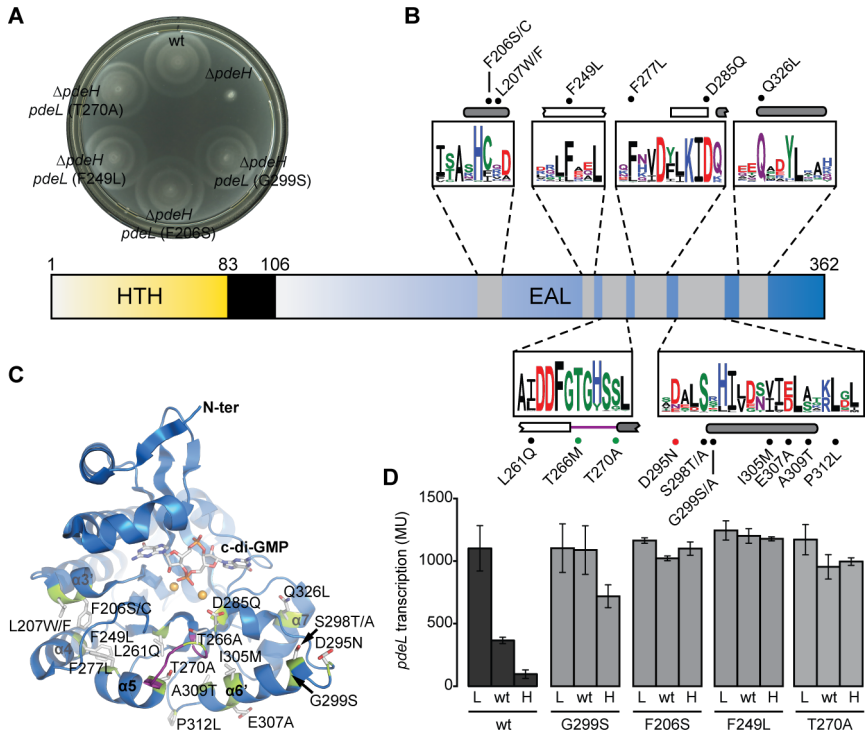
Figure S1 | Specificity and DNA-binding affinities of Cra and Pde to *pdeL* intergenic region



(A) Binding of purified Cra-StrepII to *pdeL* intergenic region as tested by electrophoretic mobility shift assay (EMSA). Binding is assayed using 5' Cy3-labeled oligonucleotides spanning the Cra-box (CB) as well as the Cra-dependent PdeL-box (CDB). DNA concentration is kept constant at 10 nM, while Cra protein titration concentration is shown. (B) Saturation binding fit of quantified band intensities. (C) EMSA and (D) binding affinity of purified PdeL-StrepII in presence of co-factor Cra using the same DNA region as indicated in (A). Cra-StrepII concentration was kept constant at 40 nM. In (D), the band intensities of the supershift (Cra-PdeL-DNA-complex) were quantified to obtain binding constant. (E) Binding of purified PdeL-StrepII to distal Cra-independent PdeL-box (CIB). DNA region containing 10 bp upstream and 33 bp downstream of the CIB was used. (F) Saturation binding fit of PdeL-DNA-bands (E) to determine binding constant. (G) Confirmation of abrogated binding of transcription factors by introducing point mutation in the recognition sequences. Left panel: binding of Cra and/or PdeL was tested at 40 nM Cra and 400 nM PdeL concentration. Right panel: binding of

PdeL to the CIB and to the mutated CIB (CIB) was tested at 200 - 600 nM PdeL concentration. **(H)** Recognition sequence of Cra and PdeL to corresponding binding boxes. Upper sequence shows recognition sequence whereas lower sequence highlighted in bold and red shows mutations introduced to abrogate binding. Note that mutations abolishing binding of PdeL to the CIB were chosen to not affect the putative H-NS consensus sequence.

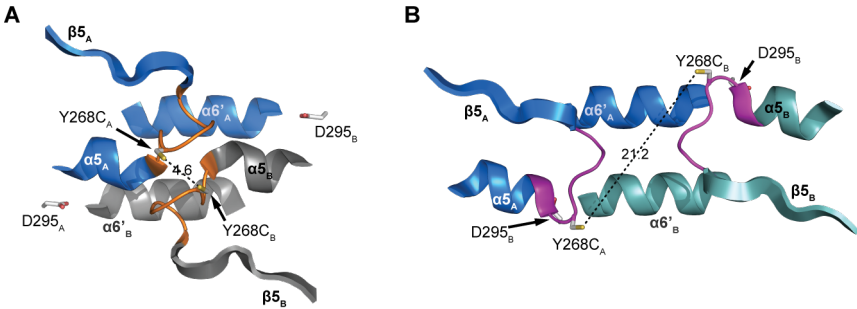
Figure S2 | Location and properties of PdeL motile suppressor alleles



(A) Swarm plate showing restoration of non-motile phenotype of $\Delta pdeH$ strain when combined with a selection of motile suppressor allele in PdeL. **(B)** Domain architecture of PdeL protein. Location of isolated motile suppressor alleles are shown as black dots. Red dot indicates aspartic acid responsible for stabilization of repulsive macro-dipole, which is generated by the N-termini of helices $\alpha 5$ and $\alpha 6$ facing each other. Green dots show position of motile suppressor alleles located within highly conserved loop 6. Secondary structural elements in EAL-domain are shown as follows (alpha-helices = rounded grey bars, b-sheets = blank rectangles = line, unstructured regions). Amino acid conservation of neighborhood of motile suppressor mutations is shown as web logo of 500 non-redundant EAL-domain proteins. **(C)** Crystal structure of monomer of non-conventional T-state PdeL_{EAL} dimer in presence of Ca²⁺ (orange spheres) and c-di-GMP as published in [62]. Conserved loop 6 is shown in purple. Residues, which resulted in motile suppressor phenotype are shown as sticks. Their position within the crystal structure is highlighted in yellow. **(D)** c-di-GMP-dependent *pdeL*.

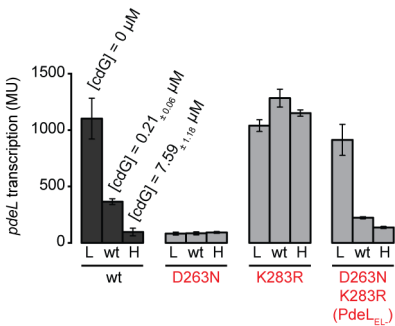
transcription of selection of motile suppressor alleles in PdeL. Wild-type PdeL is shown in grey. Note that – with exception of G299S – all tested alleles render the *pdeL* promoter irresponsive to different c-di-GMP regimes.

Figure S3 | R-state-specific cysteine-crosslink of PdeL (Y268C)



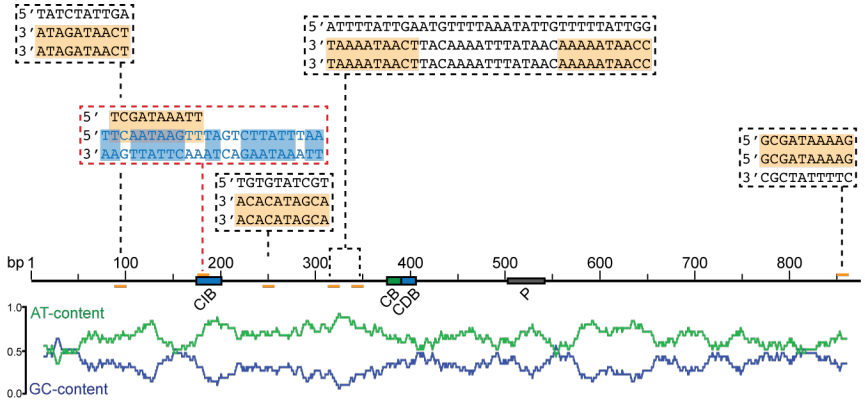
(A) Close-up of loop 6 (orange) and dimerization helices region of R-state dimer configuration of the EAL-domain of PdeL. Individual protomers are colored in marine or grey. Distance between Y268C of two protomers is shown as stippled black lines in Å. (B) Loop 6 (magenta) and dimerization helices region of T-state dimer configuration. Protomers here shown in marine and light-teal. Note the almost 5-fold higher distance of the Y268C substitutions compared to (A). Bismaleimidoethane (BMOE) is capable of crosslinking cysteines over a distance of maximal 8 Å.

Figure S4 | Characterization of enzymatic feedback loop-deficient PdeL_{EL} variant



Effect of wild type and mutant PdeL variants on c-di-GMP-dependent *pdeL* transcription measured via a chromosomal translational P_{pdeL} -*lacZ* reporter fusion. *PdeL* transcription was measured in different c-di-GMP regimes: (L = $\Delta pdeH$ strain with low c-di-GMP levels generated by 65 μM induction of plasmid-borne P_{lac} -*pdeH*; H = $\Delta pdeH$ strain with high c-di-GMP levels generated by not inducing plasmid). D263N = mutation of second aspartic acid from highly conserved DD motif (see Figure S2B) responsible for coordination of catalytic metals. K283R = mutation of conserved catalytic base. Combination of both mutations = PdeL_{EL} (enzymatic loop-deficient). C-di-GMP levels are from experiment in Figure 4D (black curve) Enzymatic activity was measured via Phosphate Sensor assay (see Materials & Methods & [79]). Enzymatically inactive PdeL variants are shown in red.

Figure S5 | Putative H-NS binding boxes within *pdeL* intergenic region



PdeL intergenic region shown with promoter (grey), PdeL binding boxes (blue) and Cra-binding box (green). Putative H-NS binding boxes, which were identified using the Virtual Footprint website <http://www.prodoric.de/vfp/> [252] are shown in orange. Individual regions are highlighted in base-pair resolution. Note that red box was not predicted *in silico* but was experimentally identified and characterized H-NS binding box (see **Figure 1A & D**). Graph below shows AT- and GC-content of *pdeL* intergenic region with a binning of 5 bp.

Chapter 6 | OUTLOOK

To this end we applied structure-function based approaches to unravel how c-di-GMP affects both the enzymatic as well as the transcriptional activity of PdeL. In the discussion, we proposed a model in which binding of PdeL to the upstream Cra-independent PdeL-box induces PdeL tetramerization, which stabilizes PdeL in the highly active R-state. This model emerges from previous evidences in which EAL-domain proteins were shown to form higher oligomers, and also from initial MALLS experiments that suggest a c-di-GMP and PdeL concentration-dependent oligomerization of PdeL. In collaboration with the structural group of Prof. Tilman Schirmer one major task will be to confirm these initial findings, structurally and biochemically characterize the tetrameric state of PdeL and unravel its implication *in vivo*.

In this study, we have acquired precise quantitative data regarding the enzymatic and transcriptional properties of PdeL and how PdeL contributes to the homeostasis of the global c-di-GMP pool on the population and on single-cell level. We suggested that PdeL is a module that responds to noise in the c-di-GMP concentration to either buffer or amplify these fluctuations, which ultimately leads to the establishment of bimodal c-di-GMP regimes. However, measuring noise in the c-di-GMP levels is a challenging endeavor experimentally. Given that the complexity of this multifactorial system easily exceeds simple two-dimensional problems, it will be paramount to apply mathematical modeling in the future. Not only can mathematical simulations of the *pdeL* regulation circuit strengthen the integrity of our proposed model but also serve to make predictions about the degree in c-di-GMP noise, which PdeL can amplify to generate bistable c-di-GMP regimes.

The fact that the central carbon metabolic regulator Cra binds to the *pdeL* promoter and growth on various carbon sources seems to affect *pdeL* transcription (data not shown), implied that the metabolic and c-di-GMP status of the cell are integrated to drive *pdeL* transcription and ultimately affect c-di-GMP levels. Combination of genetic and metabolomics will be subject to future work as an approach to understand the metabolic impact on c-di-GMP levels, and whether – in return – c-di-GMP itself might signal back into metabolism.

As a transcription factor, PdeL is likely to be involved in the regulation of more than just its own expression. It is hard to reconcile that a cell invests a high degree of energy and applies such a complex circuit to tune PdeL levels between roughly 200 and 1000 molecules per cell, although – if we neglect DNA-binding affinities – only 4 molecules are in principle required for the regulation of *pdeL* transcription. Rather it is conceivable that PdeL engages in further downstream signaling by binding and regulating secondary promoters. Initial proteomics analyses in which we compared the proteome of wild type and *pdeL* mutant in different c-di-GMP regimes already revealed several promising candidates involved in metabolism, biofilm formation and most interestingly c-di-GMP signaling itself. Future ChIP-Seq experiments will be complementary to the already performed proteomics approach and moreover will unravel direct PdeL targets

Chapter 7 | APPENDICES

References

1. Ross P, Weinhouse H, Aloni Y, Michaeli D, Weinberger-Ohana P, Mayer R, Braun S, de Vroom E, van der Marel GA, van Boom JH, et al. (1987) Regulation of cellulose synthesis in *Acetobacter xylinum* by cyclic diguanylic acid. *Nature* **325**: 279–281.
2. Witte G, Hartung S, Büttner K, Hopfner K-P (2008) Structural biochemistry of a bacterial checkpoint protein reveals diadenylate cyclase activity regulated by DNA recombination intermediates. *Molecular Cell* **30**: 167–178.
3. Davies BW, Bogard RW, Young TS, Mekalanos JJ (2012) Coordinated Regulation of Accessory Genetic Elements Produces Cyclic Di-Nucleotides for *Vibrio cholerae* Virulence. *Cell* **149**: 358–370.
4. Hornung V, Hartmann R, Ablasser A, Hopfner K-P (2014) OAS proteins and cGAS: unifying concepts in sensing and responding to cytosolic nucleic acids. *Nat Rev Immunol* **14**: 521–528.
5. Chan C, Paul R, Samoray D, Amiot NC, Giese B, Jenal U, Schirmer T (2004) Structural basis of activity and allosteric control of diguanylate cyclase. *Proc Natl Acad Sci USA* **101**: 17084–17089.
6. Kranzusch PJ, Lee ASY, Wilson SC, Solovykh MS, Vance RE, Berger JM, Doudna JA (2014) Structure-guided reprogramming of human cGAS dinucleotide linkage specificity. *Cell* **158**: 1011–1021.
7. Paul R, Weiser S, Amiot NC, Chan C, Schirmer T, Giese B, Jenal U (2004) Cell cycle-dependent dynamic localization of a bacterial response regulator with a novel diguanylate cyclase output domain. *Genes & Development* **18**: 715–727.
8. Christen M, Christen B, Folcher M, Schauerte A, Jenal U (2005) Identification and characterization of a cyclic di-GMP-specific phosphodiesterase and its allosteric control by GTP. *J Biol Chem* **280**: 30829–30837.
9. Lori C, Ozaki S, Steiner S, Böhm R, Abel S, Dubey BN, Schirmer T, Hiller S, Jenal U (2015) Cyclic di-GMP acts as a cell cycle oscillator to drive chromosome replication. *Nature* **523**: 236–239.
10. Srivastava D, Waters CM (2012) A tangled web: regulatory connections between quorum sensing and cyclic Di-GMP. *Journal of Bacteriology* **194**: 4485–4493.
11. Gupta KR, Kasetty S, Chatterji D (2015) Novel functions of (p)ppGpp and Cyclic di-GMP in mycobacterial physiology revealed by phenotype microarray analysis of wild-type and isogenic strains of *Mycobacterium smegmatis*. *Applied and Environmental Microbiology* **81**: 2571–2578.
12. An S-Q, Chin K-H, Febrer M, McCarthy Y, Yang J-G, Liu C-L, Swarbreck D, Rogers J,

- Dow JM, Chou S-H, et al. (2013) A cyclic GMP-dependent signalling pathway regulates bacterial phytopathogenesis. *EMBO J* 1–9.
13. Almlblad H, Harrison JJ, Rybtke M, Groizeleau J, Givskov M, Parsek MR, Tolker-Nielsen T (2015) The Cyclic AMP-Vfr Signaling Pathway in *Pseudomonas aeruginosa* Is Inhibited by Cyclic Di-GMP. *Journal of Bacteriology* **197**: 2190–2200.
 14. He Q, Wang F, Liu S, Zhu D, Cong H, Gao F, Li B, Wang H, Lin Z, Liao J, et al. (2015) Structural and Biochemical Insight into the Mechanism of Rv2837c from *Mycobacterium tuberculosis* as a C-di-NMP Phosphodiesterase. *Journal of Biological Chemistry*.
 15. Huynh TN, Luo S, Pensinger D, Sauer J-D, Tong L, Woodward JJ (2015) An HD-domain phosphodiesterase mediates cooperative hydrolysis of c-di-AMP to affect bacterial growth and virulence. *Proceedings of the National Academy of Sciences* **112**: E747–E756.
 16. Bai Y, Yang J, Eisele LE, Underwood AJ, Koestler BJ, Waters CM, Metzger DW, Bai G (2013) Two DHH Subfamily 1 Proteins in *Streptococcus pneumoniae* Possess Cyclic Di-AMP Phosphodiesterase Activity and Affect Bacterial Growth and Virulence. *Journal of Bacteriology* **195**: 5123–5132.
 17. Mehne FMP, Gunka K, Eilers H, Herzberg C, Kaever V, Stülke J (2013) Cyclic di-AMP homeostasis in *Bacillus subtilis*: both lack and high level accumulation of the nucleotide are detrimental for cell growth. *Journal of Biological Chemistry* **288**: 2004–2017.
 18. Witte CE, Whiteley AT, Burke TP, Sauer J-D, Portnoy DA, Woodward JJ (2013) Cyclic di-AMP is critical for *Listeria monocytogenes* growth, cell wall homeostasis, and establishment of infection. *mBio* **4**: e00282–13.
 19. Whiteley AT, Pollock AJ, Portnoy DA (2015) The PAMP c-di-AMP Is Essential for *Listeria monocytogenes* Growth in Rich but Not Minimal Media due to a Toxic Increase in (p)ppGpp. [corrected]. *Cell Host Microbe* **17**: 788–798.
 20. Kaplan Zeevi M, Shafir NS, Shaham S, Friedman S, Sigal N, Nir Paz R, Boneca IG, Herskovits AA (2013) *Listeria monocytogenes* multidrug resistance transporters and cyclic di-AMP, which contribute to type I interferon induction, play a role in cell wall stress. *Journal of Bacteriology* **195**: 5250–5261.
 21. Zhu Y, Pham TH, Nhiep THN, Vu NMT, Marcellin E, Chakrabortti A, Wang Y, Waanders J, Lo R, Huston WM, et al. (2016) Cyclic-di-AMP synthesis by the diadenylate cyclase CdaA is modulated by the peptidoglycan biosynthesis enzyme GlmM in *Lactococcus lactis*. *Mol Microbiol* **99**: 1015–1027.
 22. Luo Y, Helmann JD (2012) Analysis of the role of *Bacillus subtilis* $\sigma(M)$ in β -lactam

resistance reveals an essential role for c-di-AMP in peptidoglycan homeostasis. *Mol Microbiol* **83**: 623–639.

23. Corrigan RM, Abbott JC, Burhenne H, Kaever V, Gründling A (2011) c-di-AMP is a new second messenger in *Staphylococcus aureus* with a role in controlling cell size and envelope stress. *PLoS Pathog* **7**: e1002217.
24. Oppenheimer-Shaanan Y, Wexselblatt E, Katzhendler J, Yavin E, Ben-Yehuda S (2011) c-di-AMP reports DNA integrity during sporulation in *Bacillus subtilis*. *EMBO Rep* **12**: 594–601.
25. Gándara C, Alonso JC (2015) DisA and c-di-AMP act at the intersection between DNA-damage response and stress homeostasis in exponentially growing *Bacillus subtilis* cells. *DNA Repair (Amst)* **27**: 1–8.
26. Zhang L, He Z-G (2013) Radiation-sensitive gene A (RadA) targets DisA, DNA integrity scanning protein A, to negatively affect cyclic Di-AMP synthesis activity in *Mycobacterium smegmatis*. *Journal of Biological Chemistry* **288**: 22426–22436.
27. Corrigan RM, Campeotto I, Jeganathan T, Roelofs KG, Lee VT, Gründling A (2013) Systematic identification of conserved bacterial c-di-AMP receptor proteins. *Proceedings of the National Academy of Sciences*.
28. Chin K-H, Liang J-M, Yang J-G, Shih M-S, Tu Z-L, Wang Y-C, Sun X-H, Hu N-J, Liang Z-X, Dow JM, et al. (2015) Structural Insights into the Distinct Binding Mode of Cyclic Di-AMP with SaCpaA_RCK. *Biochemistry* **54**: 4936–4951.
29. Kim H, Youn S-J, Kim SO, Ko J, Lee J-O, Choi B-S (2015) Structural Studies of Potassium Transport Protein KtrA Regulator of Conductance of K⁺ (RCK) C Domain in Complex with Cyclic Diadenosine Monophosphate (c-di-AMP). *Journal of Biological Chemistry* **290**: 16393–16402.
30. Moscoso JA, Schramke H, Zhang Y, Tosi T, Dehbi A, Jung K, Gründling A (2015) Binding of Cyclic Di-AMP to the *Staphylococcus aureus* Sensor Kinase KdpD Occurs via the Universal Stress Protein Domain and Downregulates the Expression of the Kdp Potassium Transporter. *Journal of Bacteriology* **198**: 98–110.
31. Schuster CF, Bellows LE, Tosi T, Campeotto I, Corrigan RM, Freemont P, Gründling A (2016) The second messenger c-di-AMP inhibits the osmolyte uptake system OpuC in *Staphylococcus aureus*. *Sci Signal* **9**: ra81–ra81.
32. Huynh TN, Choi PH, Sureka K, Ledvina HE, Campillo J, Tong L, Woodward JJ (2016) Cyclic di-AMP targets the cystathionine beta-synthase domain of the osmolyte transporter OpuC. *Mol Microbiol* **102**: 233–243.
33. Zhang L, Li W, He Z-G (2013) DarR, a TetR-like transcriptional factor, is a cyclic di-AMP-responsive repressor in *Mycobacterium smegmatis*. *Journal of Biological*

- Chemistry* **288**: 3085–3096.
34. Nelson JW, Sudarsan N, Furukawa K, Weinberg Z, Wang JX, Breaker RR (2013) Riboswitches in eubacteria sense the second messenger c-di-AMP. *Nature Chemical Biology* **9**: 834–839.
 35. Gundlach J, Rath H, Herzberg C, Mäder U, Stülke J (2016) Second Messenger Signaling in *Bacillus subtilis*: Accumulation of Cyclic di-AMP Inhibits Biofilm Formation. *Front Microbiol* **7**: 804.
 36. Peng X, Zhang Y, Bai G, Zhou X, Wu H (2016) Cyclic di-AMP mediates biofilm formation. *Mol Microbiol* **99**: 945–959.
 37. Mehne FMP, Schröder-Tittmann K, Eijlander RT, Herzberg C, Hewitt L, Kaefer V, Lewis RJ, Kuipers OP, Tittmann K, Stülke J (2014) Control of the diadenylate cyclase CdaS in *Bacillus subtilis*: an autoinhibitory domain limits cyclic di-AMP production. *Journal of Biological Chemistry* **289**: 21098–21107.
 38. Sureka K, Choi PH, Precit M, Delince M, Pensinger D, Huynh TN, Jurado AR, Goo YA, Sadilek M, Iavarone AT, et al. (2014) The cyclic dinucleotide c-di-AMP is an allosteric regulator of metabolic enzyme function. *Cell* **158**: 1389–1401.
 39. Dengler V, McCallum N, Kiefer P, Christen P, Patrignani A, Vorholt JA, Berger-Bächi B, Senn MM (2013) Mutation in the C-di-AMP cyclase dacA affects fitness and resistance of methicillin resistant *Staphylococcus aureus*. *PLoS ONE* **8**: e73512.
 40. Ablasser A, Goldeck M, Cavlar T, Deimling T, Witte G, Röhl I, Hopfner K-P, Ludwig J, Hornung V (2013) cGAS produces a 2'-5'-linked cyclic dinucleotide second messenger that activates STING. *Nature* **498**: 380–384.
 41. Kato K, Ishii R, Hirano S, Ishitani R, Nureki O (2015) Structural Basis for the Catalytic Mechanism of DncV, Bacterial Homolog of Cyclic GMP-AMP Synthase. *Structure* **23**: 843–850.
 42. Nelson JW, Sudarsan N, Phillips GE, Stav S, Lünse CE, McCown PJ, Breaker RR (2015) Control of bacterial exoelectrogenesis by c-AMP-GMP. *Proceedings of the National Academy of Sciences* **112**: 5389–5394.
 43. Kellenberger CA, Wilson SC, Hickey SF, Gonzalez TL, Su Y, Hallberg ZF, Brewer TF, Iavarone AT, Carlson HK, Hsieh Y-F, et al. (2015) GEMM-I riboswitches from *Geobacter* sense the bacterial second messenger cyclic AMP-GMP. *Proceedings of the National Academy of Sciences* **112**: 5383–5388.
 44. Sun L, Wu J, Du F, Chen X, Chen ZJ (2013) Cyclic GMP-AMP synthase is a cytosolic DNA sensor that activates the type I interferon pathway. *Science* **339**: 786–791.
 45. Civril F, Deimling T, de Oliveira Mann CC, Ablasser A, Moldt M, Witte G, Hornung V, Hopfner K-P (2013) Structural mechanism of cytosolic DNA sensing by cGAS.

Nature **498**: 332–337.

46. Diner EJ, Burdette DL, Wilson SC, Monroe KM, Kellenberger CA, Hyodo M, Hayakawa Y, Hammond MC, Vance RE (2013) The innate immune DNA sensor cGAS produces a noncanonical cyclic dinucleotide that activates human STING. *CellReports* **3**: 1355–1361.
47. Kranzusch PJ, Wilson SC, Lee ASY, Berger JM, Doudna JA, Vance RE (2015) Ancient Origin of cGAS-STING Reveals Mechanism of Universal 2',3' cGAMP Signaling. *Molecular Cell* **59**: 891–903.
48. Karaolis DKR, Means TK, Yang D, Takahashi M, Yoshimura T, Muraille E, Philpott D, Schroeder JT, Hyodo M, Hayakawa Y, et al. (2007) Bacterial c-di-GMP is an immunostimulatory molecule. *J Immunol* **178**: 2171–2181.
49. McWhirter SM, Barbalat R, Monroe KM, Fontana MF, Hyodo M, Joncker NT, Ishii KJ, Akira S, Colonna M, Chen ZJ, et al. (2009) A host type I interferon response is induced by cytosolic sensing of the bacterial second messenger cyclic-di-GMP. *J Exp Med* **206**: 1899–1911.
50. Woodward JJ, Iavarone AT, Portnoy DA (2010) c-di-AMP secreted by intracellular *Listeria monocytogenes* activates a host type I interferon response. *Science* **328**: 1703–1705.
51. Andrade WA, Firon A, Schmidt T, Hornung V, Fitzgerald KA, Kurt-Jones EA, Trieu-Cuot P, Golenbock DT, Kaminski P-A (2016) Group B Streptococcus Degrades Cyclic-di-AMP to Modulate STING-Dependent Type I Interferon Production. *Cell Host Microbe* **20**: 49–59.
52. Schirmer T (2016) C-di-GMP Synthesis: Structural Aspects of Evolution, Catalysis and Regulation. *Journal of Molecular Biology* **428**: 3683–3701.
53. Gentner M, Allan MC, Zaehring F, Schirmer T, Grzesiek S (2011) Oligomer formation of the bacterial second messenger c-di-GMP: reaction rates and equilibrium constants indicate a monomeric state at physiological concentrations. *J Am Chem Soc* **133**: 111205181927003.
54. Römling U, Galperin MY, Gomelsky M (2013) Cyclic di-GMP: the first 25 years of a universal bacterial second messenger. *Microbiol Mol Biol Rev* **77**: 1–52.
55. Wassmann P, Chan C, Paul R, Beck A, Heerklotz H, Jenal U, Schirmer T (2007) Structure of BeF₃-Modified Response Regulator PleD: Implications for Diguanylate Cyclase Activation, Catalysis, and Feedback Inhibition. *Structure* **15**: 915–927.
56. Paul R, Abel S, Wassmann P, Beck A, Heerklotz H, Jenal U (2007) Activation of the diguanylate cyclase PleD by phosphorylation-mediated dimerization. *J Biol Chem* **282**: 29170–29177.

57. Christen B, Christen M, Paul R, Schmid F, Folcher M, Jenoe P, Meuwly M, Jenal U (2006) Allosteric control of cyclic di-GMP signaling. *J Biol Chem* **281**: 32015–32024.
58. De N, Pirruccello M, Krasteva PV, Bae N, Raghavan RV, Sondermann H (2008) Phosphorylation-Independent Regulation of the Diguanylate Cyclase WspR. *PLoS Biol* **6**: e67.
59. Zähringer F, Lacanna E, Jenal U, Schirmer T, Boehm A (2013) Structure and signaling mechanism of a zinc-sensory diguanylate cyclase. *Structure* **21**: 1149–1157.
60. Dahlstrom KM, Giglio KM, Sondermann H, O'Toole GA (2016) The Inhibitory Site of a Diguanylate Cyclase Is a Necessary Element for Interaction and Signaling with an Effector Protein. *Journal of Bacteriology* **198**: 1595–1603.
61. Barends TRM, Hartmann E, Griese JJ, Beitlich T, Kirienko NV, Ryjenkov DA, Reinstein J, Shoeman RL, Gomelsky M, Schlichting I (2009) Structure and mechanism of a bacterial light-regulated cyclic nucleotide phosphodiesterase. *Nature* **459**: 1015–1018.
62. Sundriyal A, Massa C, Samoray D, Zehender F, Sharpe T, Jenal U, Schirmer T (2014) Inherent regulation of EAL domain-catalyzed hydrolysis of second messenger cyclic di-GMP. *Journal of Biological Chemistry* **289**: 6978–6990.
63. Winkler A, Udvarhelyi A, Hartmann E, Reinstein J, Menzel A, Shoeman RL, Schlichting I (2014) Characterization of Elements Involved in Allosteric Light Regulation of Phosphodiesterase Activity by Comparison of Different Functional BlrP1 States. *Journal of Molecular Biology* **426**: 853–868.
64. Rao F, Qi Y, Chong HS, Kotaka M, Li B, Li J, Lescar J, Tang K, Liang Z-X (2009) The functional role of a conserved loop in EAL domain-based cyclic di-GMP-specific phosphodiesterase. *Journal of Bacteriology* **191**: 4722–4731.
65. Morgan JLW, McNamara JT, Zimmer J (2014) Mechanism of activation of bacterial cellulose synthase by cyclic di-GMP. *Nat Struct Mol Biol* **21**: 489–496.
66. Navarro MVAS, Newell PD, Krasteva PV, Chatterjee D, Madden DR, O'Toole GA, Sondermann H (2011) Structural basis for c-di-GMP-mediated inside-out signaling controlling periplasmic proteolysis. *PLoS Biol* **9**: e1000588.
67. Ryan RP, Fouhy Y, Lucey JF, Crossman LC, Spiro S, He Y-W, Zhang L-H, Heeb S, Cámara M, Williams P, et al. (2006) Cell-cell signaling in *Xanthomonas campestris* involves an HD-GYP domain protein that functions in cyclic di-GMP turnover. *Proc Natl Acad Sci USA* **103**: 6712–6717.
68. Bellini D, Caly DL, McCarthy Y, Bumann M, An S-Q, Dow JM, Ryan RP, Walsh MA (2014) Crystal structure of an HD-GYP domain cyclic-di-GMP phosphodiesterase reveals an enzyme with a novel trinuclear catalytic iron centre. *Mol Microbiol* **91**: 26–38.

69. Orr MW, Donaldson GP, Severin GB, Wang J, Sintim HO, Waters CM, Lee VT (2015) Oligoribonuclease is the primary degradative enzyme for pGpG in *Pseudomonas aeruginosa* that is required for cyclic-di-GMP turnover. *Proceedings of the National Academy of Sciences* **112**: E5048–E5057.
70. Cohen D, Mechold U, Nevenzal H, Yarmiyhu Y, Randall TE, Bay DC, Rich JD, Parsek MR, Kaever V, Harrison JJ, et al. (2015) Oligoribonuclease is a central feature of cyclic diguanylate signaling in *Pseudomonas aeruginosa*. *Proceedings of the National Academy of Sciences* **112**: 11359–11364.
71. García B, Latasa C, Solano C, Portillo FGD, Gamazo C, Lasa I (2004) Role of the GGDEF protein family in *Salmonella* cellulose biosynthesis and biofilm formation. *Mol Microbiol* **54**: 264–277.
72. Tuckerman JR, Gonzalez G, Sousa EHS, Wan X, Saito JA, Alam M, Gilles-Gonzalez M-A (2009) An Oxygen-Sensing Diguanylate Cyclase and Phosphodiesterase Couple for c-di-GMP Control. *Biochemistry* **48**: 9764–9774.
73. Plate L, Marletta MA (2012) Nitric Oxide Modulates Bacterial Biofilm Formation through a Multicomponent Cyclic-di-GMP Signaling Network. *Molecular Cell* 1–12.
74. Basu Roy A, Sauer K (2014) Diguanylate cyclase NicD-based signalling mechanism of nutrient-induced dispersion by *Pseudomonas aeruginosa*. *Mol Microbiol* **94**: 771–793.
75. Mills E, Petersen E, Kulasekara BR, Miller SI (2015) A direct screen for c-di-GMP modulators reveals a *Salmonella Typhimurium* periplasmic ι -arginine-sensing pathway. *Sci Signal* **8**: ra57–ra57.
76. O'Connor JR, Kuwada NJ, Huangyutitham V, Wiggins PA, Harwood CS (2012) Surface sensing and lateral subcellular localization of WspA, the receptor in a chemosensory-like system leading to c-di-GMP production. *Mol Microbiol* **86**: 720–729.
77. Hengge R, Galperin MY, Ghigo J-M, Gomelsky M, Green J, Hughes KT, Jenal U, Landini P (2015) Systematic nomenclature for GGDEF and EAL domain-containing c-di-GMP turnover proteins of *Escherichia coli*. *Journal of Bacteriology*.
78. Boehm A, Kaiser M, Li H, Spangler C, Kasper CA, Ackermann M, Kaever V, Sourjik V, Roth V, Jenal U (2010) Second Messenger-Mediated Adjustment of Bacterial Swimming Velocity. *Cell* **141**: 107–116.
79. Reinders A, Hee C-S, Ozaki S, Mazur A, Boehm A, Schirmer T, Jenal U (2015) Expression and Genetic Activation of Cyclic Di-GMP-Specific Phosphodiesterases in *Escherichia coli*. *Journal of Bacteriology* **198**: 448–462.
80. Lindenberg S, Klauck G, Pesavento C, Klauck E, Hengge R (2013) The EAL domain protein YciR acts as a trigger enzyme in a c-di-GMP signalling cascade in *E. coli* biofilm control. *EMBO J* **32**: 2001–2014.

81. Chou S-H, Galperin MY (2015) Diversity of c-di-GMP-binding proteins and mechanisms. *Journal of Bacteriology*.
82. Hengge R (2010) Cyclic-di-GMP reaches out into the bacterial RNA world. *Sci Signal*.
83. Krasteva PV, Fong JCN, Shikuma NJ, Beyhan S, Navarro MVAS, Yildiz FH, Sondermann H (2010) *Vibrio cholerae* VpsT regulates matrix production and motility by directly sensing cyclic di-GMP. *Science* **327**: 866–868.
84. Baraquet C, Harwood CS (2013) Cyclic diguanosine monophosphate represses bacterial flagella synthesis by interacting with the Walker A motif of the enhancer-binding protein FleQ. *Proceedings of the National Academy of Sciences*.
85. Tschowri N, Schumacher MA, Schlimpert S, Chinnam NB, Findlay KC, Brennan RG, Buttner MJ (2014) Tetrameric c-di-GMP mediates effective transcription factor dimerization to control *Streptomyces* development. *Cell* **158**: 1136–1147.
86. Habazettl J, Allan MG, Jenal U, Grzesiek S (2011) Solution structure of the PilZ domain protein PA4608 complex with cyclic di-GMP identifies charge clustering as molecular readout. *Journal of Biological Chemistry* **286**: 14304–14314.
87. Schumacher MA, Zeng W (2016) Structures of the activator of *K. pneumoniae* biofilm formation, MrkH, indicates PilZ domains involved in c-di-GMP and DNA binding. *Proceedings of the National Academy of Sciences* **113**: 10067–10072.
88. Duerig A, Abel S, Folcher M, Nicollier M, Schwede T, Amiot N, Giese B, Jenal U (2009) Second messenger-mediated spatiotemporal control of protein degradation regulates bacterial cell cycle progression. *Genes & Development* **23**: 93–104.
89. An S-Q, Caly DL, McCarthy Y, Murdoch SL, Ward J, Febrer M, Dow JM, Ryan RP (2014) Novel cyclic di-GMP effectors of the YajQ protein family control bacterial virulence. *PLoS Pathog* **10**: e1004429.
90. Fazli M, O'Connell A, Nilsson M, Niehaus K, Dow JM, Givskov M, Ryan RP, Tolker-Nielsen T (2011) The CRP/FNR family protein Bcam1349 is a c-di-GMP effector that regulates biofilm formation in the respiratory pathogen *Burkholderia cenocepacia*. *Mol Microbiol* **82**: 327–341.
91. Matsuyama BY, Krasteva PV, Baraquet C, Harwood CS, Sondermann H, Navarro MVAS (2016) Mechanistic insights into c-di-GMP-dependent control of the biofilm regulator FleQ from *Pseudomonas aeruginosa*. *Proceedings of the National Academy of Sciences* **113**: E209–E218.
92. Skotnicka D, Smaldone GT, Petters T, Trampari E, Liang J, Kaefer V, Malone JG, Singer M, Søgaard-Andersen L (2016) A Minimal Threshold of c-di-GMP Is Essential for Fruiting Body Formation and Sporulation in *Myxococcus xanthus*. *PLoS Genet* **12**: e1006080.

93. Srivastava D, Hsieh M-L, Khataokar A, Neiditch MB, Waters CM (2013) Cyclic di-GMP inhibits *Vibrio cholerae* motility by repressing induction of transcription and inducing extracellular polysaccharide production. *Mol Microbiol* **90**: 1262–1276.
94. Roelofs KG, Jones CJ, Helman SR, Shang X, Orr MW, Goodson JR, Galperin MY, Yildiz FH, Lee VT (2015) Systematic Identification of Cyclic-di-GMP Binding Proteins in *Vibrio cholerae* Reveals a Novel Class of Cyclic-di-GMP-Binding ATPases Associated with Type II Secretion Systems. *PLoS Pathog* **11**: e1005232.
95. Jones CJ, Utada A, Davis KR, Thongsomboon W, Zamorano Sanchez D, Banakar V, Cegelski L, Wong GCL, Yildiz FH (2015) C-di-GMP Regulates Motile to Sessile Transition by Modulating MshA Pili Biogenesis and Near-Surface Motility Behavior in *Vibrio cholerae*. *PLoS Pathog* **11**: e1005068.
96. Wang Y-C, Chin K-H, Tu Z-L, He J, Jones CJ, Sanchez DZ, Yildiz FH, Galperin MY, Chou S-H (2016) Nucleotide binding by the widespread high-affinity cyclic di-GMP receptor MshEN domain. *Nat Commun* **7**: 1–12.
97. Moscoso JA, Mikkelsen H, Heeb S, Williams P, Filloux A (2011) The *Pseudomonas aeruginosa* sensor RetS switches Type III and Type VI secretion via c-di-GMP signalling. *Environmental Microbiology*.
98. Trampari E, Stevenson CEM, Little RH, Wilhelm T, Lawson DM, Malone JG (2015) Bacterial Rotary Export ATPases are Allosterically Regulated by the Nucleotide Second Messenger Cyclic-di-GMP. *Journal of Biological Chemistry* jbc.M115.661439.
99. Spangler C, Böhm A, Jenal U, Seifert R, Kaever V (2010) A liquid chromatography-coupled tandem mass spectrometry method for quantitation of cyclic di-guanosine monophosphate. *Journal of Microbiological Methods* **81**: 226–231.
100. Burhenne H, Kaever V (2013) Quantification of cyclic dinucleotides by reversed-phase LC-MS/MS. *Methods Mol Biol* **1016**: 27–37.
101. Pawar SV, Messina M, Rinaldo S, Cutruzzola F, Kaever V, Rampioni G, Leoni L (2016) Novel genetic tools to tackle c-di-GMP-dependent signalling in *Pseudomonas aeruginosa*. *J Appl Microbiol* **120**: 205–217.
102. Zhou H, Zheng C, Su J, Chen B, Fu Y, Xie Y, Tang Q, Chou S-H, He J (2016) Characterization of a natural triple- tandem c-di-GMP riboswitch and application of the riboswitch-based dual- uorescence reporter. *Sci Rep* **6**: 1–13.
103. Kellenberger CA, Wilson SC, Sales-Lee J, Hammond MC (2013) RNA-Based Fluorescent Biosensors for Live Cell Imaging of Second Messengers Cyclic di-GMP and Cyclic AMP-GMP. *J Am Chem Soc* **135**: 4906–4909.
104. Rybtke MT, Borlee BR, Murakami K, Irie Y, Hentzer M, Nielsen TE, Givskov M, Parsek MR, Tolker-Nielsen T (2012) Fluorescence-based reporter for gauging cyclic di-GMP

- levels in *Pseudomonas aeruginosa*. *Applied and Environmental Microbiology* **78**: 5060–5069.
105. Christen M, Kulasekara HD, Christen B, Kulasekara BR, Hoffman LR, Miller SI (2010) Asymmetrical Distribution of the Second Messenger c-di-GMP upon Bacterial Cell Division. *Science* **328**: 1295–1297.
106. Kulasekara BR, Kamischke C, Kulasekara HD, Christen M, Wiggins PA, Miller SI (2013) c-di-GMP heterogeneity is generated by the chemotaxis machinery to regulate flagellar motility. *eLife* **2**: e01402.
107. Nesper J, Reinders A, Glatter T, Schmidt A, Jenal U (2012) A novel capture compound for the identification and analysis of cyclic di-GMP binding proteins. *Journal of Proteomics* **75**: 4874–4878.
108. Laventie B-J, Nesper J, Ahrné E, Glatter T, Schmidt A, Jenal U (2015) Capture compound mass spectrometry—a powerful tool to identify novel c-di-GMP effector proteins. *JoVE*.
109. Düvel J, Bertinetti D, Möller S, Schwede F, Morr M, Wissing J, Radamm L, Zimmermann B, Genieser H-G, Jänsch L, et al. (2011) A chemical proteomics approach to identify c-di-GMP binding proteins in *Pseudomonas aeruginosa*. *Journal of Microbiological Methods*.
110. Steiner S, Lori C, Boehm A, Jenal U (2013) Allosteric activation of exopolysaccharide synthesis through cyclic di-GMP-stimulated protein-protein interaction. *EMBO J* **32**: 354–368.
111. Rotem O, Nesper J, Borovok I, Gorovits R, Kolot M, Pasternak Z, Shin I, Glatter T, Pietrovski S, Jenal U, et al. (2015) An extended cyclic di-GMP network in the predatory bacterium *Bdellovibrio bacteriovorus*. *Journal of Bacteriology*.
112. Roelofs KG, Wang J, Sintim HO, Lee VT (2011) Differential radial capillary action of ligand assay for high-throughput detection of protein-metabolite interactions. *Proc Natl Acad Sci USA* **108**: 15528–15533.
113. Kirkpatrick CL, Viollier PH (2012) Decoding *Caulobacter* development. *FEMS Microbiology Reviews* **36**: 193–205.
114. Abel S, Chien P, Wassmann P, Schirmer T, Kaever V, Laub MT, Baker TA, Jenal U (2011) Regulatory Cohesion of Cell Cycle and Cell Differentiation through Interlinked Phosphorylation and Second Messenger Networks. *Molecular Cell* **43**: 550–560.
115. Abel S, Bucher T, Nicollier M, Hug I, Kaever V, Abel zur Wiesch P, Jenal U (2013) Bimodal Distribution of the Second Messenger c-di-GMP Controls Cell Fate and Asymmetry during the *Caulobacter* Cell Cycle. *PLoS Genet* **9**: e1003744.
116. Paul R, Jaeger T, Abel S, Wiedeker I, Folcher M, Biondi EG, Laub MT, Jenal U (2008)

Allosteric regulation of histidine kinases by their cognate response regulator determines cell fate. *Cell* **133**: 452–461.

117. Davis NJ, Cohen Y, Sanselicio S, Fumeaux C, Ozaki S, Luciano J, Guerrero-Ferreira RC, Wright ER, Jenal U, Viollier PH (2013) De- and repolarization mechanism of flagellar morphogenesis during a bacterial cell cycle. *Genes & Development* **27**: 2049–2062.
118. Ozaki S, Schalch-Moser A, Zumthor L, Manfredi P, Ebbensgaard A, Schirmer T, Jenal U (2014) Activation and polar sequestration of PopA, a c-di-GMP effector protein involved in *Caulobacter crescentus* cell cycle control. *Mol Microbiol* **94**: 580–594.
119. Smith SC, Joshi KK, Zik JJ, Trinh K, Kamajaya A, Chien P, Ryan KR (2014) Cell cycle-dependent adaptor complex for ClpXP-mediated proteolysis directly integrates phosphorylation and second messenger signals. *Proceedings of the National Academy of Sciences* **111**: 14229–14234.
120. Dubey BN, Lori C, Ozaki S, Fucile G, Plaza-Menacho I, Jenal U, Schirmer T (2016) Cyclic di-GMP mediates a histidine kinase/phosphatase switch by noncovalent domain cross-linking. *Sci Adv* **2**: e1600823.
121. Morgan DO (1997) Cyclin-dependent kinases: engines, clocks, and microprocessors. *Annu Rev Cell Dev Biol* **13**: 261–291.
122. Chen YE, Tropini C, Jonas K, Tsokos CG, Huang KC, Laub MT (2011) Spatial gradient of protein phosphorylation underlies replicative asymmetry in a bacterium. *Proceedings of the National Academy of Sciences* **108**: 1052–1057.
123. Tsokos CG, Perchuk BS, Laub MT (2011) A dynamic complex of signaling proteins uses polar localization to regulate cell-fate asymmetry in *Caulobacter crescentus*. *Dev Cell* **20**: 329–341.
124. Bush MJ, Tschowri N, Schlimpert S, Flårdh K, Buttner MJ (2015) c-di-GMP signalling and the regulation of developmental transitions in streptomycetes. *Nature Publishing Group* **13**: 749–760.
125. Petters T, Zhang X, Nesper J, Treuner-Lange A, Gomez-Santos N, Hoppert M, Jenal U, Søgaard-Andersen L (2012) The orphan histidine protein kinase SgmT is a c-di-GMP receptor and regulates composition of the extracellular matrix together with the orphan DNA binding response regulator DigR in *Myxococcus xanthus*. *Mol Microbiol* **84**: 147–165.
126. Hogley L, Fung RKY, Lambert C, Harris MATS, Dabhi JM, King SS, Basford SM, Uchida K, Till R, Ahmad R, et al. (2012) Discrete cyclic di-GMP-dependent control of bacterial predation versus axenic growth in *Bdellovibrio bacteriovorus*. *PLoS Pathog* **8**: e1002493.
127. Enomoto G, Ni-Ni-Win, Narikawa R, Ikeuchi M (2015) Three cyanobacteriochromes

- work together to form a light color-sensitive input system for c-di-GMP signaling of cell aggregation. *Proceedings of the National Academy of Sciences* **112**: 8082–8087.
128. Valentini M, Filloux A (2016) Biofilms and Cyclic di-GMP (c-di-GMP) Signaling: Lessons from *Pseudomonas aeruginosa* and Other Bacteria. *Journal of Biological Chemistry* **291**: 12547–12555.
129. Russell MH, Bible AN, Fang X, Gooding JR, Campagna SR, Gomelsky M, Alexandre G (2013) Integration of the Second Messenger c-di-GMP into the Chemotactic Signaling Pathway. *mBio* **4**: e00001–13–e00001–13.
130. Paul K, Nieto V, Carlquist WC, Blair DF, Harshey RM (2010) The c-di-GMP binding protein YcgR controls flagellar motor direction and speed to affect chemotaxis by a ‘backstop brake’ mechanism. *Molecular Cell* **38**: 128–139.
131. Fang X, Gomelsky M (2010) A post-translational, c-di-GMP-dependent mechanism regulating flagellar motility. *Mol Microbiol* **76**: 1295–1305.
132. Chen Y, Chai Y, Guo JH, Losick R (2012) Evidence for Cyclic Di-GMP-Mediated Signaling in *Bacillus subtilis*. *Journal of Bacteriology* **194**: 5080–5090.
133. Baker AE, Diepold A, Kuchma SL, Scott JE, Ha DG, Orazi G, Armitage JP, O’Toole GA (2016) PilZ Domain Protein FlgZ Mediates Cyclic Di-GMP-Dependent Swarming Motility Control in *Pseudomonas aeruginosa*. *Journal of Bacteriology* **198**: 1837–1846.
134. Martínez-Granero F, Navazo A, Barahona E, Redondo-Nieto M, González de Heredia E, Baena I, Martín-Martín I, Rivilla R, Martín M (2014) Identification of flgZ as a flagellar gene encoding a PilZ domain protein that regulates swimming motility and biofilm formation in *Pseudomonas*. *PLoS ONE* **9**: e87608.
135. Pultz IS, Christen M, Kulasekara HD, Kennard A, Kulasekara B, Miller SI (2012) The response threshold of *Salmonella* PilZ domain proteins is determined by their binding affinities for c-di-GMP. *Mol Microbiol* n/a–n/a.
136. Park JH, Jo Y, Jang SY, Kwon H, Irie Y, Parsek MR, Kim MH, Choi SH (2015) The cabABC Operon Essential for Biofilm and Rugose Colony Development in *Vibrio vulnificus*. *PLoS Pathog* **11**: e1005192.
137. Kariisa AT, Weeks K, Tamayo R (2016) The RNA Domain Vc1 Regulates Downstream Gene Expression in Response to Cyclic Diguanylate in *Vibrio cholerae*. *PLoS ONE* **11**: e0148478.
138. Skotnicka D, Petters T, Heering J, Hoppert M, Kaever V, Søgaard-Andersen L (2015) Cyclic Di-GMP Regulates Type IV Pilus-Dependent Motility in *Myxococcus xanthus*. *Journal of Bacteriology* **198**: 77–90.
139. Kazmierczak BI, Lebron MB, Murray TS (2006) Analysis of FimX, a phosphodiesterase that governs twitching motility in *Pseudomonas aeruginosa*. *Mol Microbiol* **60**: 1026–

1043.

140. Bordeleau E, Purcell EB, Lafontaine DA, Fortier L-C, Tamayo R, Burrus V (2015) Cyclic Di-GMP Riboswitch-Regulated Type IV Pili Contribute to Aggregation of *Clostridium difficile*. *Journal of Bacteriology* **197**: 819–832.
141. Serra DO, Richter AM, Klauck G, Mika F, Hengge R (2013) Microanatomy at cellular resolution and spatial order of physiological differentiation in a bacterial biofilm. *mBio* **4**: e00103–e00113.
142. Pesavento C, Becker G, Sommerfeldt N, Possling A, Tschowri N, Mehlis A, Hengge R (2008) Inverse regulatory coordination of motility and curli-mediated adhesion in *Escherichia coli*. *Genes & Development* **22**: 2434–2446.
143. Vakulskas CA, Potts AH, Babitzke P, Ahmer BMM, Romeo T (2015) Regulation of bacterial virulence by Csr (Rsm) systems. *Microbiol Mol Biol Rev* **79**: 193–224.
144. Chua SL, Hultqvist LD, Yuan M, Rybtke M, Nielsen TE, Givskov M, Tolker-Nielsen T, Yang L (2015) In vitro and in vivo generation and characterization of *Pseudomonas aeruginosa* biofilm–dispersed cells via c-di-GMP manipulation. *Nat Protoc* **10**: 1165–1180.
145. Chatterjee D, Cooley RB, Boyd CD, Mehl RA, O’Toole GA, Sondermann H (2014) Mechanistic insight into the conserved allosteric regulation of periplasmic proteolysis by the signaling molecule cyclic-di-GMP. *eLife* **3**: e03650.
146. Malone JG, Jaeger T, Manfredi P, Dötsch A, Blanka A, Bos R, Cornelis GR, Häussler S, Jenal U (2012) The YfiBNR signal transduction mechanism reveals novel targets for the evolution of persistent *Pseudomonas aeruginosa* in cystic fibrosis airways. *PLoS Pathog* **8**: e1002760.
147. Blanka A, Düvel J, Dötsch A, Klinkert B, Abraham W-R, Kaefer V, Ritter C, Narberhaus F, Häussler S (2015) Constitutive production of c-di-GMP is associated with mutations in a variant of *Pseudomonas aeruginosa* with altered membrane composition. *Sci Signal* **8**: ra36.
148. Jeffery CJ (1999) Moonlighting proteins. *Trends in Biochemical Sciences* **24**: 8–11.
149. Commichau FM, Stülke J (2007) Trigger enzymes: bifunctional proteins active in metabolism and in controlling gene expression. *Mol Microbiol* **67**: 692–702.
150. Ingerson-Mahar M, Briegel A, Werner JN, Jensen GJ, Gitai Z (2010) The metabolic enzyme CTP synthase forms cytoskeletal filaments. *Nat Cell Biol* **12**: 739–746.
151. Ostrovsky de Spicer P, O’Brien K, Maloy S (1991) Regulation of proline utilization in *Salmonella typhimurium*: a membrane-associated dehydrogenase binds DNA in vitro. *Journal of Bacteriology* **173**: 211–219.
152. Ostrovsky de Spicer P, Maloy S (1993) PutA protein, a membrane-associated flavin

- dehydrogenase, acts as a redox-dependent transcriptional regulator. *Proc Natl Acad Sci USA* **90**: 4295–4298.
153. Bordeleau E, Fortier L-C, Malouin F, Burrus V (2011) c-di-GMP turn-over in *Clostridium difficile* is controlled by a plethora of diguanylate cyclases and phosphodiesterases. *PLoS Genet* **7**: e1002039.
 154. Purcell EB, McKee RW, McBride SM, Waters CM, Tamayo R (2012) Cyclic diguanylate inversely regulates motility and aggregation in *Clostridium difficile*. *Journal of Bacteriology* **194**: 3307–3316.
 155. Soutourina OA, Monot M, Boudry P, Saujet L, Pichon C, Sismeiro O, Semenova E, Severinov K, Le Bouguenec C, Coppée J-Y, et al. (2013) Genome-wide identification of regulatory RNAs in the human pathogen *Clostridium difficile*. *PLoS Genet* **9**: e1003493.
 156. Purcell EB, McKee RW, Bordeleau E, Burrus V, Tamayo R (2015) Regulation of Type IV Pili Contributes to Surface Behaviors of Historical and Epidemic Strains of *Clostridium difficile*. *Journal of Bacteriology* **198**: 565–577.
 157. McKee RW, Mangalea MR, Purcell EB, Borchardt EK, Tamayo R (2013) The second messenger cyclic Di-GMP regulates *Clostridium difficile* toxin production by controlling expression of sigD. *Journal of Bacteriology* **195**: 5174–5185.
 158. Peltier J, Shaw HA, Couchman EC, Dawson LF, Yu L, Choudhary JS, Kaever V, Wren BW, Fairweather NF (2015) Cyclic diGMP regulates production of sortase substrates of *Clostridium difficile* and their surface exposure through ZmpI protease-mediated cleavage. *Journal of Biological Chemistry* **290**: 24453–24469.
 159. Buchholz U, Bernard H, Werber D, Böhmer MM, Remschmidt C, Wilking H, Deleré Y, an der Heiden M, Adlhoch C, Dreesman J, et al. (2011) German outbreak of *Escherichia coli* O104:H4 associated with sprouts. *N Engl J Med* **365**: 1763–1770.
 160. Richter AM, Povolotsky TL, Wieler LH, Hengge R (2014) Cyclic-di-GMP signalling and biofilm-related properties of the Shiga toxin-producing 2011 German outbreak *Escherichia coli* O104:H4. *EMBO Molecular Medicine* **6**: 1622–1637.
 161. Jenal U, Malone J (2006) Mechanisms of cyclic-di-GMP signaling in bacteria. *Annu Rev Genet* **40**: 385–407.
 162. Hengge R (2009) Principles of c-di-GMP signalling in bacteria. *Nature Publishing Group* **7**: 263–273.
 163. Lee ER, Baker JL, Weinberg Z, Sudarsan N, Breaker RR (2010) An Allosteric Self-Splicing Ribozyme Triggered by a Bacterial Second Messenger. *Science* **329**: 845–848.
 164. Li L, Yin Q, Kuss P, Maliga Z, Millán JL, Wu H, Mitchison TJ (2014) Hydrolysis of 2'3'-cGAMP by ENPP1 and design of nonhydrolyzable analogs. *Nature Chemical Biology* **10**: 1043–1048.

165. Ohana P, Delmer DP, Carlson RW, Glushka J, Azadi P, Bacic T, Benziman M (1998) Identification of a novel triterpenoid saponin from *Pisum sativum* as a specific inhibitor of the diguanylate cyclase of *Acetobacter xylinum*. *Plant Cell Physiol* **39**: 144–152.
166. Lieberman OJ, Orr MW, Wang Y, Lee VT (2014) High-throughput screening using the differential radial capillary action of ligand assay identifies ebselen as an inhibitor of diguanylate cyclases. *ACS Chem Biol* **9**: 183–192.
167. Furukawa S, Kuchma SL, O'Toole GA (2006) Keeping their options open: acute versus persistent infections. *Journal of Bacteriology* **188**: 1211–1217.
168. Schirmer T, Jenal U (2009) Structural and mechanistic determinants of c-di-GMP signalling. *Nature Publishing Group* **7**: 724–735.
169. Sondermann H, Shikuma NJ, Yildiz FH (2012) You've come a long way: c-di-GMP signaling. *Current Opinion in Microbiology* **15**: 140–146.
170. Köster H, Little DP, Luan P, Muller R, Siddiqi SM, Marappan S, Yip P (2007) Capture Compound Mass Spectrometry: A Technology for the Investigation of Small Molecule Protein Interactions. *ASSAY and Drug Development Technologies* **5**: 381–390.
171. Lenz T, Fischer JJ, Dreger M (2011) Probing small molecule-protein interactions: A new perspective for functional proteomics. *Journal of Proteomics* **75**: 100–115.
172. Cline MR, Mandel SM, Platz MS (2007) Identification of the reactive intermediates produced upon photolysis of p-azidoacetophenone and its tetrafluoro analogue in aqueous and organic solvents: implications for photoaffinity labeling. *Biochemistry* **46**: 1981–1987.
173. Hickman JW, Harwood CS (2008) Identification of FleQ from *Pseudomonas aeruginosa* as a c-di-GMP-responsive transcription factor. *Mol Microbiol* **69**: 376–389.
174. Winsor GL, Lo R, Ho Sui SJ, Ung KSE, Huang S, Cheng D, Ching W-KH, Hancock REW, Brinkman FSL (2005) *Pseudomonas aeruginosa* Genome Database and PseudoCAP: facilitating community-based, continually updated, genome annotation. *Nucleic Acids Res* **33**: D338–D343.
175. Solano C, García B, Latasa C, Toledo-Arana A, Zorraquino V, Valle J, Casals J, Pedroso E, Lasa I (2009) Genetic reductionist approach for dissecting individual roles of GGDEF proteins within the c-di-GMP signaling network in *Salmonella*. *Proceedings of the National Academy of Sciences* **106**: 7997–8002.
176. Ryjenkov DA, Simm R, Römling U, Gomelsky M (2006) The PilZ domain is a receptor for the second messenger c-di-GMP: the PilZ domain protein YcgR controls motility in enterobacteria. *J Biol Chem* **281**: 30310–30314.
177. Christen M, Christen B, Allan MG, Folcher M, Jenö P, Grzesiek S, Jenal U (2007) DgrA

- is a member of a new family of cyclic diguanosine monophosphate receptors and controls flagellar motor function in *Caulobacter crescentus*. *Proc Natl Acad Sci USA* **104**: 4112–4117.
178. Zähringer F, Massa C, Schirmer T (2010) Efficient Enzymatic Production of the Bacterial Second Messenger c-di-GMP by the Diguanylate Cyclase YdeH from *E. coli*. *Appl Biochem Biotechnol* **163**: 71–79.
179. Luo Y, Blex C, Baessler O, Glinski M, Dreger M, Sefkow M, Köster H (2009) The cAMP capture compound mass spectrometry as a novel tool for targeting cAMP-binding proteins: from protein kinase A to potassium/sodium hyperpolarization-activated cyclic nucleotide-gated channels. *Mol Cell Proteomics* **8**: 2843–2856.
180. Fischer JJ, Graebner OY, Dalhoff C, Michaelis S, Schrey AK, Ungewiss J, Andrich K, Jeske D, Kroll F, Glinski M, et al. (2010) Comprehensive Identification of Staurosporine-Binding Kinases in the Hepatocyte Cell Line HepG2 using Capture Compound Mass Spectrometry (CCMS). *J Proteome Res* **9**: 806–817.
181. Smyth GK (2004) Linear models and empirical bayes methods for assessing differential expression in microarray experiments. *Stat Appl Genet Mol Biol* **3**: Article3.
182. Hengge R, Gründling A, Jenal U, Ryan R, Yildiz F (2015) Bacterial signal transduction by c-di-GMP and other nucleotide second messengers. *Journal of Bacteriology*.
183. Lee VT, Mawehish JM, Kessler JL, Hyodo M, Hayakawa Y, Lory S (2007) A cyclic-di-GMP receptor required for bacterial exopolysaccharide production. *Mol Microbiol* **65**: 1474–1484.
184. Navarro MVA, De N, Bae N, Wang Q, Sondermann H (2009) Structural analysis of the GGDEF-EAL domain-containing c-di-GMP receptor FimX. *Structure* **17**: 1104–1116.
185. Newell PD, Boyd CD, Sondermann H, O'Toole GA (2011) A c-di-GMP effector system controls cell adhesion by inside-out signaling and surface protein cleavage. *PLoS Biol* **9**: e1000587.
186. Tschowri N, Busse S, Hengge R (2009) The BLUF-EAL protein YcgF acts as a direct anti-repressor in a blue-light response of *Escherichia coli*. *Genes & Development* **23**: 522–534.
187. Minasov G, Padavattan S, Shuvalova L, Brunzelle JS, Miller DJ, Baslé A, Massa C, Collart FR, Schirmer T, Anderson WF (2009) Crystal structures of YkuI and its complex with second messenger cyclic Di-GMP suggest catalytic mechanism of phosphodiester bond cleavage by EAL domains. *J Biol Chem* **284**: 13174–13184.
188. Schmidt AJ, Ryjenkov DA, Gomelsky M (2005) The ubiquitous protein domain EAL is a cyclic diguanylate-specific phosphodiesterase: enzymatically active and inactive EAL domains. *Journal of Bacteriology* **187**: 4774–4781.

189. Gu H, Furukawa K, Breaker RR (2012) Engineered allosteric ribozymes that sense the bacterial second messenger cyclic diguanosyl 5'-monophosphate. *Anal Chem* **84**: 4935–4941.
190. Lacey MM, Partridge JD, Green J (2010) Escherichia coli K-12 YfgF is an anaerobic cyclic di-GMP phosphodiesterase with roles in cell surface remodelling and the oxidative stress response. *Microbiology* **156**: 2873–2886.
191. Zheng Y, Sambou T, Bogomolnaya LM, Cirillo JD, McClelland M, Andrews-Polymenis H (2013) The EAL domain containing protein STM2215 (rtn) is needed during Salmonella infection and has cyclic di-GMP phosphodiesterase activity. *Mol Microbiol* **89**: 403–419.
192. Brombacher E, Baratto A, Dorel C, Landini P (2006) Gene expression regulation by the Curli activator CsgD protein: modulation of cellulose biosynthesis and control of negative determinants for microbial adhesion. *Journal of Bacteriology* **188**: 2027–2037.
193. Ko M, Park C (2000) Two novel flagellar components and H-NS are involved in the motor function of Escherichia coli. *Journal of Molecular Biology* **303**: 371–382.
194. Weber H, Pesavento C, Possling A, Tischendorf G, Hengge R (2006) Cyclic-di-GMP-mediated signalling within the sigma network of Escherichia coli. *Mol Microbiol* **62**: 1014–1034.
195. Sommerfeldt N, Possling A, Becker G, Pesavento C, Tschowri N, Hengge R (2009) Gene expression patterns and differential input into curli fimbriae regulation of all GGDEF/EAL domain proteins in Escherichia coli. *Microbiology* **155**: 1318–1331.
196. Wang X, Dubey AK, Suzuki K, Baker CS, Babitzke P, Romeo T (2005) CsrA post-transcriptionally represses pgaABCD, responsible for synthesis of a biofilm polysaccharide adhesin of Escherichia coli. *Mol Microbiol* **56**: 1648–1663.
197. Jonas K, Edwards AN, Simm R, Romeo T, Römling U, Melefors Ö (2008) The RNA binding protein CsrA controls cyclic di-GMP metabolism by directly regulating the expression of GGDEF proteins. *Mol Microbiol* **70**: 236–257.
198. Palaniyandi S, Mitra A, Herren CD, Lockett CV, Johnson DE, Zhu X, Mukhopadhyay S (2012) BarA-UvrY two-component system regulates virulence of uropathogenic E. coli CFT073. *PLoS ONE* **7**: e31348.
199. Yoong P, Cywes-Bentley C, Pier GB (2012) Poly-N-acetylglucosamine expression by wild-type Yersinia pestis is maximal at mammalian, not flea, temperatures. *mBio* **3**: e00217–12.
200. Chen K-M, Chiang M-K, Wang M, Ho H-C, Lu M-C, Lai Y-C (2014) The role of pgaC in Klebsiella pneumoniae virulence and biofilm formation. *Microb Pathog* **77**: 89–99.
201. Serra DO, Richter AM, Hengge R (2013) Cellulose as an architectural element in

- spatially structured *Escherichia coli* biofilms. *Journal of Bacteriology* **195**: 5540–5554.
202. Blattner FR, Plunkett G, Bloch CA, Perna NT, Burland V, Riley M, Collado-Vides J, Glasner JD, Rode CK, Mayhew GF, et al. (1997) The complete genome sequence of *Escherichia coli* K-12. *Science* **277**: 1453–1462.
203. Maris AE, Sawaya MR, Kaczor-Grzeskowiak M, Jarvis MR, Bearson SMD, Kopka ML, Schröder I, Gunsalus RP, Dickerson RE (2002) Dimerization allows DNA target site recognition by the NarL response regulator. *Nat Struct Biol* **9**: 771–778.
204. Li Y, Heine S, Entian M, Sauer K, Frankenberg-Dinkel N (2013) NO-induced biofilm dispersion in *Pseudomonas aeruginosa* is mediated by an MHYT domain-coupled phosphodiesterase. *Journal of Bacteriology* **195**: 3531–3542.
205. Qi Y, Rao F, Luo Z, Liang Z-X (2009) A Flavin Cofactor-Binding PAS Domain Regulates c-di-GMP Synthesis in *AxDGC2* from *Acetobacter xylinum*. *Biochemistry* **48**: 10275–10285.
206. Cao Z, Livoti E, Losi A, Gärtner W (2010) A blue light-inducible phosphodiesterase activity in the cyanobacterium *Synechococcus elongatus*. *Photochem Photobiol* **86**: 606–611.
207. Römling U (2009) Rationalizing the evolution of EAL domain-based cyclic di-GMP-specific phosphodiesterases. *Journal of Bacteriology* **191**: 4697–4700.
208. Boos W, Parkinson JS, Jenal U, Vogel J, Søgaard-Andersen L (2013) Alexander Böhm (1971-2012). *Mol Microbiol* **88**: 219–221.
209. Chung CT, Niemela SL, Miller RH (1989) One-step preparation of competent *Escherichia coli*: transformation and storage of bacterial cells in the same solution. *Proc Natl Acad Sci USA* **86**: 2172–2175.
210. Miller JH (1992) *A short course in bacterial genetics - a laboratory manual and handbook for escherichia coli and related bacteria*. Cold Spring Harbor Laboratory Press.
211. Datsenko KA, Wanner BL (2000) One-step inactivation of chromosomal genes in *Escherichia coli* K-12 using PCR products. *Proc Natl Acad Sci USA* **97**: 6640–6645.
212. Baba T, Ara T, Hasegawa M, Takai Y, Okumura Y, Baba M, Datsenko KA, Tomita M, Wanner BL, Mori H (2006) Construction of *Escherichia coli* K-12 in-frame, single-gene knockout mutants: the Keio collection. *Molecular Systems Biology* **2**.
213. Uzzau S, Figueroa-Bossi N, Rubino S, Bossi L (2001) Epitope tagging of chromosomal genes in *Salmonella*. *Proc Natl Acad Sci USA* **98**: 15264–15269.
214. Boehm A, Steiner S, Zaehring F, Casanova A, Hamburger F, Ritz D, Keck W, Ackermann M, Schirmer T, Jenal U (2009) Second messenger signalling governs *Escherichia coli* biofilm induction upon ribosomal stress. *Mol Microbiol* **72**: 1500–1516.
215. Hindley C, Philpott A (2012) Co-ordination of cell cycle and differentiation in the

developing nervous system. *Biochem J* **444**: 375–382.

216. Blanpain C, Simons BD (2013) Unravelling stem cell dynamics by lineage tracing. *Nat Rev Mol Cell Biol* **14**: 489–502.
217. Holmberg J, Perlmann T (2012) Maintaining differentiated cellular identity. *Nat Rev Genet* **13**: 429–439.
218. Pasque V, Jullien J, Miyamoto K, Halley-Stott RP, Gurdon JB (2011) Epigenetic factors influencing resistance to nuclear reprogramming. *Trends Genet* **27**: 516–525.
219. Jenal U, Reinders A, Lori C (2017) Cyclic di-GMP: second messenger extraordinaire. *Nature Publishing Group* **15**: 271–284.
220. Pratt LA, Kolter R (1999) Genetic analyses of bacterial biofilm formation. *Current Opinion in Microbiology* **2**: 598–603.
221. Southey-Pillig CJ, Davies DG, Sauer K (2005) Characterization of temporal protein production in *Pseudomonas aeruginosa* biofilms. *Journal of Bacteriology* **187**: 8114–8126.
222. Waite RD, Papakonstantinou A, Littler E, Curtis MA (2005) Transcriptome analysis of *Pseudomonas aeruginosa* growth: comparison of gene expression in planktonic cultures and developing and mature biofilms. *Journal of Bacteriology* **187**: 6571–6576.
223. Patell S, Gu M, Davenport P, Givskov M, Waite RD, Welch M (2010) Comparative microarray analysis reveals that the core biofilm-associated transcriptome of *Pseudomonas aeruginosa* comprises relatively few genes. *Environ Microbiol Rep* **2**: 440–448.
224. Lopez D, Vlamakis H, Kolter R (2009) Generation of multiple cell types in *Bacillus subtilis*. *FEMS Microbiology Reviews* **33**: 152–163.
225. Tischler AD, Camilli A (2004) Cyclic diguanylate (c-di-GMP) regulates *Vibrio cholerae* biofilm formation. *Mol Microbiol* **53**: 857–869.
226. Ferrell JE Jr (2002) Self-perpetuating states in signal transduction: positive feedback, double-negative feedback and bistability. *Current Opinion in Cell Biology* **14**: 140–148.
227. Shimada T, Fujita N, Maeda M, Ishihama A (2005) Systematic search for the Cra-binding promoters using genomic SELEX system. *Genes Cells* **10**: 907–918.
228. Shimada T, Yamamoto K, Ishihama A (2011) Novel members of the Cra regulon involved in carbon metabolism in *Escherichia coli*. *Journal of Bacteriology* **193**: 649–659.
229. Grainger DC, Hurd D, Goldberg MD, Busby SJW (2006) Association of nucleoid proteins with coding and non-coding segments of the *Escherichia coli* genome. *Nucleic Acids Res* **34**: 4642–4652.
230. Lang B, Blot N, Bouffartigues E, Buckle M, Geertz M, Gualerzi CO, Mavathur R,

- Muskhelishvili G, Pon CL, Rimsky S, et al. (2007) High-affinity DNA binding sites for H-NS provide a molecular basis for selective silencing within proteobacterial genomes. *Nucleic Acids Res* **35**: 6330–6337.
231. Fang FC, Rimsky S (2008) New insights into transcriptional regulation by H-NS. *Current Opinion in Microbiology* **11**: 113–120.
232. Sette M, Spurio R, Trotta E, Brandizi C, Brandi A, Pon CL, Barbato G, Boelens R, Gualerzi CO (2009) Sequence-specific recognition of DNA by the C-terminal domain of nucleoid-associated protein H-NS. *Journal of Biological Chemistry* **284**: 30453–30462.
233. Dorman CJ (2004) H-NS: a universal regulator for a dynamic genome. *Nature Publishing Group* **2**: 391–400.
234. Rangarajan AA, Schnetz K (2018) Interference of transcription across H-NS binding sites and repression by H-NS. *Mol Microbiol* **15**: 175–14.
235. Chen Y, Ho JML, Shis DL, Gupta C, Long J, Wagner DS, Ott W, Josić K, Bennett MR (2017) Tuning the dynamic range of bacterial promoters regulated by ligand-inducible transcription factors. *Nat Commun* 1–8.
236. Dubnau D, Losick R (2006) Bistability in bacteria. *Mol Microbiol* **61**: 564–572.
237. Losick R, Desplan C (2008) Stochasticity and cell fate. *Science* **320**: 65–68.
238. Norman TM, Lord ND, Paulsson J, Losick R (2015) Stochastic Switching of Cell Fate in Microbes. *Annu Rev Microbiol* **69**: 381–403.
239. Hsu C, Jaquet V, Maleki F, Becskei A (2016) Contribution of Bistability and Noise to Cell Fate Transitions Determined by Feedback Opening. *Journal of Molecular Biology* 1–14.
240. Ninfa AJ, Mayo AE (2004) Hysteresis vs. graded responses: the connections make all the difference. *Sci STKE* **2004**: pe20.
241. Mitrophanov AY, Groisman EA (2008) Positive feedback in cellular control systems. *Bioessays* **30**: 542–555.
242. Veening J-W, Smits WK, Kuipers OP (2008) Bistability, epigenetics, and bet-hedging in bacteria. *Annu Rev Microbiol* **62**: 193–210.
243. Ackermann M (2015) A functional perspective on phenotypic heterogeneity in microorganisms. *Nature Publishing Group* **13**: 497–508.
244. Shu C-C, Chatterjee A, Dunny G, Hu W-S, Ramkrishna D (2011) Bistability versus bimodal distributions in gene regulatory processes from population balance. *PLoS Comput Biol* **7**: e1002140.
245. Suzuki K, Wang X, Weilbacher T, Pernestig A-K, Melefors Ö, Georgellis D, Babitzke P, Romeo T (2002) Regulatory circuitry of the CsrA/CsrB and BarA/UvrY systems of

- Escherichia coli. *Journal of Bacteriology* **184**: 5130–5140.
246. Ramseier TM (1996) Cra and the control of carbon flux via metabolic pathways. *Research in Microbiology* **147**: 489–493.
247. Paintdakhi A, Parry B, Campos M, Irnov I, Elf J, Surovtsev I, Jacobs-Wagner C (2016) Oufiti: an integrated software package for high-accuracy, high-throughput quantitative microscopy analysis. *Mol Microbiol* **99**: 767–777.
248. Sprecher KS, Hug I, Nesper J, Potthoff E, Mahi M-A, Sangermani M, Kaever V, Schwede T, Vorholt J, Jenal U (2017) Cohesive Properties of the Caulobacter crescentus Holdfast Adhesin Are Regulated by a Novel c-di-GMP Effector Protein. *mBio* **8**: e00294–17–15.
249. Schmidt A, Kochanowski K, Vedelaar S, Nature EA, 2016 The quantitative and condition-dependent Escherichia coli proteome. *naturecom*
- .
250. Peterson AC, Russell JD, Bailey DJ, Westphall MS, Coon JJ (2012) Parallel reaction monitoring for high resolution and high mass accuracy quantitative, targeted proteomics. *Mol Cell Proteomics* **11**: 1475–1488.
251. Ahrné E, Glatter T, Viganò C, Schubert CV, Nigg EA, Schmidt A (2016) Evaluation and Improvement of Quantification Accuracy in Isobaric Mass Tag-Based Protein Quantification Experiments. *J Proteome Res* **15**: 2537–2547.
252. Münch R, Hiller K, Grote A, Scheer M, Klein J, Schobert M, Jahn D (2005) Virtual Footprint and PRODORIC: an integrative framework for regulon prediction in prokaryotes. *Bioinformatics* **21**: 4187–4189.

Acknowledgements

I would like to thank my supervisor Prof. Urs Jenal for the faith and support throughout my masters and PhD. Urs is a visionary and communicated his visions in a motivating clarity that fosters to willingly go the extra mile. At moments when I found myself to be “in the cloud” (self-explanatory expression of Prof. Uri Alon, Weizmann Institute, Rehovot, Israel), Urs was utterly supportive and helped to move on and establish new ideas. It was a privilege to be mentored by Urs.

I also would like to thank my PhD committee Prof. Dirk Bumann and Prof. John McKinney. Their out-of-the-box input during our annual PhD committee meetings helped to focus on the core elements of this work.

Thank goes out to past and present members of the Jenal group, especially to Dr. Shogo Ozaki, Benjamin Sellner and Dr. Matteo Sangermani and Dr. Pablo Manfredi who were heavily involved in this project. Further I would like to thank Fabienne Hamburger who – more than once – lent me her “golden-cloning-hands” and Dr. Andreas Kaczmarczyk for valuable discussions.

The progress of this work would have been impossible without the synergistic collaboration with the structural group of Prof. Tilman Schirmer. This includes Prof. Tilman Schirmer himself, whose sound biophysical knowledge and meticulous approach towards scientific problems was of utmost importance, as well as Dr. Amit Sundriyal, Dr. Chee-Seng Hee, David Hinnen and Johanna Rueher. The fruitful in-house interdisciplinarity is a hallmark of the Biozentrum and practiced with unmatched standard, which I highly appreciated throughout my scientific career at the Biozentrum.

The 2.5 years after my PhD defense have been the most exciting in terms of the scientific progress we made in the PdeL project. The deep knowledge we gained in understanding the regulatory mechanisms of PdeL made us confident to team up with the group of Prof. Terence T. Hwa and mathematically model our system. Here I would like to especially thank Dr. Jonas Cremer who made an extraordinary effort in breaking down the complex PdeL circuit into concise mathematical models and simulations. I was literally always full of anticipation to our weekly Skype meetings and couldn't imagine a better culmination of this project than seeing how the “blood and sweat” of the last 7 years of lab work are condensed into mathematical equations. I'm greatly looking forward to publish this aspect together with Jonas.

Thank goes out to Prof. Volkhard Kaever and Annette Garve at the Institut für Pharmakologie in Hannover for the roughly 2,000 c-di-GMP measurements.

I thank all the technical and administrative staff of the Biozentrum, especially Marina Kuhn, Roger Sauder, Patric Haenni as well as the past and present “kitchen-ladies”. The service provided to us scientists for making us focus on our work is of priceless value. I hope that I will enjoy such a high-quality service at any other institute.

Although already acknowledged during my graduate studies I again want to greatly thank Dr. Markus Schwab & Dr. Thomas Østergaard-Tange. It frequently dawned on me how grateful I must be for having had these two great scientist as supervisors during my work at Evolva SA. Markus and Thomas established my first contact with scientific work, gave me all the freedom to develop own ideas and sustainably helped to form my “scientific character”.

I would like to thank all my friends. Alexander, Kathrin, Heiko, Jasmin, Benjamin, Ramona, Malte & Tibor. In particular, I would like to thank my band-mates Patrick, Tobias, Sebastian, Perrine and Luana. The process of exploring unknown and initially awe-inspiring terrains in a team-based (creative) effort, which finally gives birth to a new song, is a process very reminiscent to scientific work. I am grateful for this experience.

It is said that “your basic character traits are set with the age of three, from then on it is just fine-tuning”. For both character building and fine-tuning I wish to express my humble gratitude to my parents Peter and Enrichetta, sister Dr. Federica Reinders, brother-in-law Dr. Jens Tüxen and the Knaupp family.

It is inconceivable for me how a person could endure the bipolar mania of science without a strong emotional pillar. I am utterly grateful to have been emotionally guided throughout my scientific career by my wife Kerstin. Her faith and love are an inexhaustible source of vigor. I am a lucky man!

Publication record

Jutta Nesper*, [Alberto Reinders](#)*, Timo Glatter*, Alexander Schmidt, Urs Jenal (2012) *A novel capture compound for the identification and analysis of cyclic di-GMP binding proteins*. **Journal of Proteomics** Vol. 75, Issue 15: 4874-4878.

[Alberto Reinders](#), Chee-Seng Hee, Adam Mazur, Shogo Ozaki, Alex Boehm[‡], Tilman Schirmer, Urs Jenal (2015) *Expression and genetic activation of c-di-GMP-specific phosphodiesterases in Escherichia coli*. **Journal of Bacteriology** Vol 198, Issue 3: 448-462.

Urs Jenal, [Alberto Reinders](#)*, Christian Lori* (2017) *Cyclic di-GMP: second messenger extraordinaire*. **Nature Reviews Microbiology** Vol 15, Issue 5: 271-284.

[Alberto Reinders](#), Shogo Ozaki, Johanna Rueher, Benjamin Sellner, Matteo Sangermani, Tilman Schirmer, Urs Jenal (2018) *Stay or go? A bistable molecular switch facilitating bacterial lifestyle transitions*, manuscript under preparation.

*contributed equally

[‡]deceased on November 27th, 2012

Co-author affiliations

Focal Area of Infection Biology, Biozentrum, University of Basel; Klingelbergstrasse 50-70, 4065 Basel (CH)

Alberto Reinders, Shogo Ozaki¹, Jutta Nesper², Benjamin Sellner, Matteo Sangermani, Urs Jenal

Focal Area of Structural Biology & Biophysics, University of Basel; Klingelbergstrasse 50-70, 4056 Basel (CH)

Amit Sundriyal³, Chee-Seng Hee³, David Hinnen⁴, Johanna Rueher, Tilman Schirmer

Proteomics Core Facility, Biozentrum, University of Basel; Klingelbergstrasse 50-70, 4056 Basel (CH)

Timo Glatter⁵, Alexander Schmidt

Research IT Technology Plattform, Biozentrum, University of Basel; Klingelbergstrasse 50-70, 4056 Basel (CH)

Adam Mazur

Zentrale Forschungseinrichtung (ZFA) Metabolomics, Institut für Pharmakologie, Medizinische Hochschule Hannover, Carl-Neuberg Straße 1, 30625 Hannover (D)

Volkhard Kaever

Current address

¹Associate professor at the Kyushu University, Fukuoka, Japan

²⁻⁴Exmatriculated from the University of Basel

⁵Group leader of the Proteomics and Mass Spectrometry Facility at the MPI Marburg, Germany

^{*}deceased on November 15th, 2016

Curriculum vitae

Personal details:

Name: Alberto Reinders
Address: Hauptstraße 400, D-79576 Weil am Rhein
Birth date: 29.12.1985
Place of birth: Sana'a, Yemen
Nationality: German/Italian

Education:

1990 – 1992	International School, Primary School Sana'a, Yemen
1992 – 1993	Karl-Tschamber Schule, Primary School Weil am Rhein, Germany
1993 – 1996	Rheinschule, Primary School Weil am Rhein, Germany
1996 – 2005	Immanuel Kant-Gymnasium, High School Weil am Rhein, Germany A-levels with focus on biology and music
<hr/>	
2006 – 2010	Undergraduate studies in Molecular Biology Biozentrum, University of Basel, Switzerland
2010 – 2011	Graduate studies in Molecular Microbiology Biozentrum, University of Basel, Switzerland Group: Prof. Urs Jenal Supervision: Dr. Alexander Böhm Topic: <i>Genetic dissection of c-di-GMP-specific phosphodiesterases in E. coli</i>
<hr/>	
2011 – 2016	PhD studies in Molecular Microbiology Biozentrum, University of Basel, Switzerland Group: Prof. Urs Jenal Topic: <i>Stay or go? A bistable molecular switch facilitating bacterial lifestyle transitions</i>

Work experience:

2005 – 2006	Civilian service at the Caritas Catholic Welfare Center Weil am Rhein, Germany
-------------	---

2008 – 2010 Undergraduate lab assistant at Evolva SA
Reinach (formerly in Allschwil), Switzerland

Special efforts:

08/2011 Scholarship: 'Fellowships For Excellence'
International PhD Program

2010 – 2018 Co-management of yearly undergraduate student block-course
Biozentrum, University of Basel, Switzerland

2015 – 2016 Supervision of collaborating master student
Biozentrum, University of Basel, Switzerland

Conferences:

05/2011 Molecular Microbiology Meeting
Würzburg, Germany
Poster contribution

03/2013 ESF-EMBO Symposium, Bacterial Networks (BacNet)
Pułtusk, Poland
Poster contribution

01/2014 Gordon Research Conference, Sensory Transduction in
Microorganisms (STIM)
Ventura (CA), USA
Poster contribution

06/2014 1st Fellowship For Excellence Symposium
Basel, Switzerland
Talk: *How to couple enzymatic activity to transcriptional
regulation*

04/2016 1st International Symposium on c-di-GMP Signaling in Bacteria
Berlin, Germany
Poster contribution

05/2015 ESF-EMBO Symposium, Bacterial Networks (BacNet)
Sant Feliu de Guíxols, Spain
Poster contribution

01/2016 Biozentrum Symposium
Basel, Switzerland
Talk: *A moonlighting enzyme imposes second messenger
bistability to drive lifestyle decisions in E. coli*
Awarded 'Best Talk'

01/2016

Gordon Research Conference, Sensory Transduction in
Microorganisms (STIM)
Ventura (CA), USA
Poster contribution

Languages:

German (mother tongue)
Italian (mother tongue)
English (fluent)
French (advanced)

Publications:

Jutta Nesper*, **Alberto Reinders***, **Timo Glatter***, **Alexander Schmidt**, **Urs Jenal**
A novel capture compound for the identification and analysis of cyclic di-GMP binding
proteins
Journal of Proteomics | May 2012 | Vol. 75 (15): pp. 4874-4878
*equal contribution

Alberto Reinders, **Chee-Seng Hee**, **Adam Mazur**, **Shogo Ozaki**, **Alex Böhm***, **Tilman
Schirmer**, **Urs Jenal**
Expression and genetic activation of c-di-GMP-specific phosphodiesterases in *Escherichia
coli*
Journal of Bacteriology | November 2015 | Vol. 198 (3): pp. 448-462
* deceased on November 27th, 2012

Urs Jenal, **Alberto Reinders***, **Christian Lori***
Cyclic di-GMP: second messenger extraordinaire
Nature Reviews Microbiology | February 2017 | Vol. 15 (5): pp. 271-284
*equal contribution

Alberto Reinders, **Shogo Ozaki**, **Johanna Rueher**, **Benjamin Sellner**, **Matteo Sangermani**,
Tilman Schirmer, **Urs Jenal**
Stay or go? A bistable molecular switch facilitating bacterial lifestyle transitions
Manuscript under preparation

Interests:

Music, cave- and recreational-diving, mountaineering, CrossFit, snowboarding

The 'Fellowship For Excellence' International PhD Program financially supported the research performed in this thesis by Alberto Reinders.